1

Electromagnetics, Physics, and Mathematics

Mathematics is the mother of science, science is the mother of technology and father of innovation, and technology is a gift of God.

1.1 A Brief History of Electromagnetics

Electromagnetics is a subject that entails the study of electromagnetic theory, its physical interaction with environments and objects, and its use for design and engineering applications. Electromagnetic theory is governed by a set of equations that originated from many great scientists such as Gauss (1835), Amperes (1823), Faraday (1838), and Coulomb (1785) [1–4]. However, this set of equations is now commonly known as Maxwell's equations due to the work of James Clerk Maxwell who put on them in mathematical form in 1864 and added a term to Ampere's law that included displacement current density [5, 6, 33][1].

This set of equations is used to describe static electromagnetic fields, radio waves, microwaves, optical fields, as well as x-rays. It is valid from subatomic length scale to inter-galactic length scale. The Coulomb potential due to a point charge of a proton or an electron inside an atom can be derived from Maxwell's equations. Meanwhile, the propagation of radio waves and optical signals from outer galaxies can be described by the same set of equations [7].

Before the completion of Maxwell's theory, optical fields were thought to be different from electromagnetic fields. Snell (1621), Huygens (1660), Newton (1660), and Fresnel (1814) were studying optical fields along a different line. Maxwell's theory unified electromagnetics with optics. When quantum theory is added to electromagnetic theory, quantum electrodynamics (QED) ensues, as was done by Dirac (1920). When differential geometry was used, electromagnetic theory inspired Yang-Mills theory which has been regarded as a generalized electromagnetic theory (see Figure 1.1).

Moreover, the impact and importance of electromagnetics on modern technologies are unquestionable. This knowledge is pervasively used in engineering, and is used as a supporting technology for many aspects of scientific investigation. For instance, in high-energy physics, particles are accelerated by an electromagnetic field [8, 9], and

1 The theory was presented to the British Royal Society in 1864, published in 1865, and a treatise was written in 1873. The equations were later beautified by O. Heaviside.

The Nyström Method in Electromagnetics, First Edition. Mei Song Tong and Weng Cho Chew.

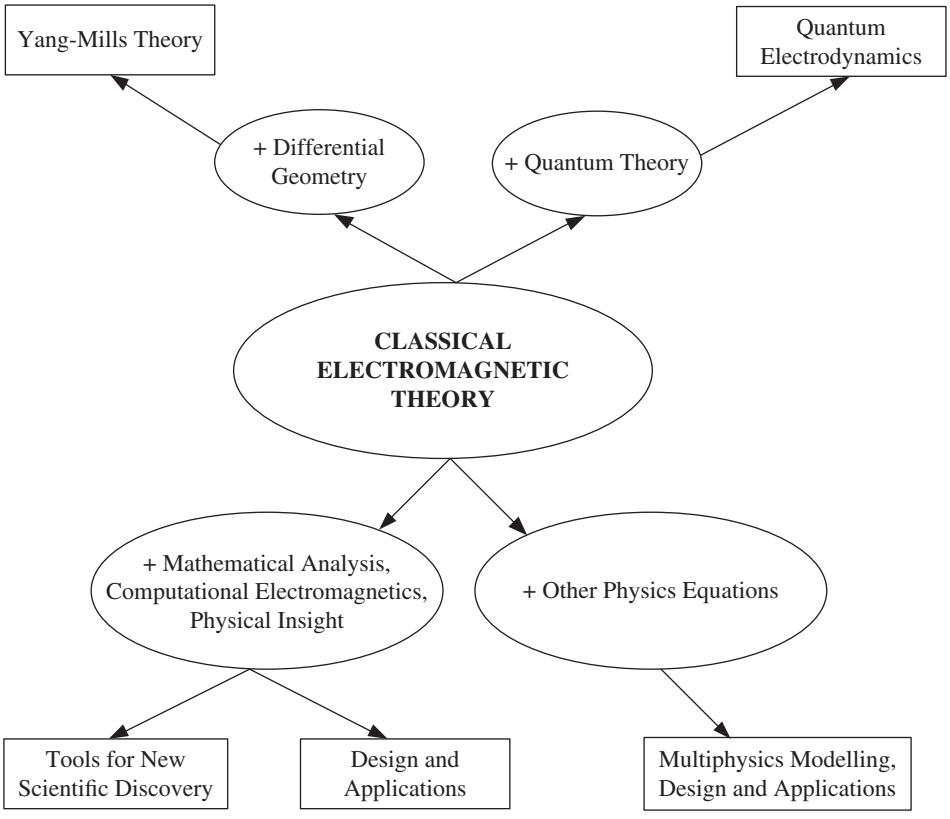

Figure 1.1 The relationship of classical electromagnetic theory with other knowledge areas.

hence electromagnetic engineering is needed. The measurement of electromagnetic fields and optical signals arriving to the earth from the outer universe is used in astronomy to enhance our understanding of the universe. Electromagnetic fields are used in electrophoresis in electrochemistry [10, 11] and biomolecular electrostatics [12, 13]. The electromagnetic force is a predominant force in nano-electronic transport [14–17]. The Poisson-Boltzmann equation is usually solved in these contexts [18–25]. More recently, electromagnetics is of fundamental importance in wireless power transfer and also in bioelectromagnetics.

Electromagnetics is also important in the design of rotating machineries, electric generators, energy conversion devices, and electric power distribution networks, as well as green energy such as solar cells and solar collectors [26–32]. It is important for antenna design for wireless communication, radar, and remote sensing. The maser was first invented at microwave frequency (1952) before its close cousin, laser, was invented (1958). As the field of optics grows, many technologies that were first proven at microwave frequencies are now being realized at optical frequencies, such as optical interferometric imaging, optical coherence tomography, and nano-antennas. Electromagnetics also becomes increasingly important in electromagnetic interference (EMI) and electromagnetic compatibility (EMC) as more electronic components are packed into smaller spaces in, e.g., the cellphone industry.

The recent advent in nano-fabrication technology, where structures on the order of tens of nanometers can be made, has spurred strong interest in nano-optics. The advent of single photon measurement, and the validation of the Bell's theorem in favor of the interpretation of Copenhagen school in the 1980s, spurred new interest in quantum optics and quantum information. Quantum electromagnetics is emerging. The validation of the Casimir force in 1997 also spurred new interest in this force.

1.2 Enduring Legacy of Electromagnetic Theory–Why?

Electromagnetic theory as completed by James Clerk Maxwell in 1865 [5] is just over 150 years old now. It has withstood the test of time, and the emergence of new physics theories such as relativity and quantum theory. This is unlike Newton's laws of mechanics that were quickly superseded by new theories.

Putatively, Maxwell's equations were difficult to understand [33]; distillation and cleaning of the equations were done by Heaviside and Hertz [34]; experimental confirmations of these equations were not done until some 20 years later in 1888 by Hertz [35].

As is the case with the emergence of new knowledge, it is often confusing at times, and inaccessible to many people. Numerous developments of electromagnetic theory have ensued since Maxwell's time and we shall discuss them in the next section.

Since the advent of Maxwell's equations in 1865, the enduring legacy of these equations has been pervasive in many fields. As aforementioned, Hertz confirmed the remote induction effect in 1888. And in 1893, Tesla [36] demonstrated the possibility of radio. In 1897, Marconi [37] demonstrated wireless transmission, followed by transatlantic transmission in 1901. Maxwell did not know the importance of the equations that he had completed. Much advanced understanding of electromagnetic theory in its modern form did not emerge until many years after his death; it will be interesting to recount these facts.

- Since Maxwell's equations unify the theories of electromagnetics and optics, they are valid over a vast length scale. Electromagnetic theory is valid for subatomic particle interaction, as well as being responsible for the propagation of light waves and radio waves across the galaxies.
- With the theory of special relativity developed by Einstein in 1905 [38], these equations were known to be relativistically invariant. In other words, Maxwell's equations remain the same in a spaceship irrespective of how fast it is moving. Electrostatic theory in one spaceship becomes electrodynamic theory in a moving spaceship relative to the first one.
- The development of QED by Dirac in 1927 [39] indicated that Maxwell's equations are valid in the quantum regime as well. Initially, QED was studied by Dyson, Feynman, Schwinger, and Tomonaga, mainly to understand the interparticle interactions in the context of quantum field theory to determine fine structure constants and their anomalies due to quantum electromagnetic fluctuations [40]. However, the recent increase in quantum information has spurred on the application of QED in optics, giving rise to the field of quantum optics [41–47].

- Later, with the development of differential forms by Cartan in 1945 [48, 49], it was found that electromagnetic theory is intimately related to differential geometry. Electromagnetic theory inspired the Yang-Mills theory, which was developed in 1954 [50, 51]; it is regarded as a generalized electromagnetic theory. In fact, as quoted by Misner, Thorne, and Wheeler, it is said that "differential forms illuminate electromagnetic theory, and electromagnetic theory illuminates differential forms" [52, 53].
- In 1985, Feynman wrote that quantum electrodynamics (a superset of electromagnetic theory) had been validated to be one of the most accurate equations to a few parts in a billion [54]. This is equivalent to an error of a few human hair widths compared to the distance from New York to Los Angeles. More recently, Styer wrote in 2012 [55] that the accuracy had been improved to a few parts in a trillion [56]; such an error is equivalent to a few human hair widths in the distance from the Earth to the Moon.
- More importantly, since Maxwell's equations have been around for over 150 years, they have pervasively influenced the development of a large number of scientific technologies. This impact is particularly profound in electrical engineering, ranging from rotating machinery, oil-gas exploration, and magnetic resonance imaging, to optics, wireless and optical communications, computers, remote sensing, bioelectromagnetics, etc.

Despite the cleaning up of Maxwell's equations by Heaviside, he has great admiration for Maxwell as seen from his following statement [34], "A part of us lives after us, diffused through all humanity – more or less – and through all nature. This is the immortality of the soul. There are large souls and small souls. The immoral soul of the 'scienticulists'[2] is a small affair, scarcely visible. Indeed its existence has been doubted. That of a Shakespeare or Newton is stupendously big. Such men live the bigger part of their lives after they are dead. Maxwell is one of these men. His soul will live and grow for long to come, and hundreds of years hence will shine as one of the bright stars of the past, whose light takes ages to reach us."

1.3 The Rise of Quantum Optics and Electromagnetics

The rise of the importance of quantum electromagnetics has been spurred on by technologies for single photon sources and measurements [57, 58], the validation of Bell's theorem [59], and the leaps and bounds progress in nanofabrication technologies.

The validation of Bell's theorem in favor of the interpretation of Copenhagen school opens up new possibilities for quantum information, computing, cryptography, and communication [60]. Nanofabrication techniques further allow the construction of artificial atoms such as quantum dots that are microscopic in scale. Moreover, the potential for using such artificial atoms to manipulate quantum information abounds. In this case, semi-classical calculations where the fields are treated classically and the atoms treated quantum mechanically [61, 62] do not suffice to support many of the emerging technologies when the number of photons is limited, such as single photon

2 This term was coined by Heaviside for his nemesis, Preece [34].

based devices and high sensitivity photo-detectors. Another interesting example is circuit QED at microwave frequencies where a superconducting quantum interference device (SQUID) based artificial atom is entangled with coplanar waveguide microwave resonators [63]. For these situations, full quantum field-artificial-atom calculations need to be undertaken [64].

The recent progress in nano-fabrication technology underscores the importance of quantum effects at nanoscale, first on electron transport [65], and now on the importance of photon-artificial-atom interaction at nanoscale. Moreover, nanofabrication emphasizes the importance of photons and the accompanying quantum effects in heat transfer. While phonons require material media for heat transfer, photons can account for near-field heat transfer through vacuum where the classical heat conduction equation and Kirchhoff's law of thermal radiation are invalid. Furthermore, the confirmation of the Casimir force in 1997 [66] revived it as an interesting research topic. Several experiments confirmed that the Casimir force is in fact real, and entirely quantum in origin: it can be only explained using quantum theory of electromagnetic fields in its quantized form [67, 68]. Also, the Casimir force cannot be explained by classic electromagnetics theory, which assumes null electromagnetic field in vacuum.

More importantly, the use of the ubiquitous Green's function is still present in many quantum calculations [69, 71]. Hence, the knowledge and effort in computational electromagnetics for computing the Green's functions of complicated systems have not become obsolete or in vain [72, 74–76]. Therefore, the development of computational electromagnetics, which has been important for decades for the development of many classical electromagnetics technologies all across the electromagnetic spectrum, will be equally important in the development of quantum technologies.

1.3.1 Connection of Quantum Electromagnetics to Classical Electromagnetics

Vacuum space consists of electron-positron (e–p) pairs that represent nothingness. However, when an electromagnetic wave passes through vacuum, the e–p pairs are polarized to form simple harmonic oscillators. The propagation of electromagnetic waves through vacuum is due to the coupling of these simple harmonic oscillators [79]. From this concept, the quantum Maxwell's equations are derived to be [80, 81]:

$$\nabla \times \hat{\mathbf{H}}(\mathbf{r}, t) - \partial_t \hat{\mathbf{D}}(\mathbf{r}, t) = \hat{\mathbf{J}}_{\text{ext}}(\mathbf{r}, t) \tag{1.1}$$

$$\nabla \times \hat{\mathbf{E}}(\mathbf{r}, t) + \partial_t \hat{\mathbf{B}}(\mathbf{r}, t) = 0 \tag{1.2}$$

$$\nabla \cdot \hat{\mathbf{D}}(\mathbf{r}, t) = \hat{\rho}_{\text{ext}}(\mathbf{r}, t) \tag{1.3}$$

$$\nabla \cdot \hat{\mathbf{B}}(\mathbf{r}, t) = 0. \tag{1.4}$$

The Green's function technique applies when the quantum system is linearly time-invariant. Hence, past knowledge in classical computational electromagnetics can be invoked to arrive at these Green's functions. These quantum Maxwell's equations portend well for a better understanding of quantum effects that are observed in many branches of electromagnetics, as well as in quantum optics, quantum information, communication, computing, encryption and related fields. More details about this work can be found in [62, 80–83]. Hence, the combination of computational electromagnetics with quantum theory is cogent for the development of computational quantum optics.

1.4 The Early Days – Descendent from Fluid Physics

In the early days, mathematics was developed to describe different physical laws such as Newton's laws. Later, calculus was developed to study solid mechanics, elasticity, and fluid mechanics. In fluids and elastomechanics, the concepts of field and its conservative and rotational properties were introduced. Such concepts were later carried over to describe the physics of electromagnetic fields. The concepts of gradient, curl, and divergence operators have originated in fluid mechanics. The concepts of scalar field and vector field also occur in fluids. The gradient of a scalar field gives rise to a vector field that could be a velocity field. For instance, in acoustics, the gradient of the pressure, which is a scalar field, gives rise to a force field density, which is a vector field, namely, $\mathbf{F} = -\nabla\phi$.

The curl operator is a measure of the rotation of a vector field. Hence, it is a good measure of angular momentum that exists in a fluid field. It also reflects on the torsional field that exists in the force field in a solid when it is deformed. For instance, $\boldsymbol{\omega} = \nabla \times \mathbf{v}$ is a measure of rotation in the velocity field $\mathbf{v}$.

The divergence operator indicates how much field actually oozes from a point in space. It is useful for measuring the conservation of "things", such as conservation of mass and momentum in fluid mechanics. For example, the conservation of mass in fluid can be written as

$$\nabla \cdot (\mathbf{v}\rho) + \frac{\partial \rho}{\partial t} = 0 \tag{1.5}$$

where $\mathbf{v}$ is the velocity field, while ρ is the mass density.

The divergence operator has been used to describe Coulomb's law that the total electric flux that emerges from a charge source is proportional to the charge [3], i.e.

$$\nabla \cdot \mathbf{D} = \rho \tag{1.6}$$

where ρ is the charge density. The concept of electric flux density $\mathbf{D}$ was introduced to relate $\mathbf{D}$ to the surface charge density. The above has a conservative concept in the sense that a fixed amount of flux emerges from a fixed amount of charge.

Similarly, the Gauss' law [4] was introduced for the conservation of magnetic flux, and the concept of magnetic flux density $\mathbf{B}$ was introduced, namely,

$$\nabla \cdot \mathbf{B} = 0 \tag{1.7}$$

which represents the conservation of magnetic flux density. It also points to the non-existence of magnetic charges.

Ampere's law [2] was introduced by experimental observation that a wire carrying an electric current produces a swirling magnetic field that "circulates" around the current, i.e.

$$\nabla \times \mathbf{H} = \mathbf{J}. \tag{1.8}$$

Taking the divergence of the above yields $\nabla \cdot \mathbf{J} = 0$, which implies the conservation of current flow. It also implies Kirchhoff's current law in circuit theory.

Faraday's law has been formulated following the observation that a time-varying magnetic flux induces a voltage in a loop of wire. Consequently,

$$\nabla \times \mathbf{E} = -\frac{\partial \mathbf{B}}{\partial t}. \tag{1.9}$$

The above equations can be written in an integral form, but the physics is entailed in the differential form as lucidly as they are in integral form. However, much of circuit theory is derived from the integral form. The integral form of Maxwell's equations brings out the fact that it is the topology that governs the laws of circuits. So if two circuits may look very different in shape, but their behavior is similar if they are topologically the same. The above equations (1.8) and (1.9) are pre-Maxwellian, and the development of telegraphy very much depends on them [34].

1.5 The Complete Development of Maxwell's Equations

Maxwell's equations are descended from Gauss', Coulomb's, Ampere's, and Faraday's laws. Maxwell's contribution was to add a displacement current term to Ampere's law making it into the generalized Ampere's law. The displacement current is produced by the time variation of the electric flux density **D** (also called the displacement field). The generalized Ampere's law can be written as

$$\nabla \times \mathbf{H} = \mathbf{J} + \frac{\partial \mathbf{D}}{\partial t}. \tag{1.10}$$

It is the addition of this displacement current term $\frac{\partial \mathbf{D}}{\partial t}$ that connects the laws of electricity and magnetism with the laws of optics. Prior to this, the group of four equations without the displacement current was used to describe the theory of electricity and magnetism, and did not predict the existence of wave phenomena.

The term $\frac{\partial \mathbf{D}}{\partial t}$ introduces "springiness" into the electromagnetic media like a capacitor. This displacement current, in turn, produces a magnetic field. The time-varying magnetic field produces an electric field that opposes the flow of the displacement current, or a reluctance (analogous to the inertial of a mass) as in Lenz's law. This inductance together with the capacitive effect yield a simple harmonic oscillator[3].

For material media,

$$\mathbf{D} = \epsilon_0 \mathbf{E} + \mathbf{P} \tag{1.11}$$

where **P** is the dipole density. The dipoles in material media are polarized by the electric field that exerts a force that pulls the positive and negative charge of a molecule or an atom apart, forming a dipole. For a time harmonic field, the time-varying charge produces a current, and hence a magnetic field like an inductor. The dipole together with the inductor forms a resonant circuit very much like an LC tank circuit. For a weak field, **P** is linearly related to **E**, and we can write $\mathbf{P} = \epsilon_0 \chi \mathbf{E}$. Therefore, for material media, we introduce $\epsilon = \epsilon_0(1 + \chi)$ so that $\mathbf{D} = \epsilon \mathbf{E}$.

For a vacuum, $\mathbf{D} = \epsilon_0 \mathbf{E}$, implying that even a vacuum has "springiness". It is this springiness of vacuum and material media that gives rise to electromagnetic waves

3 The equation for capacitance, $V = Q/C$ is similar to Hook's law in that $F = kx$ where k is the spring constant. The voltage across an inductor $V = L\dot{I} = L\ddot{Q}$ is similar to Newton's law in that $F = m\ddot{x}$. Hence, the harmonic oscillator of a mass on a spring is similar to the harmonic oscillator formed by an LC tank circuit.

in material and even in vacuum. Electron-positron pairs that lurk in vacuum, in their quiescent state, constitute nothingness. It has also been observed that when vacuum is bombarded with energetic photons (or energetic electromagnetic fields), electron-positron pairs are produced [79, 84, 85].

Electromagnetic theory in the classical sense is hence completely described by the four equations:

$$\nabla \times \mathbf{H} = \mathbf{J} + \frac{\partial \mathbf{D}}{\partial t} \tag{1.12}$$

$$\nabla \times \mathbf{E} = -\frac{\partial \mathbf{B}}{\partial t} \tag{1.13}$$

$$\nabla \cdot \mathbf{D} = \rho \tag{1.14}$$

$$\nabla \cdot \mathbf{B} = 0. \tag{1.15}$$

When Maxwell's equations were first derived by Maxwell, they were not as elegant and succinct as the above. It was the work of Heaviside and Herz that cast them into the above form [34, 86]. It was deemed that the electric field and the magnetic field are the measurable quantities.

The above equations look deceptively simple, but they have very profound meanings. They are relativistically correct in all inertial frames of special relativity [9, 74]. They are also intimately related to geometry.

It is to be noted that for time-varying solutions, the second two equations above are derivable from the first two. For instance, if we take the divergence $(\nabla\cdot)$ of the first equation (1.12), and make use of the fact that $\nabla \cdot (\nabla \times \mathbf{H}) = 0$, we obtain that

$$0 = \nabla \cdot \mathbf{J} + \frac{\partial(\nabla \cdot \mathbf{D})}{\partial t}. \tag{1.16}$$

The conservation of charge necessitates that

$$\nabla \cdot \mathbf{J} + \frac{\partial \rho}{\partial t} = 0. \tag{1.17}$$

Using this fact in (1.16) yields

$$\frac{\partial(\nabla \cdot \mathbf{D} - \rho)}{\partial t} = 0. \tag{1.18}$$

The above implies that

$$\nabla \cdot \mathbf{D} - \rho = \rho_{\text{const}} \tag{1.19}$$

where ρ_{const} corresponds to a constant charge independent of time. We can assume such a charge to be zero, or that it produces a static field that does not contribute to our time-varying field. Then (1.14) follows from (1.12). Equation (1.15) can be similarly derived from (1.13). Therefore, for time-varying fields or electrodynamics, Equations (1.12) and (1.13) are sufficient. However, when a numerical code is written for a time-varying field, it often breaks down when the frequency is lowered, because at low frequencies, the first two of Maxwell's equations are not stable, as they do not reduce to the last two equations when the frequency is identically zero [73].

To preclude the low-frequency breakdown, the vector and scalar potential formulation has been suggested [73]. This formulation solves all four Maxwell's equations concurrently, and hence, does not have low-frequency breakdown. This formulation is in fact closer to the original formulation of Maxwell's [33].

However, there are four vector unknowns **E**, **H**, **D**, **B**, with two vector equations. To increase the number of equations, we rely on the constitutive relations. A set of general constitutive relations are

$$\mathbf{D} = \overline{\epsilon} \cdot \mathbf{E} + \overline{\xi} \cdot \mathbf{H} \tag{1.20}$$

$$\mathbf{B} = \overline{\zeta} \cdot \mathbf{E} + \overline{\mu} \cdot \mathbf{H} \tag{1.21}$$

where $\overline{\epsilon}$, $\overline{\xi}$, $\overline{\zeta}$, and $\overline{\mu}$ are tensors. The medium with the above relations is known as a bianisotropic medium [74]. When $\overline{\xi} = \overline{\zeta} = 0$, the medium is anisotropic. When the tensors are replaced with scalars, the medium is isotropic. Other non-local relations are possible such as a convolutional relation in space

$$\mathbf{D}(\mathbf{r}) = \int d\mathbf{r}' \epsilon(\mathbf{r} - \mathbf{r}')\mathbf{E}(\mathbf{r}'). \tag{1.22}$$

When Fourier transformed to the **k** space or spatial frequency space, the above becomes

$$\mathbf{D}(\mathbf{k}) = \epsilon(\mathbf{k})\mathbf{E}(\mathbf{k}) \tag{1.23}$$

which is a scalar relationship. Such a medium is known as spatially dispersive. Certain multiple scattering media that are translationally invariant in space can be described by such constitutive relations. Also, a relationship involving convolution in time is also possible. When transformed into the ω or the frequency space, the permittivity is a function of frequency. Such media are termed frequency dispersive. When the constitutive parameters are functions of space, the media are inhomogeneous.

The constitutive relations describe the physical properties of the media. Most media can be described by simpler constitutive relations

$$\mathbf{D} = \epsilon\mathbf{E} \tag{1.24}$$

$$\mathbf{B} = \mu\mathbf{H} \tag{1.25}$$

where ϵ is the permittivty and μ is the permeability. Then Equations (1.12) and (1.13) and the constitutive relations are sufficient to be solved for the unknowns **E** and **H** if the current **J** is given. In some media, the electric current **J** is induced. Then we divide $\mathbf{J} = \mathbf{J}_{\text{imp}} + \mathbf{J}_{\text{ind}}$, where $\mathbf{J}_{\text{imp}}$ is the impressed current into the equations, while $\mathbf{J}_{\text{ind}}$ is the induced current in the medium[4]. For instance, for a simple conductive medium,

$$\mathbf{J}_{\text{ind}} = \sigma\mathbf{E} \tag{1.26}$$

where σ is the conductivity.

1.5.1 Derivation of Wave Equation[5]

To show the existence of the wave solution, we take the curl of (1.13) and one gets

$$\begin{aligned} \nabla \times \nabla \times \mathbf{E} &= -\frac{\partial(\nabla \times \mathbf{B})}{\partial t} = -\mu \frac{\partial(\nabla \times \mathbf{H})}{\partial t} \\ &= -\mu \frac{\partial\left(\mathbf{J} + \frac{\partial \mathbf{D}}{\partial t}\right)}{\partial t} = -\mu \frac{\partial \mathbf{J}}{\partial t} - \mu\epsilon \frac{\partial^2 \mathbf{E}}{\partial t^2} \end{aligned} \tag{1.27}$$

4 An impressed current is a current put into Maxwell's equations that is immutable irrespective of what the environment is.

5 This can be skipped for the initiated.

or

$$\nabla \times \nabla \times \mathbf{E} + \mu\epsilon \frac{\partial^2 \mathbf{E}}{\partial t^2} = -\mu \frac{\partial \mathbf{J}}{\partial t}. \tag{1.28}$$

The above is the vector wave equation with a source term **J**. In the absence of a source, it reduces to

$$\nabla \times \nabla \times \mathbf{E} + \mu\epsilon \frac{\partial^2 \mathbf{E}}{\partial t^2} = 0 \tag{1.29}$$

whose solutions are the homogeneous solutions to (1.28). It can be simplified to the scalar wave equation, verifying the existence of a wave solution to Maxwell's equations. By using the vector identity that

$$\nabla \times \nabla \times \mathbf{E} = -\nabla \cdot \nabla \mathbf{E} + \nabla \nabla \cdot \mathbf{E} \tag{1.30}$$

and that for a source free region $\nabla \cdot \mathbf{E} = 0$, (1.29) becomes

$$\nabla^2 \mathbf{E} - \mu\epsilon \frac{\partial^2 \mathbf{E}}{\partial t^2} = 0 \tag{1.31}$$

which manifestly resembles the scalar wave equation. When written in Cartesian coordinates, the above becomes three scalar wave equations for E_x, E_y, E_z. However, one has to be mindful that these field components are not independent of each other since $\nabla \cdot \mathbf{E} = 0$.

1.6 Circuit Physics, Wave Physics, Ray Physics, and Plasmonic Resonances

Even though Maxwell's equations are deceptively simple, there are three regimes of physical phenomena described by them that are distinctly different. At low frequencies or long wavelengths, circuit physics prevails. When the object size is *on the order of* [6] the wavelength, wave physics prevails. However, when the wavelength is very short compared to the size of the object, ray physics predominates [87].

When the frequency is very low, or at statics, the **E** and **H** fields are decoupled in free space. This is the regime of circuit physics, where we have the world of the inductors and the world of the capacitors. The inductive world encompasses devices that store magnetic energy, while the capacitive world encompasses devices that store electric energy. Moreover, at low frequencies, devices in these two worlds are weakly coupled to each other.

1.6.1 Circuit Physics

When $\omega \to 0$ or $\partial/\partial t \to 0$, the four Maxwell's equations reduce to:

$$\nabla \times \mathbf{H} = \mathbf{J} \tag{1.32}$$

$$\nabla \times \mathbf{E} = 0 \tag{1.33}$$

$$\nabla \cdot \mathbf{D} = \rho \tag{1.34}$$

$$\nabla \cdot \mathbf{B} = 0. \tag{1.35}$$

6 This is the mathematical parlance for "about".

In this case, the bottom two equations are not derivable from the top two. Hence, In the low frequency regime, all four of Maxwell's equations are important. Moreover, the electric field and the magnetic field are decoupled in free space. Namely, $\{\mathbf{E}, \mathbf{D}, \rho\}$ are decoupled from $\{\mathbf{H}, \mathbf{B}, \mathbf{J}\}$ in free space. This is the circuit physics regime where topology is more important than shape.

At very low frequencies,

$$\nabla \times \mathbf{E} = -\frac{\partial \mathbf{B}}{\partial t} \approx 0 \tag{1.36}$$

can be interpreted as Kirchhoff's voltage law. When written in integral form, it implies that the sum of voltages in a loop is zero. The above implies that the electric field $\mathbf{E}$ is a conservative field: The total work done by such a field in a loop is zero.

Similarly, by taking the divergence of the generalized Ampere's law (1.10), and making use of $\nabla \cdot \mathbf{D} = \rho$, we deduce that

$$\nabla \cdot \mathbf{J} = -\frac{\partial \varrho}{\partial t} \approx 0 \tag{1.37}$$

which is Kirchhoff's current law. It implies the conservation of current flow.

The above two laws, together with the voltage-current (V–I) relations of lumped elements such as resistors, capacitors, inductors, form the basic equations in circuit theory. Nonlinear elements such as diodes and transistors can be added to further enrich circuit physics. Notice that in the static or direct current (DC) limit, taking the divergence of (1.32) implies that $\nabla \cdot \mathbf{J} = 0$. However, the current, by Helmholtz decomposition, can be decomposed into curl-free (irrotational) and divergence-free (solenoidal) currents, namely, $\mathbf{J} = \mathbf{J}_{\text{irr}} + \mathbf{J}_{\text{sol}}$. It implies that $\nabla \cdot \mathbf{J}_{\text{irr}} = 0$ but $\mathbf{J}_{\text{irr}}$ need not be zero. The DC current $\mathbf{J}$ can be coupled to the magnetic field only, as in the super-conducting current loop case. A current can flow in a superconducting loop to generate a DC magnetic field without the need for an electric field to push the current along, viz., $\mathbf{E} = 0$.

On the other hand, the DC current $\mathbf{J}$ can be a conduction current. In this case, $\mathbf{J} = \sigma \mathbf{E}$ where σ is the conductivity of the medium in which the current is flowing. It couples the electric field to the magnetic field via (1.32). Since $\nabla \times \mathbf{E} = 0$, it follows that

$$\nabla \times \frac{\mathbf{J}}{\sigma} = 0. \tag{1.38}$$

By applying the above around a loop of resistors and using Ohm's law that $V = IR$, which follows from $\mathbf{E} = \sigma^{-1}\mathbf{J}$, we obtain

$$\sum_{i=1}^{N} I_i R_i = 0 \tag{1.39}$$

which is Kirchhoff's voltage law. Since by $\nabla \cdot \mathbf{J} = 0$, the current must be conserved at every node (Kirchhoff's current law), the above can be zero only if one or more of terms $I_i R_i$ is negative. One way that $I_i R_i$ can be negative is to have a negative resistor (see Figure 1.2). This can be understood by summing the above over a simple loop. In the negative resistor, the current flows in the opposite direction to the electric field. A battery can be modeled by a negative resistor. We can make the negative resistor dependent on current to model a voltage source, or make it dependent on voltage to model a current source.

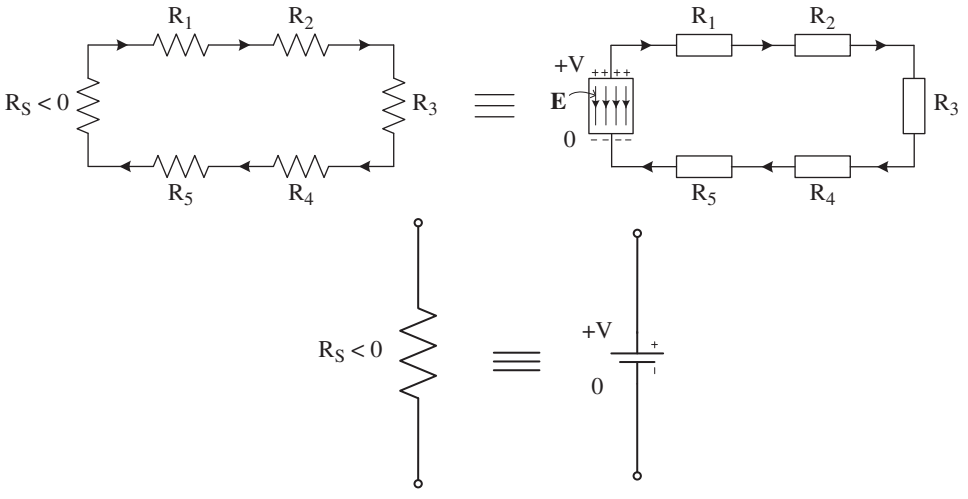

Figure 1.2 A negative resistor is needed in order for the total voltage drop in a loop to add up to zero. A battery can be modeled by a negative resistor.

For some devices such as an inductor, the $\frac{\partial \mathbf{B}}{\partial t}$ term can be made large by concentrating the magnetic field. In such a case, its V–I relation is

$$V = L\frac{\mathrm{d}I}{\mathrm{d}t} \tag{1.40}$$

which follows from Faraday's law that states $\nabla \times \mathbf{E} = -\partial \mathbf{B}/\partial t = -\mu \partial \mathbf{H}/\partial t$. By studying this law for a current loop, and using the fact that the magnetic field $\mathbf{H}$ can be related to the current I in the loop, one can derive (1.40).

From $\nabla \cdot \mathbf{J} = 0$, we derive Kirchoff's current law, which is

$$\sum_{i=1}^{N_j} I_i = 0. \tag{1.41}$$

Similarly, for a capacitor, its charge storage capability is enhanced and the right-hand side of (1.37) is non-negligible. In other words, the current is now coupled to the displacement current. Then its V–I relation is

$$I = C\frac{\mathrm{d}V}{\mathrm{d}t} \tag{1.42}$$

where the right-hand side is due to the displacement current $\mathbf{J}_D = \epsilon \partial \mathbf{E}/\partial t$.

From these circuit equations, one can also derive the telegrapher's equations, which describe the propagation of signals (or waves) on a telegraph line. These equations predate Maxwell's equations [88, 89]. By approximating a transmission line as a ladder of inductors and capacitors (see Figure 1.3), one can easily show that

$$\Delta V \approx -\Delta z L\frac{\mathrm{d}I}{\mathrm{d}t} \tag{1.43}$$

$$\Delta I \approx -\Delta z C\frac{\mathrm{d}V}{\mathrm{d}t}. \tag{1.44}$$

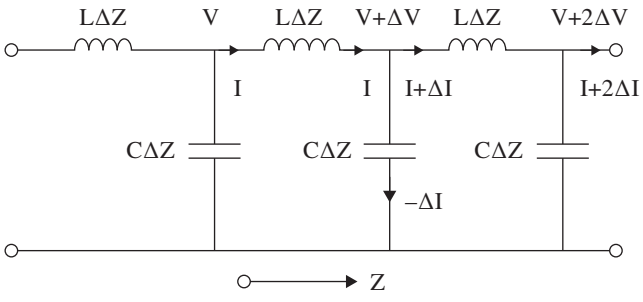

Figure 1.3 Two pieces of wire constituting a transmission line can be approximated with a ladder of inductors and capacitors.

In the limit when $\Delta z \to 0$, we obtain the telegrapher's equations:

$$\frac{\partial V}{\partial z} = -L\frac{\partial I}{\partial t} \tag{1.45}$$

and

$$\frac{\partial I}{\partial z} = -C\frac{\partial V}{\partial t}. \tag{1.46}$$

With this historical setting, it is inevitable that the missing displacement current in Ampere's law be discovered.

In general, in the low frequency regime, the electric field and the magnetic field are weakly coupled through space, except via energy storage devices such as capacitors and inductors where the electric field and magnetic field are enhanced, or via resistors where the current and electric field are coupled. It is through the lumped elements that the dynamic $(\partial/\partial t)$ terms or the whole bounty of Maxwell's equations are retained. This gives rise to the richness of circuit physics even though the circuits may be confined to a domain that is much smaller than wavelength.

Moreover, when the tiny objects are coupled to electronic devices such as transistors and diodes, the physics of circuits is richly endowed, and wonderful electronic technology has emerged which allows the devices to be packed in miniaturized dimensions. This is almost like the Alice in Wonderland story, where when one descends to nanometer dimensions, one can see a whole different world of physics in action. This is also reflected in the singularity of the electromagnetic dyadic Green's function [78], which is more elaborate than that of the elastodynamic dyadic Green's function. There was an avid interest in the dyadic Green's function singularity [76, 77].

The electromagnetic field is related to the electric current by

$$\mathbf{E}(\mathbf{r}) = \mathrm{i}\omega\mu \int_V \overline{\mathbf{G}}(\mathbf{r}, \mathbf{r}') \cdot \mathbf{J}(\mathbf{r}') \tag{1.47}$$

where

$$\overline{\mathbf{G}}(\mathbf{r}, \mathbf{r}') = \left(\bar{\mathbf{I}} g(\mathbf{r}, \mathbf{r}') + \frac{\nabla g(\mathbf{r}, \mathbf{r}') \nabla}{k_0^2} \right) \tag{1.48}$$

and

$$g(\mathbf{r}, \mathbf{r}') = \frac{\mathrm{e}^{\mathrm{i}k_0|\mathbf{r}-\mathbf{r}'|}}{4\pi|\mathbf{r}-\mathbf{r}'|}. \tag{1.49}$$

The second term is related to the electric field produced by charges in the system, which is very important in the near field to the source or when capacitance physics is important. The first term is related to the electric field produced by magnetic induction. However, if we take the curl of the above equation to obtain the magnetic field via $\mathbf{H} = \nabla \times \mathbf{E}/(\mathrm{i}\omega\mu)$, the second term disappears completely, yielding

$$\mathbf{H}(\mathbf{r}) = \nabla \times \int_V g(\mathbf{r}, \mathbf{r}')\mathbf{J}(\mathbf{r}). \tag{1.50}$$

Moreover, if the dyadic Green's function acts on a divergence-free current, only the first term, or the induction term, is important. Hence, the rich interplay between inductance physics and capacitance physics occurs in the dyadic Green's function.

In contrast, the elastodynamic Green's function is

$$\overline{\mathbf{G}}(\mathbf{r}, \mathbf{r}') = \frac{1}{\mu}\left(\bar{\mathbf{I}} + \frac{\nabla\nabla}{k_s^2}\right)\frac{\mathrm{e}^{\mathrm{i}k_s|\mathbf{r}-\mathbf{r}'|}}{4\pi|\mathbf{r}-\mathbf{r}'|} - \frac{1}{\lambda+2\mu}\frac{\nabla\nabla}{k_c^2}\frac{\mathrm{e}^{\mathrm{i}k_c|\mathbf{r}-\mathbf{r}'|}}{4\pi|\mathbf{r}-\mathbf{r}'|}. \tag{1.51}$$

It can be shown that the leading singularities produced by the $\nabla\nabla$ term will cancel each other, making its physics close to the source point quite different from that of electromagnetics.

1.6.2 Wave Physics

When the frequency is higher, the **E** and **H** fields are tightly coupled in space. As a consequence, oscillatory behavior through space is possible. The oscillation comes about due to the exchange of stored energies in the form of electric field and magnetic field. In the early days, this was possible in a telegraph line where inductors and capacitors coexist to enhance the magnetic field and electric field.

The wave physics regime is important for radio frequency (RF) and microwave when the wavelength is on the order of the dimension of the objects. In the past, the optical wavelength was usually much smaller than the size of the objects. However, wave physics has recently been important in optics and nano-optics due to the advent of nanofabrication. It is now possible to fabricate objects on the order of optical wavelength or smaller [90].

The wave physics regime is the regime in which the solutions to Maxwell's equations are the most difficult. The vector nature and the wave nature of the electromagnetic field have to be accounted for. It is also in this regime that computational electromagnetics plays an important role in seeking viable solutions to Maxwell's equations.

The physics of waves is quite different from the physics of static fields. Waves can be used to send information over a long distance, as in communication, remote sensing, and geophysical probing. However, a static field cannot be used to send information over a long distance [87]. Hence, when we look at the moon through an optical telescope, we can observe the fine details on the moon's surface. The gravitational field of the moon is a Coulombic or Laplacian field. If we observe the moon through its gravitational field, a big blob with no detail is observed [87, 91].

It turns out that the presence of $\epsilon\partial\mathbf{E}/\partial t$ implies the existence of "capacitance" in space, and the presence of $\mu\partial\mathbf{H}/\partial t$ implies the existence of "inductance" in space. Due to the "smallness" of this phenomenon (because ϵ and μ are small numbers), the velocity of the wave is tremendous, given by $c = 1/\sqrt{\mu\epsilon}$. In other words, the coupling becomes

significant only when **E** and **H** are varying rapidly with respect to time. For instance, for the same wavelength, electromagnetic wave oscillates much more rapidly compared to an acoustic wave.

The coupling allows the existence of electromagnetic waves even in vacuum. In wave physics, both **E** and **H** are equally important since stored energies are exchanged between them. When this physics exists, the yardstick is the wavelength λ of the electromagnetic wave at the pertinent frequency, viz., $\lambda = c/f$ where f is the frequency of the field. When electromagnetic field interacts with objects that are on the order of wavelength, wave physics is important. On the other hand, when electromagnetic field interacts with objects that are much smaller than the wavelength, then circuit physics predominates.

The aforementioned fact can be appreciated by eye-balling the scalar wave equation

$$\nabla^2\phi - \mu\epsilon\frac{\partial^2\phi}{\partial t^2} = 0 \tag{1.52}$$

which is valid for a Cartesian component of the electromagnetic field. When the field is time harmonic, the above simplifies to

$$\nabla^2\phi + k^2\phi = 0 \tag{1.53}$$

where $k = \omega^2\mu\epsilon$. When an object is small, and is of length scale L, such that $kL \ll 1$, then the field has to vary rapidly on the length scale L around the object in order to satisfy the boundary condition on it. We can do a coordinate stretching transformation by letting $x = Lx'$, $y = Ly'$, and $z = Lz'$ [92]. In other words, x', y', and z' are of $\mathcal{O}(1)$ when x, y, and z are of $\mathcal{O}(L)$. Consequently, $\nabla^2 = \nabla'^2/L^2$ where ∇' is of $\mathcal{O}(1)$. For time-harmonic field, the above becomes

$$\nabla'^2\phi + k^2L^2\phi = 0. \tag{1.54}$$

Therefore, if $k^2L^2 \ll 1$, then the above equation becomes

$$\nabla'^2\phi = 0 \tag{1.55}$$

which is just the Laplace equation describing the static (circuit) physics of electromagnetics. On the other hand, if $k^2L^2 \approx 1$, then the full wave equation has to be solved [93].

1.6.3 Ray Physics

When the frequency becomes exceedingly high, electromagnetic physics morphs into another regime, making electromagnetic waves behave like particles. This is the ray physics regime. In this regime, since the wavelength is very short, most electromagnetic fields can be locally approximated by a plane wave. A plane wave can be thought of as a ray. A ray bounces off surfaces and penetrates media very much like a particle. Surprisingly, it is in this regime that the quantization of an electromagnetic field is important [94], and that electromagnetic energy propagating through space should be thought of as packets of energy [95–99]. In the ray physics regime, solutions are amenable to asymptotic approximations [100–105].

In the early days, optics was studied primarily with scalar wave equations: the polarization effect of light was de-emphasized in those studies [106]. It was because light, by its nature, is randomly polarized, hence washing out the importance of the vector

nature of light. Due to the short wavelength of light, the concept of coherence comes into play [107, 108]. A light may not be able to maintain the purity of its polarization over long distances due to the short wavelength nature of light and the environmental perturbation of the wave.

Ray Equations

In the extremely-high frequency limit, the wave equation can be further simplified. In this regime, the wave that propagates through the medium is locally a plane wave. In other words, the magnitude variation of the field in one direction is much more rapid than the phase variation of the field in other directions. The dominant variation of the field is in the phase. Therefore, we let [76]

$$\phi(\mathbf{r}) = A\mathrm{e}^{\mathrm{i}\omega\tau(\mathbf{r})} \tag{1.56}$$

where A is a constant. Substituting the above into (1.53), we have

$$\nabla\tau(\mathbf{r}) = \mathrm{i}\omega\phi(\mathbf{r})\nabla\tau(\mathbf{r}) \tag{1.57}$$

and

$$\nabla\cdot\nabla\phi(\mathbf{r}) = \left\{\mathrm{i}\omega\nabla^2\tau(\mathbf{r}) - \omega^2\left[\nabla\tau(\mathbf{r})\right]^2\right\}\phi(\mathbf{r}). \tag{1.58}$$

Using the above in (1.53), we have

$$\mathrm{i}\omega\nabla^2\tau(\mathbf{r}) - \omega^2(\nabla\tau)^2 + k^2(\mathbf{r}) = 0. \tag{1.59}$$

At this point, (1.59) is still exact but nonlinear. However, we can solve (1.59) perturbatively by letting $\omega\to\infty$. In this limit, we let

$$\tau(\mathbf{r}) = \tau_0(\mathbf{r}) + \omega^{-1}\tau_1(\mathbf{r}) + \cdots, \quad \omega\to\infty. \tag{1.60}$$

If the series is used in (1.59), the ω^2 terms in the equation balance each other, yielding a leading order approximation that

$$\left[\omega\nabla\psi_0(\mathbf{r})\right]^2 = k^2(\mathbf{r}) = \omega^2 s^2(\mathbf{r}) \tag{1.61}$$

where $s = k/\omega = \sqrt{\mu\epsilon}$ is the slowness of the wave. The above equation can be written as

$$\nabla\psi_0(\mathbf{r}) = \pm s(\mathbf{r})\hat{s} \tag{1.62}$$

where $\hat{s}$ is an arbitrary unit vector. The above equation can be integrated to yield the ray passing through a point. This is known as the eikonal equation. Along the ray direction or in one dimension, it can be written as

$$\tau_0'(z) = \pm s(z). \tag{1.63}$$

It can be easily integrated to yield

$$\tau_0(z) = \pm\int_{z_0}^{z}\mathrm{d}z'\ s(z') + C_0. \tag{1.64}$$

By collecting the first order terms, we have

$$\mathrm{i}\omega\nabla\cdot\nabla\tau_0(\mathbf{r}) - 2\omega\nabla\tau_0(\mathbf{r})\cdot\nabla\tau_1(\mathbf{r}) = 0. \tag{1.65}$$

The above is the transport equation. In one dimension, or along the ray direction, it can be written as

$$i\tau_0''(z) - 2\tau_0'(z)\tau_1'(z) = 0. \tag{1.66}$$

The above can be solved to yield

$$\tau_1(z) = \frac{\mathrm{i}}{2}\ln\tau_0'(z) + C_1 = \frac{\mathrm{i}}{2}\ln s(z) + C_{1\pm}. \tag{1.67}$$

Consequently, along the ray direction, or in one dimension, the solution to the wave equation in a slowly varying inhomogeneous medium is

$$\phi(z) \sim \frac{A_+}{\sqrt{s}}\exp\left[\mathrm{i}\omega\int_{z_0}^{z} s(z')\,dz'\right] + \frac{A_-}{\sqrt{s}}\exp\left[-\mathrm{i}\omega\int_{z_0}^{z} s(z')\,\mathrm{d}z'\right]. \tag{1.68}$$

The eikonal equation contributes to describing the phase variation of the field, while the transport equation contributes to the $1/\sqrt{s}$ factor, which is important for energy conservation.

Importance of Polarization Charges

When a light impinges on a dielectric interface, the Fresnel reflection coefficients for TE (transverse electric) and TM (transverse magnetic) fields are quite different. This is because for TM fields, a component of electric field normal to the dielectric interface exists and gives rise to polarization charges. However, when the medium is slowly varying, and the frequency is high, these polarization charges are less important [76]. The inhomogeneity at optical frequencies usually is with the dielectric permittivity ϵ and we can assume that the permeability μ is a constant. We start with the vector wave equation for magnetic field $\mathbf{H}$, or

$$\nabla\times\epsilon^{-1}\nabla\times\mathbf{H} - \omega^2\mu\mathbf{H} = 0 \tag{1.69}$$

where a time-harmonic field is assumed with frequency ω. Using the vector identity, we rewrite the above as

$$\epsilon^{-1}\nabla\times\nabla\times\mathbf{H} + (\nabla\epsilon^{-1})\times\nabla\times\mathbf{H} - \omega^2\mu\mathbf{H} = 0. \tag{1.70}$$

If the field is locally a plane wave, then $\nabla = \mathrm{i}\mathbf{k}$. If the permittivity is slowly varying, then $\nabla\epsilon^{-1}$ is small. Only the first term and the last term are needed to balance the equation when $\omega\to\infty$. Hence, the vector wave equation for high frequency and slowly varying inhomogeneity simplifies to

$$\nabla\times\nabla\times\mathbf{H} - \omega^2\mu\epsilon\mathbf{H} = 0. \tag{1.71}$$

Again, the above reduces to the scalar Helmholtz wave equation

$$\nabla^2\phi + k^2\phi = 0 \tag{1.72}$$

where $k^2 = \omega^2\mu\epsilon$.

1.6.4 Plasmonic Resonance

Even though we have attributed the resonance/oscillation behavior of an electromagnetic field to energy exchange between $\mathbf{E}$ and $\mathbf{H}$ fields, there is an emerging technology that relies on another physics for resonances; this is the field of plasmonic resonances. In this system, the resonance is due to the exchange between the stored energy in the

electric field and the kinetic energy of the electrons. In plasma, free electrons abound such as in the ionosphere. In certain metal, such as gold and silver, the sea of electrons in the metal behaves like plasma. It can acquire enough kinetic energy at high-enough frequencies (optical frequencies) to exchange energy with that stored in the electric field, giving rise to resonance behavior. In this regime, the permittivity of the material medium is negative [74, 109], as shall be shown below.

One can easily show by Newton's law that the acceleration of the electron due to an applied electric field is given by

$$m_e\ddot{x} = qE \tag{1.73}$$

where x is the displacement of the electron from the mean, m_e is the effective mass of the electron[7], q is the charge of the electron, and E is the applied electric field. By assuming a time-harmonic field, so that $\ddot{x} = -\omega^2 x$, one deduces that

$$x = -\frac{qE}{m_e\omega^2}. \tag{1.74}$$

Since the polarization density $P = n_e q x$, where n_e is the electron density, one deduces that

$$\mathbf{P} = -\frac{n_e q^2}{m_e\omega^2}\mathbf{E}. \tag{1.75}$$

Hence, using the fact that $\mathbf{D} = \epsilon_0\mathbf{E} + \mathbf{P}$, one gets

$$\epsilon = \epsilon_0\left(1 - \frac{\omega_p}{\omega^2}\right) \tag{1.76}$$

where $\omega_p = \sqrt{n_e q^2/(m_e\epsilon_0)}$. In the above, the plasma medium becomes ϵ-zero material when $\omega = \omega_p$.

Simple Drude-Lorentz-Sommerfeld Model

This is often just called the Drude model. Since Lorentz and Sommerfeld also made significant contributions to this model, we will call it the Drude-Lorentz-Sommerfeld model. To begin, we have

$$m\ddot{x} + \frac{m}{\tau}\dot{x} = qE \tag{1.77}$$

$$\dot{p} + \frac{p}{\tau} = qE \tag{1.78}$$

$$-\mathrm{i}\omega p + \frac{p}{\tau} = qE \tag{1.79}$$

where $p = m\dot{x}$ and $I \sim p$. Using the fact that the kinetic energy (KE) density of the electrons is

$$\mathrm{KE} = \frac{1}{2}n_e m_e(\dot{x})^2 = \frac{1}{2}n_e m_e\omega^2 x^2 \tag{1.80}$$

7 The plasma effect is also observed in some metallic nano-particles. In this case, the electron moves in a lattice with an effective mass [98, 99].

and that the displacement x is given by (1.74), one can show that at $\omega = \omega_p$, the kinetic energy density is exactly equal to the electric field energy density [109], i.e.

$$\mathrm{KE} = \frac{1}{2}\frac{\partial \omega \epsilon E^2}{\partial \omega}. \tag{1.81}$$

Hence, at the plasma frequency, the material becomes ϵ-zero, the velocity of the wave is infinite, and all the electrons are in a time-harmonic motion but in phase with each other. In other words, the particles move in unison and oscillate as a block; the medium is in bulk plasma resonance.

When the frequency is below the plasma frequency, the material is ϵ-negative, and the wave is evanescent in the medium. This is because the electrons are light and agile; they can shield the electromagnetic field by annulling its effect to induce positive polarization current in a medium. However, above the plasma frequency, the inertia of the electrons prevents them from following the rapidly-varying electric field; they lose their shielding effect, and the electromagnetic field penetrates the plasma medium.

Surface Plasmons

When the plasma medium is ϵ-negative, the kinetic energy storage is dominant. This kinetic energy can be exchanged with the stored electric field energy. At an air-plasma interface, when the electric field has a normal component to the interface, a strong electric field is produced. The stored energy in the electric field of the charges can be exchanged with the stored kinetic energy of the electrons, yielding surface plasmon resonance. A surface plasmon mode can propagate on an interface with this energy exchange.

The guidance condition for the surface plasmon can be derived by finding the pole of the Fresnel reflection coefficient

$$R^{TM} = \frac{\epsilon_1 k_{0z} - \epsilon_0 k_{1z}}{\epsilon_1 k_{0z} + \epsilon_0 k_{1z}} \tag{1.82}$$

where $k_{iz} = \sqrt{k_i^2 - k_x^2}$, $(i = 0, 1)$ and k_x is the wavenumber along the interface, and k_{iz} is the wavenumber normal to it. The pole of the reflection coefficient is obtained by solving the equation

$$\epsilon_1 k_{0z} = -\epsilon_0 k_{1z}. \tag{1.83}$$

Assuming that the medium is non-magnetic material, solving the above yields the guidance condition that

$$\epsilon_1 k_{0z} = -\epsilon_0 k_{1z} \tag{1.84}$$

which further gives

$$k_x = \omega \sqrt{\frac{\mu_0 \epsilon_0 \epsilon_1}{\epsilon_0 + \epsilon_1}}. \tag{1.85}$$

This is the same as the condition for the Brewster angle, except that they are on different Riemann sheets of the complex plane [76]. This is the rare case where an electromagnetic wave can be guided by a single interface, whereas in elastic waves, single interface guided waves exist as Rayleigh waves [110], and Stoneley waves [111].

Since the stored energy of electric field need not exchange with the stored energy of magnetic field, plasmonic resonance can occur in nanoparticles even when they are

much smaller than the wavelength. When an ϵ-negative particle is immersed in an electric field, much electric field energy is stored outside the particle. Hence, resonance by exchanging its kinetic energy with the stored electric field energy can occur. The resonance occurs despite the fact that the particle is much smaller than a wavelength.

If a dielectric spherical particle with a radius a is immersed in a long wavelength electric field, it has a dipole moment given by

$$p = 4\pi\epsilon_0 a^3 E_0 \frac{\epsilon_s - \epsilon_0}{\epsilon_s + 2\epsilon_0} \tag{1.86}$$

where ϵ_s is the permittivity of the particle. For an ϵ-negative material, the denominator of the above can become zero, giving rise to plasmonic resonance of the nanoparticle. This is observed in gold and silver nanoparticles immersed in the optical field, where the particles can be in tens of nanometers, while the wavelength of the optical field is in hundreds of nanometers [90, 112, 113].

1.7 The Age of Closed Form Solutions

Maxwell's equations have extremely high predictive power compared to many other physical laws. The range of length scales and the range of frequencies over which they are valid make these equations become the bedrock of many technologies. Moreover, since many electromagnetic phenomena are linear, Maxwell's equations are relatively simple to solve compared to many other physics equations. By comparison, fluid equations are nonlinear, and often break into turbulence when loss or viscosity is considered [114].

Hence, there has been great interest in finding closed form solutions of Maxwell's equations. These closed form solutions offer researchers physical insights into the interactions of electromagnetic fields with simple shape objects [115–118].

The derivation of closed form solutions was preceded by mathematical knowledge in the field of fluids and acoustics that predated electromagnetics. In fluids, non-turbulent flows are amenable to closed form solutions, such as high viscosity flow (low Reynolds number) and Helmholtz flow. In fluids, the onset of turbulence is due to the existence of viscosity. In an ideal fluid with no viscosity, called inviscid fluid, turbulence cannot occur, and closed form solutions can be found [114]. Also, the acoustic wave equation, which is scalar and linear, is also amenable to closed form solutions. Many special functions and mathematical knowledge of ordinary differential equations were derived before Maxwell's equations [116]. Hence, they helped set the stage for deriving closed form solutions for electromagnetics.

1.7.1 Separable Coordinate Systems

The early closed form solutions were obtained by objects in separable coordinate systems for which the separation-of-variables technique applies. For example, scattering solution of a sphere can be obtained in the spherical coordinate system. Solutions to Maxwell's equations are derivable from solutions to the scalar wave equation. The solutions to the vector wave equation in spherical coordinates can be expressed by the derivatives of two scalar Debye potentials. The Debye potentials are in turn solutions to the scalar wave equation in spherical coordinates [113, 119].

The scalar wave equation in spherical coordinates can be expressed by separation of variables into solutions of the spherical Bessel equation, the Legendre equation, and cylindrical harmonics. These functions together are called spherical harmonics. When the solution is expressed in terms of a summation of series involving spherical harmonics, it is called the Mie-series solution [113].

When the sphere size is small compared to wavelength, the approximate solution, the Rayleigh scattering solution, can be obtained [120]. It provides insight that a wave experiences more scattering when the frequency increases, hence, explaining why the sky is blue and the sunset is red. When the scatterer is comparable to wavelength, the solution is computed via the Mie scattering solution. A typical Mie-series solution has Debye potentials that are of the form

$$\Phi_{\text{sca}}(\mathbf{r}) = \sum_{n=0}^{\infty} \sum_{m=-n}^{n} a_{n,m} h_n^{(1)}(kr) P_n^m(\cos\theta) \mathrm{e}^{\mathrm{i}m\phi} \tag{1.87}$$

where $a_{n,m}$ is selected to match boundary conditions. The above solution is given in the frequency domain, or the Fourier transform space where the time dependence is $\exp(-\mathrm{i}\omega t)$. The spherical Hankel function of the first kind, $h_n^{(1)}(kr)$, is chosen to correspond to an outgoing wave at infinity, $P_n^m(x)$ is a Legendre's polynomial, and r, θ, and ϕ are variables in the spherical coordinate system. For an incident wave, one would replace the spherical Hankel function above with spherical Bessel function $j_n(kr)$ [121]. These special functions are often discussed in standard textbooks in electromagnetics [74, 122–126].

The scattering solution of a cylinder can be obtained in the cylindrical coordinate system. Again, the solution to the vector wave equation in cylindrical coordinates can be derived from two scalar potentials representing the transverse[8] electric and transverse magnetic waves. The solution is expressed in terms of the cylindrical Hankel function $H_n^{(1)}(k\rho)$, and Bessel function $J_n(k\rho)$ and cylindrical harmonics $\mathrm{e}^{\mathrm{i}n\phi}$. Other closed form solutions are possible by similar reduction to scalar wave equations, when such solutions are available, e.g., in spherical coordinates, elliptical coordinates, etc.

In addition to the scattering problems, the inside-out solutions of cavity resonances in spherical coordinates, waveguide solutions of a cylinder can be derived by similar mathematical techniques. The above solutions can also be generalized to layered media.

A quirky problem is the case of the cavity resonances of a cuboid formed by perfect electric conducting wall or perfect magnetic conducting wall. While the inside-out problem is separable and can be solved in closed form, the outside-in scattering problem of a cuboid has no closed-form solution. The same case applies to a rectangular waveguide that has a closed form solution, while the outside-in problem has no closed form solution.

1.7.2 Integral Transform Solution

Other important problems with closed form solutions using integral transform techniques include the solutions of a point source on top of layered media, which were used to explain the propagation of radio wave over the layered earth. This problem was first solved by Sommerfeld [127]. The field due to a point source can be expanded in terms

8 Transverse here implies transverse to the axial direction of the cylinder.

of plane waves, which can be easily propagated through the planar layered media. An important mathematical identity to this end is the Weyl identity [128]

$$\frac{e^{ik_0 r}}{r} = \frac{i}{2\pi}\int\int_{-\infty}^{\infty} dk_x dk_y \frac{e^{ik_x x + ik_y y + ik_z|z|}}{k_z} \tag{1.88}$$

where $k_x^2 + k_y^2 + k_z^2 = k_0^2$, or $k_z = (k_0^2 - k_x^2 - k_y^2)^{1/2}$. It expands the spherical wave due to a point source in terms of plane waves emanating from the $z = 0$ plane. Both propagating and evanescent waves are included in the above expansion. The double integral above can be reduced to a single integral using the integral representation for Bessel function, yielding the Sommerfeld identities [76]

$$\frac{e^{ik_0 r}}{r} = i\int_0^{\infty} dk_\rho \frac{k_\rho}{k_z} J_0(k_\rho \rho) e^{ik_z|z|} = \frac{i}{2}\int_{-\infty}^{\infty} dk_\rho \frac{k_\rho}{k_z} H_0^{(1)}(k_\rho \rho) e^{ik_z|z|} \tag{1.89}$$

where $\rho = \sqrt{x^2 + y^2}$ and $k_\rho = \sqrt{k_x^2 + k_y^2}$. The above identity was first used by Sommerfeld to solve for the solution of a point source over a half-space. The transform integrals thus obtained are known as Sommerfeld integrals. Various kinds of potential were defined to solve this problem. It was later generalized to layered media using the Kong formulation with just E_z and H_z components of the electromagnetic fields [129].

Similarly, when a point source field is expanded in terms of cylindrical harmonics, or spherical harmonics, they can be propagated through layered cylinders or layered spheres.

Another problem of great importance with a closed form solution is the Sommerfeld half-plane problem [130–132]. While this problem is deceptively simple, it resists a closed form solution unless the Fourier transform technique is applied. When the Fourier transform technique is applied with the Wiener-Hopf technique [133], a closed form solution in terms of an integral is obtained[9]. The Wiener-Hopf technique is used to deconvolve a function that has semi-infinite support and the convolved result is known only over semi-infinite support. A typical problem of this type can be written as

$$\Phi_s(x) = g(x) * j(x) = -\Phi_i(x), \quad x \geq 0, \tag{1.90}$$

$$j(x) = 0, \quad x < 0 \tag{1.91}$$

where $*$ implies a convolution. In the above, $\Phi_i(x)$, which represents the incident field, is known for $x \geq 0$ while $j(x)$ is unknown to be solved with a support for $x \geq 0$. The above integral equation is a special class of the integral equation that can be deconvolved using the Wiener-Hopf technique, which seems like a lost art. The final solution to the Sommerfeld half-plane problem can be expressed in terms of the Fourier integral as

$$\Phi_s(x, y) = -\frac{e_0 (k + k_x^i)^{1/2}}{2\pi i}\int_{-\infty}^{\infty} \frac{e^{i(k_x x + k_y y)}}{(k_x - k_x^i)(k_x + k)^{1/2}} dk_x \tag{1.92}$$

where the incident field is $e_0 e^{i(k_x^i x - k_y^i y)}$, $k = \omega/c$, and $k_x^2 + k_y^2 = k^2$.

When asymptotic expansion using the contour deformation technique and the method of steepest descent is performed on the Fourier integral, the physics of the

9 Sommerfeld obtained his own solution by inspection, which is quite different from the Wiener-Hopf technique, but his method cannot be generalized.

scattering of a plane wave by a half plane can be elucidated. One can clearly see the contribution of edge diffraction, specular reflection, and the existence of reflection boundary and the shadow boundary in the above solution. This problem forms the canonical solution that explains the high-frequency scattering physics of a half plane.

1.8 The Age of Approximations

Many closed form solutions are in terms of integral transforms, or a summation of series. For instance, the solution of the point source on top of layered media is in terms of the Sommerfeld integral, which offers little physical insight into the problem. However, when the frequency is high, asymptotic approximations can be derived so as to offer more physical insight. This was done for the Sommerfeld half-plane problem, but it can also be done for the Sommerfeld integrals.

1.8.1 Asymptotic Expansions

While the asymptotic expansion for the half-plane problem could be easily obtained due to the simplicity of the integrand, it was more difficult to obtain the asymptotic solution to the Sommerfeld integrals for layered media. This was due to the presence of poles corresponding to guided waves and leaky waves in the integrand. The presence of branch cuts can be related to lateral waves, or surface waves [76, 134, 135]. A typical Sommerfeld integral is

$$E_{1z} = \frac{-I\ell}{8\pi\omega\epsilon_1}\int_{-\infty}^{\infty} \mathrm{d}k_\rho \frac{k_\rho^3}{k_{1z}} H_0^{(1)}(k_\rho\rho)\left[\mathrm{e}^{\mathrm{i}k_{1z}|z|} + \tilde{R}_{12}^{TM}\mathrm{e}^{\mathrm{i}k_{1z}z+2\mathrm{i}k_{1z}d_1}\right] \tag{1.93}$$

where $k_{1z} = (k_1^2 - k_\rho^2)^{\frac{1}{2}}$, and $k_1^2 = \omega^2\mu_1\epsilon_1$ which is the wave number in Region 1. In the above, $\tilde{R}_{12}^{TM}$ is the generalized reflection coefficient given by

$$\tilde{R}_{i,i+1} = R_{i,i+1} + \frac{T_{i,i+1}\tilde{R}_{i+1,i+2}\ T_{i+1,i}\mathrm{e}^{2\mathrm{i}k_{i+1,z}(d_{i+1}-d_i)}}{1 - R_{i+1,i}\tilde{R}_{i+1,i+2}\mathrm{e}^{2\mathrm{i}k_{i+1,z}(d_{i+1}-d_i)}} \tag{1.94}$$

where $R_{ij} = \frac{p_j k_{iz} - p_i k_{jz}}{p_j k_{iz} - p_i k_{jz}}$, $T_{ij} = 1 + R_{ij}$, $p_i = \epsilon_i$ for TM waves and $p_i = \mu_i$ for TE waves. Furthermore, $k_{iz} = \sqrt{k_i^2 - k_\rho^2}$. It appears that there is a branch point at $k_\rho = k_i$ for each of the layered media, but it can be proved that the branch point exists only for the first and the last layer [76, 135, 136]. It is a beautiful harmony between physics and mathematics as the branch points correspond to space waves that can only exist in the first and the last regions.

One important lesson to learn from the exercise of deriving asymptotic expansions for spectral integrals that follow from the Sommerfeld problems is that the approximations are associated with critical points on the complex plane: poles, branch points, saddle point (stationary phase point) [76, 137]. When the far field can be approximated by a simple critical point, simple ray-optics physics follows. However, when the critical points start to merge on the complex plane, the approximation of the spectral integral with simple functions becomes difficult and special functions have to be used [76, 137]. This usually corresponds to observation points near the shadow boundary, reflection

boundary, or caustics, where simple ray optics does not work. Uniform asymptotic approximations have to be designed in the vicinity of such boundaries [101–103, 138]. Since integrals are amenable to asymptotic expansions, even when a series solution, such as a Mie-series solution, is obtained, attempts will be made to express it into an integral by Watson's transformation to facilitate its asymptotic approximations [135, 139–141]. Watson's transformation elucidates the physics of the creeping waves, as well as the radiation from the lit-shadow boundary, which can be corrected with the incremental length diffraction coefficient [142].

Approximate asymptotic solutions offer physical insight not available with many closed form solutions. They have also motivated other asymptotic-based approximate solutions to many problems [100]. This was because the cases of solvable geometries were quickly exhausted by researchers. However, there was still a quest for solutions of more complex geometries to increase the predictive power of theoretical modeling of physical problems using mathematics. Nevertheless, many problems have no closed form solutions and are amenable only to approximate solutions.

1.8.2 Matched Asymptotic Expansions

A notable approximate method is the method of matched asymptotic expansions [92]. It was used in fluids to solve many boundary layer problems, involving the problems of different length scales. For instance, when fluid flows near a surface, the fluid velocity varies rapidly normal to the surface compared to the tangential direction. For this type of problem, it can be divided into an inner solution and an outer solution. Coordinate stretching technique is used to emphasize the variation of the fluid normal to the surface when one seeks the inner solution. For the outer solution, the inner solution provides an effective "boundary condition" for it [143].

One can view the Rayleigh scattering solution of a small particle [120] as a simple matched asymptotic solution. When one is close to the particle, which is much smaller than a wavelength, electrostatic physics prevails. The field is rapidly varying in the vicinity of the particle, but an electrostatic solution is sufficient to capture the interaction of the field with the particle. Hence, one can solve a static problem in the vicinity of the particle, to derive the induced dipole moment by a field. But far away from the particle, the radiation field of the particle is important to produce wave physics results. Hence, one can match the far field solution to obtain the dipole scattering strength [74].

A place where matched asymptotics is useful is in the WKB (Wentzel, Kramers, Brillouin) [144–146] solution in an inhomogeneous profile by assuming that the profile is smooth, and that the frequency is high [76]. If the profile is becoming optically less dense (decreasing refractive index profile) as the wave penetrates into the medium, eventually, at one point called the turning point, the wave will be refracted back and totally reflected by total internal reflection (Figure 1.4). At the region before the turning point, it can be described by ray optics. At the region beyond the turning point, the wave can be described by the evanescent wave of total internal reflection. However, at the turning point region, only a special function can be used to describe the field. In this case, it is the Airy function [121]. Solutions can be written down in each region, and asymptotic matching is used to find the coefficients of the solution in each region. The turning point region is where ray optics breaks down, because of the convergence of the rays into a tiny region. This is a caustic region [76].

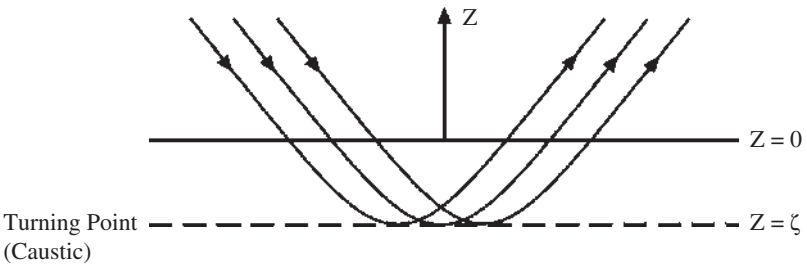

Figure 1.4 In an inhomogeneous profile with decreasing index, the ray will be continuously refracted until it turns around at the turning point.

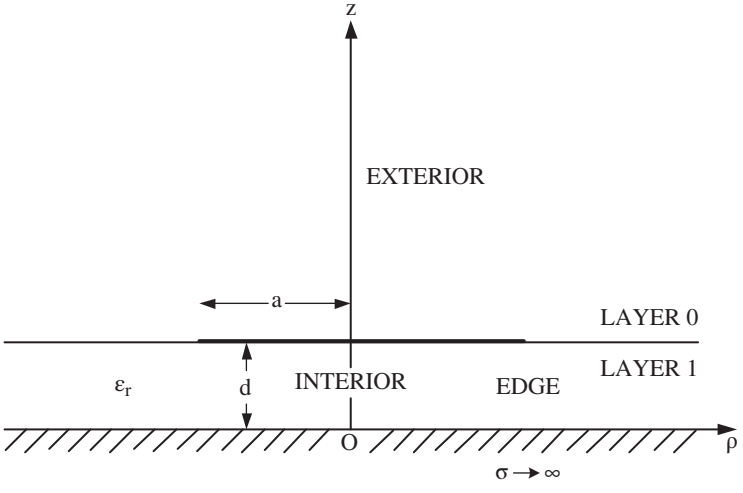

Figure 1.5 Matched asymptotics can be used to find the solution of the capacitance between two disks. The solution is divided into edge solution near the edge, inner solution between the plate, and outer solution outside the two plates.

Another place where matched asymptotics has been used is to find the capacitance of the two circular parallel plates. When the separation between the two plates is small, the solution near the edge, or the edge solution, is rapidly varying, and is quite different from the solution in the region between the two parallel plates, or the inner solution, and outside the plates, or the outer solution (see Figure 1.5). The solution near the edge can be obtained by coordinate stretching when $\delta = d/a$ is small. After coordinate stretching, the edge solution to leading order is similar to the solution of a straight edge which can be solved by conformal mapping or the Wiener-Hopf technique [133]. The outer solution can be easily sought. The first approximate solution to such a problem was obtained by Kirchhoff [147] heuristically, but was correct asymptotically:

$$C \sim \frac{\pi\epsilon_0 a^2}{2d} + \epsilon_0 a \log\left(\frac{a}{d}\right) + \epsilon_0 a\,(\log 8\pi - 1), \quad \frac{d}{a} \to 0 \tag{1.95}$$

where $2d$ is the separation of the disks, and a is their radii. It was generalized to the case of two disks separated by a dielectric slab by Chew and Kong [148]. The formula in this

case is

$$C \sim \frac{\pi \epsilon_r \epsilon_0 a^2}{2d} + \epsilon_0 a \log\left(\frac{a}{d}\right) + \epsilon_0 a \left[\log 8 - 1 - 2\epsilon_r \sum_{n=1}^{\infty} \left(\frac{1-\epsilon_r}{1+\epsilon_r}\right)^n \log n + (\epsilon_r - 1)\log 2 + \epsilon_r \log \pi\right], \quad \frac{d}{a} \to 0. \tag{1.96}$$

The Wiener-Hopf method was used to find the edge solution in the above problem. The above reduces to Kirchhoff's formula when $\epsilon_r = 1$.

Leppington and Levine [149] obtained a correction to Kirchhoff's formula, and Shaw [150] further refined the correction given by

$$C \sim \frac{\pi \epsilon_0 a^2}{2d} + \epsilon_0 a \log\left(\frac{a}{d}\right) + \epsilon_0 a (\log 8\pi - 1) + \frac{\epsilon_0 d}{2\pi}\left[\log\left(\frac{d}{8\pi a}\right)\right]^2, \quad \frac{d}{a} \to 0. \tag{1.97}$$

The conformal mapping technique [151] was used to find the edge solution since a dielectric slab was absent.

A formula to the same order of approximation as Shaw's formula has also been given by Chew and Kong in [152] when a dielectric slab is present.

$$C \sim \frac{\pi \epsilon_r \epsilon_0 a^2}{2d} + \epsilon_0 a \log\left(\frac{a}{d}\right) + \epsilon_0 a (\log 8\pi - 2 + A) + \frac{\epsilon_0 d}{2\pi}\left\{\left[\log\left(\frac{8a}{d}\right) + A - 1\right]^2 - 2\right\}, \quad \frac{d}{a} \to 0 \tag{1.98}$$

where

$$A = -2\epsilon_r \sum_{n=1}^{\infty} \left(\frac{1-\epsilon_r}{1+\epsilon_r}\right)^n \log n + (\epsilon_r - 1)\log 2 + \epsilon_r \log \pi + 1. \tag{1.99}$$

When $\epsilon_r = 1$, the above reproduces Shaw's formula but with a correction term to her formula.

A similar formula for capacitance per unit length of two parallel strips, with width w separated by a dielectric slab of thickness d, has also been derived in [148] with an improvement in [153]. It is

$$C \sim \frac{\epsilon_r \epsilon_0 w}{2d} + \frac{\epsilon_0}{\pi}\left[\log\left(\frac{w}{d}\right) + A\right] + \frac{2\epsilon_0 d}{w\pi^2 \epsilon_r}\left[\log\left(\frac{w}{d}\right) + A - \frac{1}{2}\right], \quad \frac{w}{b} \to 0. \tag{1.100}$$

When $\epsilon_r = 1$, the first two terms reduce to the result of Michell, Bromwich, and Love [154–156]. The higher order correction to the above is an improvement over Shaw's formula [150].

The matched asymptotic technique has also been generalized to find the resonance frequencies and guidance condition of a microstrip line where wave physics is included in the outer solution while static physics is involved in the edge solution [157, 158]. The matched asymptotic expansion method has also been applied to understand the interaction of electromagnetic field with electrical double layer in electrochemistry.

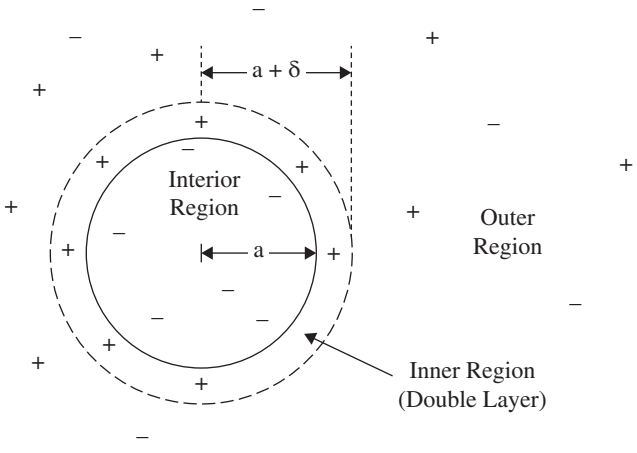

Figure 1.6 The occurrence of a thin double layer outside a charged particle makes the problem suitable for matched asymptotics analysis [10].

It helps explain the dielectric dispersion and electrophoretic properties of colloidal suspension of particles in ionic solutions [10, 159–161]. For instance, when a positively charged polystyrene particle is immersed in an ionic solution, it acquires negative counter-ion charges on its surface, forming a thin double layer. The thin double layer, where the ionic density varies rapidly, is the inner solution of a matched asymptotic analysis (see Figure 1.6).

1.8.3 Ansatz-Based Approximations

When a scatterer is very complex, a high frequency scattering solution can be motivated by physical insight derived from asymptotic approximations of closed form solutions. The approximate solutions can be derived based on an ansatz. It is assumed that at high frequencies the dominant contribution of a scatterer comes primarily from important critical points (see Figure 1.7). Moreover, the scattering phenomena are localized, meaning that the scattered field will come from localized points on surfaces, edges, vertices [100, 162–164]. At high frequencies, the specular reflection from an object is of leading order whereas the scattered field from edges and vertices are of increasingly higher order or weaker.

Since in ray physics the interaction of the field with the object is local, one can use canonical solutions such as the Sommerfeld half-plane solution to ascertain the amplitude of the scattered fields from the critical points. By studying Watson's transformation, one can understand the physics of the surface or creeping wave contribution on a curved surface. On a convex curved surface, the surface wave is radiative, meaning that it sheds energy as it creeps on the curved surface. Hence, it decays along its creeping direction, implying that in the high-frequency limit, their contributions are exponentially small, but in the twilight zone between wave physics and ray physics they may be important. In the high frequency limit, in the order of importance, the scattering events are: specular reflection, edge diffraction, vertex diffraction, and creeping wave.

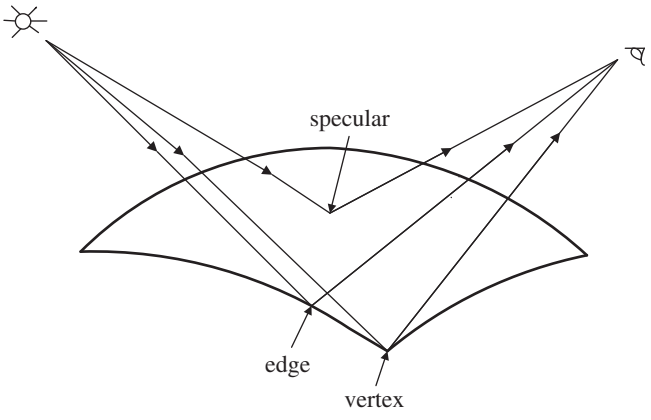

Figure 1.7 The essential physics of high-frequency scattering is controlled by critical point reflections and diffractions.

Moreover, many ray-optics approximations break down near shadow boundaries and caustics. Uniform solutions with the help of special functions and asymptotic matching are needed for solutions in this region [142].

1.9 The Age of Computations

The untenability of many problems in order to meet the demand of science and technology developments calls for new mathematical modeling methods of solving intricate equations with complex geometries. Numerical methods were the most promising general purpose methods to solve nonlinear differential equations involving elaborate geometries.

During the Second World War, a bevy of women were hired to do numerical computing by hand, but it was far too laborious. These women were actually called computers. Hence, there was a pressing need to use machines to replace humans as computers [165, 166]. Mechanical computing machines have been around for a while, but they were not feasible for high-speed computations [167]: machines with moving parts were slow and too unwieldy. Therefore, the electronic computer, with no moving mechanical parts, that promised high speed computation was developed in 1946 (Eniac) [168, 169] and an all-transistor computer was developed in 1951 (Illiac) [170].

The invention of the computer heralded in a new era and motivated many researchers to investigate alternative methods of solving sophisticated problems. In engineering, many researchers were using the finite element method (FEM) and the finite difference method (FDM) to solve complex engineering problems [171–178]. The final equation becomes a sparse matrix equation that is best solved by numerical methods and methodically by machines.

The basic equations describing many science and engineering problems involving fields, such as fluid dynamics and electromagnetics, are partial differential equations. These partial differential equations can be linear or nonlinear. The fields are functions of space as well as time. When the problems are nonlinear, they need to be solved in their original form in the time domain.

However, if the problem is linear, the Fourier transform technique can convert these equations from the time domain to the frequency domain. When the frequency is fixed, then the fields are functions of space alone, making them easier to solve. Furthermore, for linear problems, one can define a Green's function to further convert the differential equations into integral equations by using the principle of linear superposition [122, 123]. Consequently, numerical methods for solving integral equations have become important and popular [179, 181]. It is important to note that reduction to the frequency domain and integral equations is only possible for linear problems. It is, however, possible to solve a nonlinear problem in the frequency domain by considering multiple frequencies simultaneously, and to use the harmonic balancing method [182–185] to seek the solutions.

Numerical methods can be easily developed for linear problems. When a non-linear problem is encountered, it is linearized, and then an approximate solution is sought and iterated until convergence is reached. This is a Newton related method. In one dimension, this is called the Newton-Raphson method, while in higher dimensions, it is called the Gauss-Newton method or by other variants [186–188].

For inhomogeneous media, the electromagnetic equation reduces to

$$\nabla \times \mu^{-1} \nabla \times \mathbf{E} + \epsilon \frac{\partial^2 \mathbf{E}}{\partial t^2} = -\frac{\partial \mathbf{J}}{\partial t}. \tag{1.101}$$

Finite element or finite difference techniques can be applied directly to solve the above equation in the time domain. These techniques can be applied to nonlinear problems as well, for instance, when ϵ or μ are functions of $\mathbf{E}$ or $\mathbf{H}$. However, if the problem is linear, then the above equation can be transformed to the frequency domain and it becomes

$$\nabla \times \mu^{-1} \nabla \times \mathbf{E} - \omega^2 \epsilon \mathbf{E} = \mathrm{i}\omega \mathbf{J}. \tag{1.102}$$

The above can be rewritten as

$$\mathcal{L}\mathbf{E} = \mathrm{i}\omega \mathbf{J} \tag{1.103}$$

where $\mathcal{L}$ is a linear operator. This equation can be solved with the finite-element frequency domain method or the finite-difference frequency domain method.

By rearranging terms, the above equation can be rewritten as [76, 123]

$$\nabla \times \mu_0^{-1} \nabla \times \mathbf{E} - \omega^2 \epsilon_0 \mathbf{E} = \mathrm{i}\omega \mathbf{J} - \omega^2 (\epsilon_0 - \epsilon)\mathbf{E} + \nabla \times (\mu_0^{-1} - \mu^{-1}) \nabla \times \mathbf{E}. \tag{1.104}$$

Assuming that μ_0 is a constant, it can be multiplied through the equation to arrive at

$$\nabla \times \nabla \times \mathbf{E} - \omega^2 \mu_0 \epsilon_0 \mathbf{E} = \mathrm{i}\omega \mu_0 \mathbf{J} - \omega^2 \mu_0 (\epsilon_0 - \epsilon)\mathbf{E} + \mu_0 \nabla \times (\mu_0^{-1} - \mu^{-1}) \nabla \times \mathbf{E}. \tag{1.105}$$

Now if we have a closed form solution to the following equation

$$\nabla \times \mu_0^{-1} \nabla \times \overline{\mathbf{G}}(\mathbf{r} - \mathbf{r}') - \omega^2 \epsilon_0 \overline{\mathbf{G}}(\mathbf{r} - \mathbf{r}') = \bar{\mathbf{I}} \delta(\mathbf{r} - \mathbf{r}') \tag{1.106}$$

the solution is the point source response to the vector wave equation [72, 77]. Using the principle of linear superposition, we can treat the right-hand side of (1.105) as sources, and write down the solution of it as

$$\begin{aligned} \mathbf{E}(\mathbf{r}) = \mathrm{i}\omega \mu_0 \int \mathrm{d}\mathbf{r}' \overline{\mathbf{G}}(\mathbf{r} - \mathbf{r}') \cdot \mathbf{J}(\mathbf{r}') - \omega^2 \mu_0 \int \mathrm{d}\mathbf{r}' \overline{\mathbf{G}}(\mathbf{r} - \mathbf{r}') \cdot \left[\epsilon_0 - \epsilon(\mathbf{r}')\right] \mathbf{E}(\mathbf{r}') \\ + \mu_0 \int d\mathbf{r}' \overline{\mathbf{G}}(\mathbf{r} - \mathbf{r}') \cdot \nabla \times \left[\mu_0^{-1} - \mu(\mathbf{r}')^{-1}\right] \nabla \times \mathbf{E}(\mathbf{r}'). \end{aligned} \tag{1.107}$$

The above equation can be simplified further if needed. Assuming that **J** is known, the first term on the right-hand side can be regarded as the incident field on the inhomogeneity, and then the above is an integral equation for the unknown **E**. We can rewrite the above as

$$\mathbf{E} = \mathbf{E}_{\text{inc}} + \mathcal{L}_v \mathbf{E} \tag{1.108}$$

where $\mathcal{L}_v$ represents the integral operator associated with the second and the third terms on the right-hand side of (1.107).

Since the unknown is inside the integral as well as outside the integral, it is an integral equation of the second kind. Moreover, it is a volume integral equation, and the integration need only be over the domain where $\epsilon_0 - \epsilon(\mathbf{r}')$ and $\mu_0 - \mu(\mathbf{r}')$ are non-zero. So if the scatterer is of finite support, this domain is finite. The unknown **E** needs only to be solved over a smaller domain compared to the original differential equations [76, 93, 179, references therein]. The early concepts were formulated in 2D [180] and gradually evolved to 3D.

If the domains are piecewise homogenous, then the vector Green's theorem can be used to derive integral equations where only surface unknowns are needed [189]. The support of the unknown domain is even further reduced. These are surface (or boundary) integral equations. The number of unknowns is greatly reduced, beating the cruelty of dimensionality that shall be discussed later.

1.9.1 Computations and Mathematics

Mathematics is useful for classifying partial differential equations (PDEs) that are encountered in electromagnetics. For electromagneitcs, when the equations involve no derivative in time, the PDEs are considered elliptic. Such PDEs cannot propagate a singularity such as the Laplace's equation or the Poisson's equation. The field solutions of such equations are highly smooth. When the PDEs involve the first-order derivative in time only, such as the diffusion equation, they are classified as parabolic. These equations only evolve in one direction in time: the singularity can only propagate forward in time. When the PDEs involve the second-order derivatives in time, such as the wave equation, they are classified as hyperbolic. Such equations can propagate the field or singularity both forward and backward in time [190, 191].

Partial differential equations need to be solved with boundary conditions in order to guarantee unique solutions [192]. However, when internal resonance solutions exist, uniqueness is not guaranteed. Internal resonances can exist in wave-like solutions. Both hyperbolic and parabolic equations can have wave-like solutions. Internal resonance corresponds to a homogeneous solution without excitation, and hence, is equivalent to the existence of a null space solution. The solution is non-unique for PDEs when such resonance solutions exist.

Derivation of Integral Equations

When a problem is cast into an integral equation, the Green's function becomes the kernel of the integral equation. For example, in the integral equation

$$\int \mathrm{d}\mathbf{r}' g(\mathbf{r}, \mathbf{r}') f(\mathbf{r}') = h(\mathbf{r}) \tag{1.109}$$

where $g(\mathbf{r}, \mathbf{r}') = \exp(ik|\mathbf{r} - \mathbf{r}'|)$ is the Green's function and also the kernel. For wave problems, $k \neq 0$, and the Green's function is oscillatory. The oscillatory nature of the Green's function implies that it can send information over a long distance. For static problems or low-frequency problems, $k = 0$, and the Green's function is smooth (non-oscillatory); it cannot send information over a long distance [87]. These two distinct physics affect how these integral equations can be solved. Internal resonances can affect integral equations to give rise to non-uniqueness in their solutions, just as for differential equations [193–208]. An excellent review was given by Peterson [204].

Most problems are linear problems in electromagnetics. In the case when the problem is nonlinear, it is linearized and solved iteratively as a set of linear problems. For instance, differential equations and integral equations in electromagnetics are often linear. Hence, we shall discuss next the numerical methods to solve a linear equation [76, 93, 179].

Subspace Projection Methods

We can describe a general linear problem with a linear operator equation

$$\mathcal{L}f = h \tag{1.110}$$

$$\mathcal{L}^t f_a = h_a \tag{1.111}$$

where $\mathcal{L}$ represents a linear operator. The second equation is the auxiliary equation, which is discussed in conjunction with the first equation. It represents a differential operator in the case of differential equations, while it represents an integral operator for integral equations. In mathematical notation, one often writes $\mathcal{L} : V \to W$, meaning that it is a linear operator that maps elements of the vector space V to the elements of the vector space W, where V is known as the domain space and W the range space of the operator $\mathcal{L}$.

For a differential operator, an explicit form may be

$$(\nabla^2 + k^2) f(\mathbf{r}) = h(\mathbf{r}) \tag{1.112}$$

which is the Helmholtz wave equation or the frequency domain version of the wave equation. A boundary condition and a loss condition have to be stipulated in order to make the solution to the above equation unique. The Laplacian operator ∇^2 can be proved to be a negative definite operator because by using integration by parts or using the fact that $\nabla \cdot (f\nabla f) = (\nabla f)^2 + f\nabla^2 f$, we have

$$\langle f, \nabla^2 f \rangle = \int_V \mathrm{d}\mathbf{r} f(\mathbf{r}) \nabla^2 f(\mathbf{r}) = -\int_V \mathrm{d}\mathbf{r} (\nabla f(\mathbf{r}))^2 + \int_S \mathrm{d}\mathbf{S} \cdot f(\mathbf{r}) \nabla f(\mathbf{r}). \tag{1.113}$$

When $f(\mathbf{r})$ satisfies the appropriate boundary condition on the surface S, the second term on the right-hand side disappears and the first term is always negative for real $f(\mathbf{r})$. Hence, for real k^2, the operator $\nabla^2 + k^2$ is indefinite, implying that it can have a null space. This null space corresponds to the resonance solution of the wave equation.

For an integral equation, an explicit form is given in (1.109). These equations are not amenable to computation. They are equations in infinitely dimensional Hilbert space with uncountably infinite indices. To make them computable, we find a subspace in which an approximate solution of the above equations can be found, and then project the solution into this subspace. This process can be methodically described as follows.

We choose a basis set with N basis functions $f_n, n = 1, \cdots, N$ that spans the subspace that can approximate the domain space of the operator. We expand the unknown f in

terms of the basis functions in this subspace, and the auxiliary unknown f_a in terms of the auxiliary basis functions, namely

$$f(\mathbf{r}) \doteq \sum_{n=1}^{N} a_n f_n(\mathbf{r}) \tag{1.114}$$

$$f_a(\mathbf{r}) \doteq \sum_{n=1}^{N} a'_n f'_n(\mathbf{r}) \tag{1.115}$$

The linear operator equation can then be written as

$$\sum_{n=1}^{N} a_n \mathcal{L} f_n \doteq h. \tag{1.116}$$

The above equation can only be approximately satisfied since we have picked a finite number of basis functions. Moreover, the solution to (1.116) is still untenable. To make it more easily solvable, we convert (1.116) into a matrix equation by weighting or testing the equation with $w_m(\mathbf{r}), m = 1, \cdots, N$. Consequently, we have

$$\sum_{n=1}^{N} a_n \langle w_m, \mathcal{L} f_n \rangle = \langle w_m, h \rangle, \quad m = 1, \cdots, N \tag{1.117}$$

where the inner product is defined by

$$\langle u, v \rangle = \int u(\mathbf{r}) v(\mathbf{r}). \tag{1.118}$$

The above equation (1.117) implies that it can be exactly satisfied if we project (1.116) onto a subspace spanned by $w_m(\mathbf{r}), m = 1, \cdots, N$. Recent research has shown that if the testing functions w_m are chosen from the dual space of the range space, the above can be a good approximation or matrix representation of the original operator equation [210]. The dual space can be larger or smaller than the range space.

Equation (1.117) now constitutes a matrix equation

$$\bar{\mathbf{L}} \cdot \mathbf{a} = \mathbf{h} \tag{1.119}$$

$$(\bar{\mathbf{L}})_{mn} = \langle w_m, \mathcal{L} f_n \rangle \tag{1.120}$$

$$(\mathbf{a})_n = a_n \tag{1.121}$$

$$(\mathbf{h})_m = \langle w_m, h \rangle \tag{1.122}$$

$$\bar{\mathbf{L}}^t \cdot \mathbf{a}' = \mathbf{h}_a \tag{1.123}$$

$$(\bar{\mathbf{L}})_{mn} = \langle w_m, \mathcal{L} f_n \rangle \tag{1.124}$$

$$(\mathbf{a}')_n = a'_n \tag{1.125}$$

$$(\mathbf{h}_a)_m = \langle w_m, g_a \rangle \tag{1.126}$$

In the above, the choice of the testing function is determined by the auxiliary equation [76]. The testing function should be chosen so that the auxiliary equation is solved accurately, whereas the choice of the expansion or basis function is to solve the primary equation accurately. The auxiliary equation is the adjoint or the transpose of the original equation where the range space and the domain space are swapped. It can be shown that the left domain space of an operator is the dual space of the range space. Hence,

if the testing functions solve the auxiliary equation well, they can well approximate the left domain space of the original operator, which is the dual space of the range space of the original equation. This is in agreement with the aforementioned recent findings.

The above procedure of converting the operator equation into a matrix equation is the underpinning method behind the finite element method, or the method of moments. They are variously known as Galerkin's method, Petrov-Galerkin's method, method of weighted residuals, collocation method, and point matching method [212–214]. However, they are all subspace projection methods [215, 216].

When $\mathcal{L}$ is a differential operator, the matrix $\overline{\mathbf{L}}$ is sparse because a differential operator is a local operator. However, when $\mathcal{L}$ is an integral operator, the matrix $\overline{\mathbf{L}}$ is dense. In differential equations, the unknown is the field that permeates all of space. Hence, the unknown count is usually larger in differential equation solvers. However, they come with sparse matrix systems that are cheaper to solve and store.

For integral equations, the unknown is the induced current on the scatterer. Hence, the unknown count is smaller since the current resides only on or in a scatterer with finite support. However, the ensuing matrix system is dense and is hard to store. Moreover, the matrix assembly of forming the matrix elements

$$\langle w_m, \mathcal{L} f_n \rangle \tag{1.127}$$

is tedious since the operator involves singularities that have to be evaluated with care [217, 218].

1.9.2 Sobolev Space and Dual Space

Since many quantities (fields and currents) in electromagnetics correspond to finite energy, they are square integrable over a finite volume. In mathematical parlance, these quantities live in the $L2$ space. For instance,

$$\int_V |\mathbf{E}(\mathbf{r})|^2 \mathrm{d}V < \infty \tag{1.128}$$

for physical reasons. Hence, $\mathbf{E}(\mathbf{r})$ lives in the $L2$ space. However, the above is not specific enough to describe the space in which $\mathbf{E}$ lives. Since $\nabla \times \mathbf{E}$ produces the magnetic field $\mathbf{H}$, which must have finite energy and hence, the square integrable $\mathbf{E}$ lives in a space where itself plus its curl are square integrable. We can define such a space to be

$$H(\mathrm{curl}) = \{\mathbf{E} \in L2 \,:\, \nabla \times \mathbf{E} \in L2\}. \tag{1.129}$$

Spaces where the function is in Lp as well as its certain-order derivatives are also in Lp are known as Sobolev spaces. The particular Sobolev space above is also called curl conforming space. A Sobolev space imposes smoothness constraint on a function, and hence, it is a smaller space than $L2$.

What kind of space does $\mathbf{J}$ live in? If $\mathbf{J}$ is physical, then its divergence exists since from the continuity equation, $\nabla \cdot \mathbf{J} = -\mathrm{i}\omega\rho$ where ρ is charge density. Since both the current density $\mathbf{J}$ and the associated charge density ρ are finite energy functions that are square integrable, $\mathbf{J}$ lives in the space

$$H(\mathrm{div}) = \{\mathbf{J} \in L2 \,:\, \nabla \cdot \mathbf{J} \in L2\}. \tag{1.130}$$

Given an inner product $\langle f, h\rangle$ that exists where h is chosen from a vector space V, then f is said to live in the dual space of V. For instance, in electromagnetics, the reaction $\langle \mathbf{E}, \mathbf{J}\rangle$ always exists corresponding to a physical $\mathbf{E}$ field and a physical current $\mathbf{J}$. If all physical currents live in a space V, then $\mathbf{E}$ must live in the dual space of V.

Iterative Methods

When the unknown count is large, the matrix $\overline{\mathbf{L}}$ is never generated. Instead, iterative matrix-free methods in numerical linear algebra are used to solve the matrix equation. Iterative methods can be made matrix-free because one needs only to write a code to produce the result

$$\overline{\mathbf{L}} \cdot \mathbf{a} \tag{1.131}$$

namely, the result of the action of a matrix on a vector, but not the matrix itself. For sparse matrices, this action can be effected with $\mathcal{O}(N)$ operations. For dense matrices, it costs $\mathcal{O}(N^2)$ to effect this action. However, various fast solvers have been developed that allow this action to be effected in $\mathcal{O}(N)$ or $\mathcal{O}(N \log N)$ operations [115, 219–224].

When it comes to solve a matrix equation iteratively, numerical linear algebra plays an important role [225]. The condition number and the distribution of the eigenvalues of the system matrix determine the convergence rate of iterative methods. The Krylov subspace method [225–228] is a popular way to understand the convergence rate of iterative methods. In this method, one finds the solution to the matrix equation by finding the best fit solution in a subspace called Krylov subspace

$$\mathcal{K}^K(\overline{\mathbf{L}}, \mathbf{r}_0) = \left\{ \mathbf{r}_0, \overline{\mathbf{A}} \cdot \mathbf{r}_0, \overline{\mathbf{A}}^2 \cdot \mathbf{r}_0, \cdots, \overline{\mathbf{A}}^{K-1} \cdot \mathbf{r}_0 \right\} \tag{1.132}$$

where $\mathbf{r}_0 = \mathbf{h} - \overline{\mathbf{L}} \cdot \mathbf{a}_0$ where a_0 is the initial guess to the solution. Thus, $\mathbf{r}_0$ is the residual error in the first iteration in the method. The above Krylov subspace can be generated by performing a $K-1$ matrix-vector product with the matrix $\overline{\mathbf{L}}$ on the vector $\mathbf{r}_0$. The method finds the optimal solution at the Kth iteration, $\mathbf{a}_K$, by letting it be $\mathbf{a}_K = \mathbf{a}_0 + \mathbf{z}_K$, such that $\mathbf{z}_K \in \mathcal{K}^K(\overline{\mathbf{L}}, \mathbf{r}_0)$. By doing so, the residual at the Kth iteration is

$$\begin{aligned} \mathbf{r}_K &= \mathbf{h} - \overline{\mathbf{L}} \cdot \mathbf{a}_K \\ &= \mathbf{r}_0 - \overline{\mathbf{L}} \cdot \mathbf{z}_K \in \left\{ \mathbf{r}_0, \overline{\mathbf{L}} \cdot \mathbf{r}_0, \overline{\mathbf{L}}^2 \cdot \mathbf{r}_0, \cdots, \overline{\mathbf{L}}^K \cdot \mathbf{r}_0 \right\} \\ &\in \mathcal{K}^{K+1}(\overline{\mathbf{L}}, \mathbf{r}_0). \end{aligned} \tag{1.133}$$

In other words, the residual error that is to be minimized can be written as

$$\begin{aligned} \mathbf{r}_K &= \mathbf{r}_0 + \alpha_1 \overline{\mathbf{L}} \cdot \mathbf{r}_0 + \alpha_2 \overline{\mathbf{L}}^2 \cdot \mathbf{r}_0 + \cdots + \alpha_K \overline{\mathbf{L}}^K \cdot \mathbf{r}_0 \\ &= \sum_{k=0}^{K} \alpha_k \overline{\mathbf{L}}^k \cdot \mathbf{r}_0 = P_K^o(\overline{\mathbf{L}}) \cdot \mathbf{r}_0 \end{aligned} \tag{1.134}$$

where $P_K^o(x)$ is an optimal polynomial with $\alpha_0 = 1$, and the coefficients $\alpha_1, \cdots, \alpha_K$ are chosen to minimize $\mathbf{r}_K$.

To understand the convergence of the above matrix polynomial, we expand $\mathbf{r}_0$ in terms of the left and right eigenvectors of $\overline{\mathbf{L}}$, or [229–233]

$$\mathbf{r}_0 = \sum_{n=1}^{N} \mathbf{v}_n \left(\mathbf{w}_n^t \cdot \mathbf{r}_0\right) \tag{1.135}$$

where $\mathbf{v}_n$ is the right eigenvector, while $\mathbf{w}_n$ is the left eigenvector. They can be shown to share the same set of eigenvalues, and are mutually orthogonal. That is $\mathbf{w}_n \cdot \mathbf{v}_{n'} = \delta_{nn'}$. Therefore,

$$\overline{\mathbf{L}} \cdot \mathbf{v}_n = \lambda_n \mathbf{v}_n \tag{1.136}$$

$$\mathbf{w}_n^t \cdot \overline{\mathbf{L}} = \lambda_n \mathbf{w}_n^t \tag{1.137}$$

where the eigenvalue λ_n can be complex. We can easily show that

$$\overline{\mathbf{L}}^k \cdot \mathbf{r}_0 = \sum_{n=1}^{N} \lambda_n^k \mathbf{v}_n (\mathbf{w}_n^t \cdot \mathbf{r}_0). \tag{1.138}$$

By substituting the above into (1.134), we have

$$\mathbf{r}_K = \sum_{n=1}^{N} \sum_{k=0}^{K} \alpha_k \lambda_n^k \mathbf{v}_n \left(\mathbf{w}_n^t \cdot \mathbf{r}_0\right) = \sum_{n=1}^{N} P_K^o \left(\lambda_n\right) \mathbf{v}_n \left(\mathbf{w}_n^t \cdot \mathbf{r}_0\right) \tag{1.139}$$

$$\mathbf{r}_K = \sum_{k=0}^{K} \overline{\mathbf{L}}^k \cdot \mathbf{r}_0 = \sum_{n=1}^{N} P_K^o \left(\lambda_n\right) \mathbf{v}_n \left(\mathbf{w}_n^t \cdot \mathbf{r}_0\right) \tag{1.140}$$

$$\mathbf{r}_0 = \mathbf{h} - \overline{\mathbf{L}} \cdot \mathbf{a}_0 \tag{1.141}$$

$$\mathbf{r}_1 = \mathbf{r}_0 + \alpha_1' \overline{\mathbf{L}} \cdot \mathbf{r}_0. \tag{1.142}$$

It is seen that the residual error in the Kth iteration is proportional to the optimal polynomial $P_K^o(\lambda_n)$ at the N eigenvalues λ_n. If $K = N$, a polynomial can be found such that $P_K^o(\lambda_n)$ is exactly zero at all these eigenvalues, meaning that the residual error is zero. When K is less than N, if the eigenvalues are clustered together on the complex plane, the residual error can still be made small. Since the polynomial has a value such that $P_K^0(0) = 1$, if there are many eigenvalues near the origin, it is difficult to fit the polynomial so that it is small close to the origin.

1.10 Fast Algorithms

Due to the increased workload of numerical methods when the scatterer becomes electrically large (large compared to wavelength), there has been much interest in fast methods to solve the ensuing matrix equations derived from Maxwell's equations.

Differential equation solvers naturally give rise to sparse matrices. The solution process can be made matrix-free easily. The down side is the existence of grid dispersion error whose deleterious effect increases with the size of the problem [234]. In this case, the effort has been in reducing the unknown counts as the unknowns are fields that permeate space pervasively. Also, accuracy improvement is necessary to mitigate grid dispersion errors. A higher-order method is used to reduce unknown counts, but with the peril of reducing the sparsity of the matrix. Also, the unknowns in differential equation solvers grow with the volume of the simulation region, and hence suffer from the cruelty of dimensionality as we shall discuss later.

Methods to invert the finite-element matrix directly have been studied extensively. Because of the sparsity of the FEM matrix for differential equations, it can be directly inverted in $\mathcal{O}(N^{1.5})$ in 2D and $\mathcal{O}(N^2)$ in 3D by the nested dissection ordering method

[235, 236]. Moreover, for domains where the shapes are oblong, frontal method proves popular in inverting the finite-element matrix [237, 238].

Another hot area of research in differential equation solvers is the design of absorbing boundary conditions (ABCs) [239–250]. Berenger's perfectly matched layers (PMLs) [251], and coordinate-stretching PMLs [252] have become highly popular among numericists in this area. Coordinate-stretching PMLs draw inspirations from the area of matched asymptotics where coordinate stretching is used to emphasize a certain physics of the problem [252]. Furthermore, an anisotropic medium PML has been developed [253]. This topic has spurred the interest of many researchers [254–261].

The coordinate stretching PML is quite general, as coordinate stretching can be applied to any derivative operators. So it can be applied to different types of PDEs, and hence, it has allowed the generalization of PMLs to curvilinear coordinates, and other equations of physics easily [261–264].

Most ABCs are not perfect; a rigorous, perfect ABC is actually a boundary integral equation truncation of a differential equation solution domain solved by FEM or FDM [174–178]. This has been avoided in the past because boundary integral equations give rise to dense matrix systems that are expensive to solve and store. However, the advent of fast algorithms has changed the landscape [115, 265]. Boundary integral equations accelerated by fast algorithms have been used to reduce the domain size of finite element methods since they act as absorbing boundary conditions.

1.10.1 Cruelty of Computational Complexity

Integral equations were difficult and expensive to solve in the past. They usually give rise to dense matrix system requiring $\mathcal{O}(N^3)$ computer time and $\mathcal{O}(N^2)$ memory to solve. These computational complexities are just too unwieldy for large problems. However, advances in fast methods have eliminated this bottleneck by reducing the size of α in the exponent in $\mathcal{O}(N^\alpha)$ in these computational complexity scalings.

First, direct solvers such as RATMA (recursive aggregate T matrix method) [266, 267] have been designed to solve integral equations in $\mathcal{O}(N^2)$ in 2D, and $\mathcal{O}(N^{7/3})$ in 3D, faster than the $\mathcal{O}(N^3)$ time needed to solve a dense matrix system. A method similar to the nested dissection ordering method, called the nested equivalence principle algorithm (NEPAL) [268, 269] can directly solve a matrix in $\mathcal{O}(N^{1.5})$ in 2D and $\mathcal{O}(N^2)$ in 3D. When the object is oblong, it can be reduced to $\mathcal{O}(N \log^2 N)$ [270, 271]. Recently, some direct solver work has been done to produce low-complexity solutions to scattering problems [272, 273].

For iterative solvers, a sleuthing of the method can reduce the computational time complexity to $\mathcal{O}(N \log N)$. Moreover, many of these methods can be made matrix-free so that only the unknown vector, and only the diagonal part of the matrix, need to be stored. Hence, the memory requirements can be reduced to $\mathcal{O}(N)$. There are essentially three popular methods to speed up the solutions of integral equations.

- Fast Fourier transform (FFT) based techniques: In this technique, the integral operator is cast into a form that resembles a convolutional integral as much as possible. Then FFT is used to expedite the convolution enabling its evaluation of a matrix-vector products in $\mathcal{O}(N \log N)$ operations. For surface scatterers with a lot of zero-padding in the FFT, the complexity is worse and is not optimal [274–285].
- Matrix compression based techniques: the method of moments matrix that follows from solving integral equations is of low rank. The reasons for low rank are two: over

discretization of mesh density; and far interactions between currents on the object. The Nyquist sampling theorem necessitates the discretization of at least two points per wavelength in order to capture the oscillatory nature of the currents on an object. However, oftentimes, discretization far above the Nyquist sampling rate is used. In this case, redundancies are created in the unknown counts, and the ensuing matrix system is of lower rank than the unknown counts. Such matrix systems can be easily compressed using matrix compression techniques, such as wavelets [286–295], adaptive cross approximations, simple fast multipole, etc. [219, 296–305]. Interaction matrices with low-ranks due to far interactions are harder to compress. They cannot be compressed beyond the Nyquist barrier [291], even though ray-physics based methods have been used to compress them further beyond the Nyquist barrier [306–310]. When wave physics is involved, the only viable way to compress the matrices for far interaction efficiently is the multipole based methods [222, 223]. However, recent advances in direct solvers [272, 273] herald new possibility for further matrix compression.

- Multipole-based methods: the simple fast multipole method can expedite the solution involving circuit physics or Laplace solutions very easily [219, 311, 312]. Extension of such an algorithm for wave physics cases has been proposed, but its verbatim use for wave physics cases does not work [313, 314]. The only viable method of expediting the wave physics case is the multilevel fast multipole algorithm [222, 223], where anterpolation and interpolation [315] between levels are added. The algorithm is a tree-based algorithm. The matrices for far interactions are analytically diagonalized [313, 316, 317] on paper rather than by algebraic or numerical means. The number of diagonal elements needed is proportional to the rank of the matrices. The reason is that the ranks of the matrices increase with the group size compared to wavelength. Near the upper levels of the inverted tree, the ranks of the matrices are higher, while near the lower levels, their ranks are lower.

  To be of the varying ranks of these matrices, their dimensions are different for different levels even if they are diagonalized. Hence, anterpolation and interpolation are needed between levels due to their different ranks, very much in the spirit of multilevel multigrid schemes [318]. With this augmentation, the multilevel fast multipole algorithm provides optimal complexity of performing a matrix-vector product with $\mathcal{O}(N \log N)$ complexity. It is with this algorithm that wave physics problems with tens of millions to hundreds of millions, and over a billion unknowns have been solved [115, 319–324].

The key to the multilevel fast multipole algorithm is the factorization of the the matrix element L_{ij} when elements i and j are far apart. Then one can express [115, 223]

$$L_{ij} = \tilde{\mathbf{V}}^t_{f,i,i_1} \cdot \bar{\mathbf{I}}^t_1 \cdot \bar{\bar{\boldsymbol{\beta}}}_{i_1,i_2} \cdot \bar{\mathbf{I}}^t_2 \cdots \bar{\bar{\boldsymbol{\beta}}}_{i_N,L} \cdot \bar{\bar{\boldsymbol{\alpha}}}_{LL'} \cdot \bar{\bar{\boldsymbol{\beta}}}_{L',j_N} \cdots \bar{\mathbf{I}}_2 \cdot \bar{\bar{\boldsymbol{\beta}}}_{j_2,j_1} \cdot \bar{\mathbf{I}}_1 \cdot \tilde{\mathbf{V}}_{s,j_1,j}. \quad (1.143)$$

The factorization allows a matrix-vector product to emulate a multilevel telephone network connection, as shown in Figure 1.8, where the number of telephone lines can be greatly reduced compared to direct telephone connection. In the above, the $\bar{\bar{\boldsymbol{\alpha}}}$ and $\bar{\bar{\boldsymbol{\beta}}}$ matrices are diagonal, while the $\bar{\mathbf{I}}$ matrices are quasi-diagonal interpolation and anterpolation matrices that are not square. Hence, the storage requirement of the factorized matrices is small, and they can be reused in a tree algorithm. Other factorizations do not lead to $\mathcal{O}(N \log N)$ complexity. There has been much activity in this field as well [325–336].

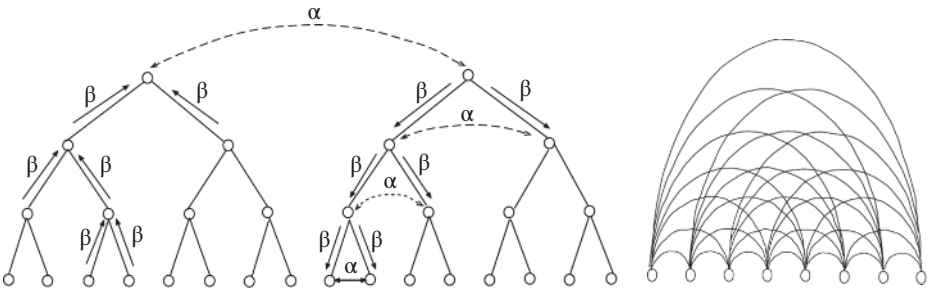

Figure 1.8 The factorization of the matrix L_{ij} in (1.143) allows the matrix-vector product to emulate a telephone network connection (left) [115]. The direct line connections between telephones (right) require a large number of lines.

1.10.2 Curse of Dimensionality

If the discretization density is in terms of n per wavelength, it implies that n is linearly proportional to $k = 2\pi/\lambda$. The fact that the total $N = n^d$ where d is the dimensionality of the problem can make N exorbitantly large if d is 3. For some problems, like the finite difference problem, the grid dispersion error makes the frequency scaling of n as $n = C_0 k^{1.5}$ [234]. Consequently, in 3D,

$$N = Ck^{4.5} \tag{1.144}$$

which is a rather pathological scaling.

One way to reduce the grid dispersion error is to use higher-order methods. Another way to reduce the dimensionality of the problem is to combine it with analytic methods. Integral equation techniques generally can reduce a volume problem to a surface problem. The use of the closed-form Green's function as a propagator reduces the grid dispersion error, as it is an exact propagator.

Yet another way to reduce the dimensionality of the problem is to use the semi-analytic, or numerical mode-matching method [337–339]. In this method, the problem is decomposed into the propagation dimension and the transverse dimensions. The transverse dimension is usually one less than the original dimensions of the problem. The problem is solved numerically in the traverse dimension, and the solution is analytically propagated in the propagation dimension (see Figure 1.9). These methods are variously known as the R-matrix method, rigorous coupled wave analysis, numerical mode matching, the recursive Green's function method, and the contact block recursion approaches [337, 338, 340–344]. They are also pervasively used in nano-electronic simulation involving Schrödinger equations. The use of the FEM or FDM to solve the transverse dimension can give rise to an increase in speed of orders of magnitude compared to a full 3D method [338, 345].

1.10.3 Multiscale Problems

As the complexity of a geometry increases, there is a need for multiscale modeling of complex geometry. Certain parts of the geometry may need discretization sizes much smaller than wavelengths, while other parts may be modeled with much larger discretization sizes. This can happen in the modeling of complex antennas mounted on

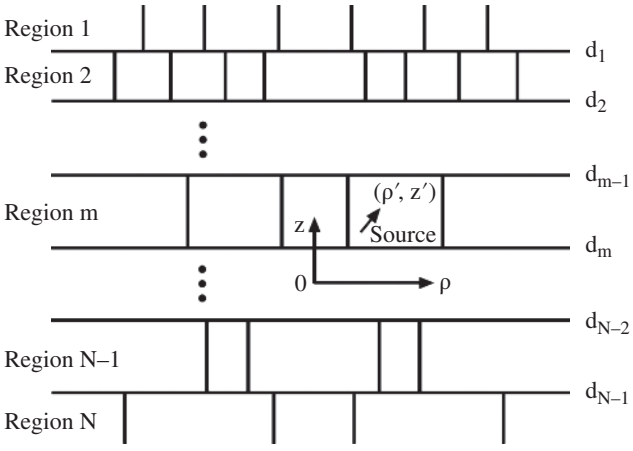

Figure 1.9 A multiregion problem can be solved semi-analytically using numerical mode matching, where the problem is solved numerically in the transverse dimension, but analytically in the longitudinal *z* direction [76].

a platform or inside a computer. The modeling of the fineries of an antenna structure is important in capturing the circuit physics necessary for the functioning of the antenna. This part may need fine meshes for its modeling. On the other hand, the interaction of the radiation field from the antenna with the rest of the platform does not involve circuit physics, and hence can be modeled with much coarser meshes.

The concurrent existence of disparate mesh sizes can be dealt with using a number of methods. In the case of multilevel FMM (fast multipole method), tree structures of different depths have been proposed for its solution, or different multiscale methods have been developed [210, 346–349].

However, the disparate mesh sizes often give rise to ill-conditioned matrix systems. Hence, a divide and defeat (DAD) scheme is more expedient to overcome such problems [265, 350]. For instance, the regions of fine meshes can be solved first with a different method, and later on sewn with the other regions. In the FEM, the domain decomposition method (DDM) [265] is best suited to solve such problems. For integral equation solvers, the equivalence principle algorithm (EPA) [350] can be used to overcome the ill-conditioning of the matrix system due to disparate mesh sizes. More recently, well-conditioned formulations such as the augmented electric field integral equation [351] and the Calderon multiplicative preconditioner have been designed to overcome such problems [209, 210].

1.10.4 Fast Algorithm for Multiscale Problems

When the discretization sizes are uneven, some parts of the object can be in the circuit-physics regime, while the long-range interactions between different parts of the object are in the wave-physics regime. A simple fast multipole algorithm that works only in the circuit physics (low frequency), or the fast multipole algorithm that captures only wave physics, is insufficient to model such problems. For these problems, the mixed-form fast multipole algorithm has been specially designed to overcome these problems [352–355]. More importantly, a recent advance has been made in

developing a low-complexity fast multipole algorithm that is valid from the static to the wave-physics regime [356].

1.10.5 Domain Decomposition Methods

A popular way to attack large scale problem is via the DAD scheme by DDMs. In this scheme, a large problem is subdivided into smaller subproblems. Then each subproblem is solved using a method that requires less resource. DDM has been applied first to differential equation solvers. Examples of such solvers are the frontal algorithms [357], Schwarz algorithms [358], as well as the nested dissection ordering method [235].

The precursor to domain decomposition method is the diakoptic approach where a complex problem is broken into simpler subproblems [359]. The subproblems are easily solved and pieced together to obtain the solution to the larger problem [360–365]. This subsequently gives rise to the DDM. The domain of numerical simulation is systematically divided into smaller subdomains, and the problem is solved for each subdomain using a numerical method, and usually, the FEM. This allows for ease of parallel computing. Then the solution for the entire domain is sewn together by imposing boundary conditions at the interface of the domain. Overlapping domains are also used, called the overlapping Schwarz method [358]. When a condition is imposed at an interface, it is also called the finite element tearing interconnect method [265, 366–388]

Other DDM methods include the frontal algorithm [357], and the nested dissection ordering (NDO) algorithm [235]. Recently, an integral equation approach of domain decomposition has been proposed using Huygens' equivalence principle [268, 269, 389–397]. This is particularly useful when each domain contains "white space" due to free space or a homogeneous medium. A differential equation solver would have wasted many unknowns by having to discretize and represent such white space with many unknowns. An integral equation solver, however, would propagate the field through such white space using the closed-form Green's function. The DDM for an integral equation was first proposed in 1993 known as the NEPAL [268, 269]. It is similar to the NDO for differential equation solvers. Its advantage is that there is little grid dispersion error, as in differential equation solvers, and the radiation boundary condition is automatically satisfied due to the used Green's function. Subsequently, a simpler version of it was used to solve practical problems involving complex structures. The simple version is known as the EPA [389, 390].

While the NEPAL does a multilevel subdivision of a domain into smaller subdomains, the EPA does a single-level division of a domain into smaller subdomains. The EPA is particularly useful for solving multiscale problems. Interaction between subdomains is calculated using surface equivalence currents on equivalence surfaces. A scattering operator (also called equivalence principle operator) is defined to encapsulate the scattering physics of an object within the operator. The mesh for capturing the physics of surface equivalence current is usually coarser than the fine mesh needed to capture the physics of a multiscale structure. Hence, the system matrix equation is better conditioned, and easier to solve, by iterative methods.

The EPA has been applied to solve for the solution of a microstrip patch antenna mounted on a car or a large ground plane. The EPA allows for solutions of large problems when it is accelerated with the multilevel fast multipole algorithm [115, 223, 395]. Hence, a problem size with several million unknowns has been solved on a single CPU

personal computer. More recently, a version of the EPA known as the augmented-EPA (A-EPA) has been developed to preclude low-frequency breakdown [391, 392]. Consequently, the A-EPA has been used to solve low-frequency micro-chip problems where the structures are much smaller than the wavelength. In this regime, both circuit physics and wave physics have to be captured concurrently. A more efficient version of the EPA using a single source rather than both electric and magnetic currents has also been developed [393]. Other methods that can be classified as an integral equation DDM are: (1) the self-box inclusion preconditioner method, where a parallel code has been used to solve problems with several million unknowns [115, 223, 394, 395]. (2) The generalized impedance boundary condition where the scattering solution is encapsulated within an impedance operator [396]. Some problems involving nano-optics have been solved using such a method [397].

1.11 High Frequency Solutions

When the frequency is extremely high, electromagnetic problems are not easily solved with numerical methods. Most numerical methods are based on the discretization of complex objects into smaller pieces, each of which is much smaller than the wavelength. Hence, the number of discretizations or unknowns grows exorbitantly as the frequency becomes high.

In the high frequency limit, the dominant contribution comes from specular reflections and diffractions off critical points of an object. Ray tracing technique can be used to find these dominant contributions. Moreover, as the wavelength becomes short, the phase of the wave becomes random and unimportant. In the infra-red (IR) and optical regime, the phase of the field is often neglected.

However, in the microwave regime, there is some interest in keeping track of the phase of the wave. The shooting-and-bouncing ray method is popular in seeking solutions in this regime [398]. For complex targets, the current on the object is approximated with the physical optics approximation. Then the radiation integral is evaluated to find the scattered field. But these integrals are highly oscillatory in nature. One pressing need is the efficient evaluation of highly oscillatory integrals making the workload frequency-independent. This has been a subject of avid study by a number of researchers [100–103, 105, 162–164, 398–414]. Also, efficient numerical methods have also been developed to enable them to solve higher frequency problems [115, 313, 315, 415].

Another approach is to solve the integral equation directly using techniques that are frequency-independent. This has also been a subject of avid study [416–419].

1.12 Inverse Problems

Since an electromagnetic field has been used in remote sensing, geophysical prospection, microwave imaging, and optical coherence tomography, inverse problems are an important aspect of this field. Inverse problems in 1D, surprisingly, are driven by incredible tour-de-force mathematics. Many inverse problems are not solvable, but the 1D inverse problems can be tackled with many mathematical techniques, such as the Gelfand-Levitan-Marchenko method [76, 420].

In multidimensions, there is no closed form solution for the inverse problems except when linear approximations are made. If only single scattering is assumed, which is also called the Born approximation, one can show that the scattered field data in the far field are related to the Fourier transform of the object. Hence, one can perform a Fourier inverse transform to obtain the object. This is used in synthetic aperture radar (SAR) with the production of marvelous pictures of the Earth surface from remotely sensed data. Diffraction tomography is another example of linear inverse problem that can be performed rapidly. Since FFT can be used in the reconstruction, the complexity of the image reconstruction is proportional to $O(N \log N)$ [421–424].

In general, inverse problems in multidimensions have no closed-form solutions, and are usually solved as an optimization problem, where the forward problem is solved with a scatterer. Then a scatterer that generates the best fit data is searched and selected as the solution. Such a method generally gives rise to non-uniqueness of solutions. The way to overcome the non-uniqueness is to arrive at the minimum norm solution [76, 425].

This is very much in the spirit of finding the Fourier inverse transform. If one knows the Fourier transform of an object up to a finite spectrum, the inverse Fourier transform of the object is indeterminate. This is because if we can add an object with spectrum outside the finite spectrum, it will produce the same Fourier transform within the same window. The way to remove the non-uniqueness is to define a minimum norm inverse that is equivalent to pad the data outside the finite window with zero values.

When multiple scattering is accounted for in inverse problems, the multiple scattering (nonlinear) solution can be solved by minimization of the cost functional. A cost functional can be set up and the minimum of the cost functional can be found by a gradient search approach. The gradient in multidimensional space, called the Frechet derivative, can be found by the distorted Born approximation, or other Gauss-Newton methods [426–441]. The Gauss-Newton method is the general name for a nonlinear problem solver, whereas the distorted Born approximation relates this multiple scattering (nonlinear) method directly to the inverse problems.

1.12.1 Distorted Born Iterative Method

By the above approaches, it can be shown that the calculation of the Frechet derivative is equivalent to the solving of the forward scattering problem. Hence, if the forward problem can be solved rapidly, it portends a rapid solution to the inverse problem. With the advent in computer technologies, there is hope that the multiple scattering (nonlinear) inverse problem can be solved rapidly and made practical [442].

Since inverse scattering involves a volume scatterer, we can write the volume integral equation of the Green's function as

$$\mathbf{E}(\mathbf{r}) = \mathbf{E}_{\text{inc}}(\mathbf{r}) + \int_V \mathrm{d}\mathbf{r}' \, \overline{\mathbf{G}}_0(\mathbf{r}, \mathbf{r}') \cdot \left[k^2(\mathbf{r}') - k_0^2\right] \mathbf{E}(\mathbf{r}'), \tag{1.145}$$

where k_0^2 is a constant wavenumber for the homogeneous background. Here, $\overline{\mathbf{G}}_0(\mathbf{r}, \mathbf{r}')$ is a homogeneous medium Green's function with wavenumber k_0. Hence, $\mathbf{E}_{\text{inc}}$ is the field in the absence of the scatterer, but $\mathbf{E}(\mathbf{r})$ is the total field in the presence of the scatterer. By letting

$$\mathbf{E}(\mathbf{r}) = \overline{\mathbf{G}}(\mathbf{r}, \mathbf{r}'') \cdot \mathbf{a} \tag{1.146}$$

$$\mathbf{E}_{\text{inc}}(\mathbf{r}) = \overline{\mathbf{G}}_0(\mathbf{r}, \mathbf{r}'') \cdot \mathbf{a} \tag{1.147}$$

(1.145) can be written as

$$\overline{\mathbf{G}}(\mathbf{r},\mathbf{r}'') = \overline{\mathbf{G}}_0(\mathbf{r},\mathbf{r}'') + \int_V \mathrm{d}\mathbf{r}'\ \overline{\mathbf{G}}_0(\mathbf{r},\mathbf{r}') \cdot \left[k^2(\mathbf{r}') - k_0^2\right] \overline{\mathbf{G}}(\mathbf{r}',\mathbf{r}''). \tag{1.148}$$

The above can be written as an operator equation

$$\overline{\mathcal{G}} = \overline{\mathcal{G}}_0 + \overline{\mathcal{G}}_0 \cdot \overline{\mathcal{O}} \cdot \overline{\mathcal{G}} \tag{1.149}$$

where $\overline{\mathcal{O}}$ is the operator representation of $k^2(\mathbf{r}') - k_0^2$. The above can be solved formally

$$\overline{\mathcal{G}} = (\overline{\mathcal{I}} - \overline{\mathcal{G}}_0 \cdot \overline{\mathcal{O}})^{-1} \cdot \overline{\mathcal{G}}_0 \tag{1.150}$$

where $\overline{\mathcal{G}}$ is manifestly nonlinear with respect to $\overline{\mathcal{O}}$. If one lets

$$\overline{\mathcal{O}} = \overline{\mathcal{O}}_b + \delta\overline{\mathcal{O}} \tag{1.151}$$

$$\overline{\mathcal{G}} = \overline{\mathcal{G}}_b + \delta\overline{\mathcal{G}} \tag{1.152}$$

where $\overline{\mathcal{G}}_b = (\overline{\mathcal{I}} - \overline{\mathcal{G}}_0 \cdot \overline{\mathcal{O}}_b)^{-1} \cdot \overline{\mathcal{G}}_0$, then it can be easily shown that

$$\delta\overline{\mathcal{G}} = \overline{\mathcal{G}}_b \cdot \delta\overline{\mathcal{O}} \cdot \overline{\mathcal{G}}_b. \tag{1.153}$$

The above is the functional or Frechet derivation that can be used in conjunction with a gradient search method such as the Gauss-Newton method. However, it is also a distorted Born approximation for finding the perturbed Green's operator $\delta\overline{\mathcal{G}}$. We have called the iterative method of solving the inverse problem the distorted Born iterative method (DBIM).

1.12.2 Super-Resolution Reconstruction

The use of the DBIM has been shown to yield super-resolution reconstruction of objects with subwavelength resolution (see Figure 1.10) [443–448]. The super-resolution can be ascribed to the fact that the data used for reconstruction have been embedded in the multiple scattering information. The high-resolution information of an object is buried in the evanescent wave spectrum of the scattered field. When single scattering is assumed, the evanescent wave remains localized to the vicinity of the scatterer. Hence, the far field has no super-resolution information of the object. However, when multiple scattering is accounted for, evanescent waves can be converted to propagating waves due to multiple scattering. The multiply-scattered propagating wave hence contains super-resolution information on the object. Thus, if a reconstruction algorithm includes the multiple-scattering physics in the model, super-resolution reconstruction of an object is possible. Super-resolution phenomena have also been observed in [449, 450].

1.12.3 Super-Resolution and the Weyl-Sommerfeld Identity

The physics of super-resolution can be gleaned from the Weyl (1919) identity given as

$$\frac{\mathrm{e}^{\mathrm{i}k_0 r}}{r} = \frac{i}{2\pi} \iint_{-\infty}^{\infty} \mathrm{d}k_x \mathrm{d}k_y\ \frac{\mathrm{e}^{\mathrm{i}k_x x + \mathrm{i}k_y y + \mathrm{i}k_z |z|}}{k_z} \tag{1.154}$$

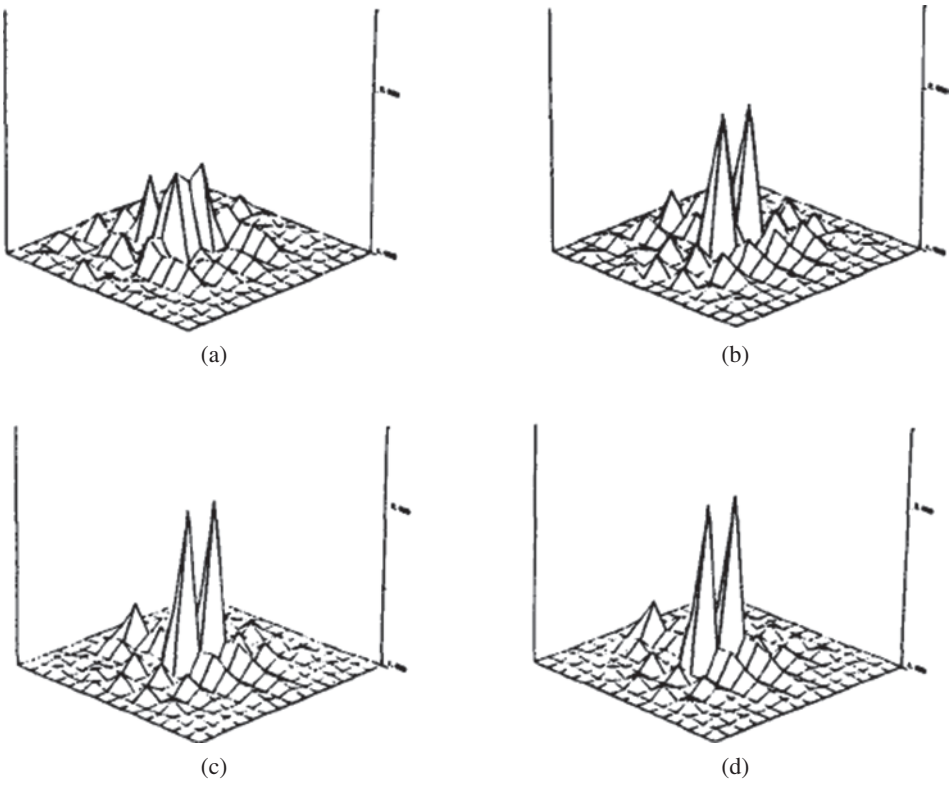

Figure 1.10 The use of multiple-scattering information in multiple scattering (nonlinear) inverse scattering algorithm allows the super-resolution reconstruction of two objects spaced 0.1λ apart [443].

where $k_x^2 + k_y^2 + k_z^2 = k_0^2$ or $k_z = (k_0^2 - k_x^2 - k_y^2)^{1/2}$. The above expression says that a point source generates a spherical wave that can be expressed as an integral summation of plane waves propagating in all directions. Notably, k_z becomes pure imaginary corresponding to an evanescent wave when $k_x^2 + k_y^2 > k_0^2$. If we view the above right-hand side as the Fourier transform of the left-hand side, the field is from a point source. It is clear that the Fourier data for $k_x^2 + k_y^2 > k_0^2$ cannot propagate to a large z location. For large z, the Fourier data that can propagate over long distances are within the Ewald circle $k_x^2 + k_y^2 < k_0^2$. Hence, a low-pass filtered version of the source field is accessible at long distances. This is the source of the Rayleigh limit for the resolution of a point source.

The bunches of plane waves only interfere constructively when they are almost parallel to each other. In other words, the plane wave bundles become rays in the long distance limit or high-frequency limit. If one is to collect the Fourier data with a lens of radius a and subtending an angle θ at the source location, the Fourier data are collected with a circular disk of radius $k_0 \sin\theta$, even smaller than the Eward circle aforementioned. Here, $\sin\theta$ is the numerical aperture of the lens. It is seen that the larger its numerical aperture, the more Fourier data the lens can collect, and hence, of the higher resolution the image that can be reconstructed.

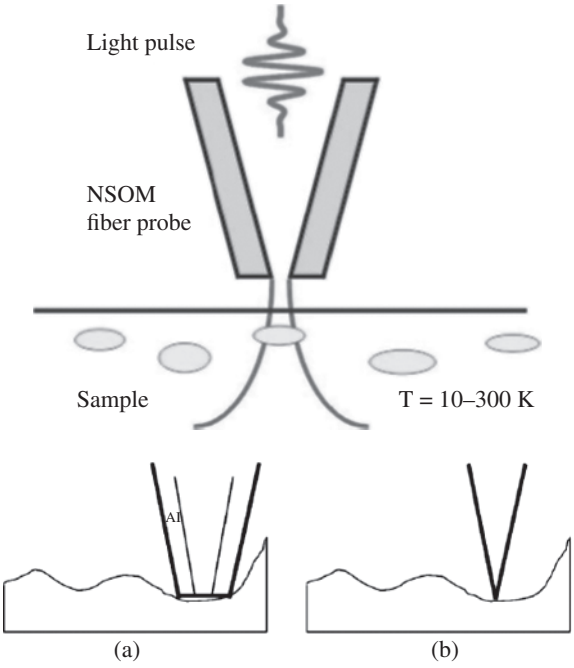

Figure 1.11 Since super-resolution information is buried in the evanescent field of the wave, near-field scanning optical microscopy (NSOM) exploits this fact by using subwavelength sharp tips to generate and sense evanescent field (courtesy of Wiki).

A space propagator for wave is a Fourier transformer, as indicated by the following formula

$$\phi(\mathbf{r}) = \int_V \mathrm{d}\mathbf{r}' g(\mathbf{r}, \mathbf{r}') s(\mathbf{r}') \approx \frac{\mathrm{e}^{\mathrm{i}k_0 r}}{4\pi r} \int_V \mathrm{d}\mathbf{r}' \mathrm{e}^{-\mathrm{i}\mathbf{k}\cdot\mathbf{r}'} s(\mathbf{r}') = \frac{\mathrm{e}^{\mathrm{i}k_0 r}}{4\pi r} \tilde{S}(\mathbf{k}) \tag{1.155}$$

where $\tilde{S}(\mathbf{k})$ is the Fourier transform of $s(\mathbf{r})$. A lens is a phase-shift provider so that after the wave field has passed through it, its Fourier transform by space creates the image of the original object.

If a lens has a numerical aperture of $\sin\theta$, the Fourier data are provided by a circle of radius $k_0 \sin\theta$ on the k_x-k_y Fourier space. A precise point source field cannot be created. It is interesting to note that

$$\frac{\partial}{\partial z} \frac{\mathrm{e}^{\mathrm{i}k_0 r}}{r}\bigg|_{z=0} = \delta(x)\delta(y). \tag{1.156}$$

The above can be proved easily by using Weyl's identity. The space propagator takes the Fourier of the field at $z = 0$ and propagates to the lens location. The lens adds the appropriate phase shift to the wave field so that the second part of the space propagator essentially does a Fourier inverse transform of the wave field at $z = h$, which tries to reconstruct the wave field at $z = 0$. However, due to low-pass filtering and the finite numerical aperture of the lens, the point image reconstructed is

$$I(x, y) = \int_0^{k_0 \sin\theta} \mathrm{d}k_\rho k_\rho J_0(k_\rho \rho). \tag{1.157}$$

The above can be evaluated to

$$I(\rho) = \frac{J_1(k_0 \sin\theta)}{k_0 \sin\theta} \tag{1.158}$$

which is also called the Airy disk function. It is the point-spread function of the low-pass filter system that will propagate a point image at $z = 0$ to the focal point of a lens.

1.13 Metamaterials

The study of metamaterials has become a hot topic in recent years mainly due to two recent concepts proposed by Pendry [451, 452]. One was the use of double-negative materials to obtain super-resolution. The second was to engineer a reflectionless body by cloaking so that the object is invisible to a field [453, 454].

While super-resolution was possible on paper, it was never realized to satisfaction. The high-resolution information of a point source is embedded in the evanescent spectrum of the field. However, the evanescent spectrum decays rapidly away from the source point, and hence this information is lost as one moves away from the source point. However, if one can amplify this evanescent spectrum, it can potentially recover the high-resolution information and give rise to super-resolution. This is the gist of the concept of super-resolution in a double-negative slab [455].

When a double negative material with $\mu = -\mu_0$ and $\epsilon = -\epsilon_0$ interfaces with a vacuum, it can be shown that plasmonic-type resonances occur at the interface for all frequencies. For a double negative slab placed in vacuum, the plasmon resonances occur at both surfaces. The character of a surface plasmon mode is that it is exponentially decaying away from the surface. So when a point source is placed next to the slab, the evanescent spectrum of the point source will excite the surface plasmon resonance at the interface. The surface plasmon resonance at the first interface will excite the surface plasmon resonance at the second interface. The surface plasmon of the second interface, though exponentially decaying from the interface, is exponentially growing with respect to the first interface. Hence, within the slab, it will appear that the evanescent spectrum is exponentially growing, but it is actually due to resonance coupling between two surface plasmon modes. This amplification of the evanescent mode is the source of the proposed super-resolution in a double-negative slab.

However, this amplification process is a very fragile process. The evanescent field, by the time it reaches the first interface, could be in the noise floor of the system. When such an evanescent wave is amplified by resonance coupling, the noise content of the amplified field can be high. So in practice, even if such double-negative material exists in nature, the physics behind this amplification is highly fragile. Any system imperfection or loss could annul this physics [455, 456].

The second difficulty is to construct an artificial double negative material. This has been mimicked at microwave frequencies due to the longer wavelength and larger component sizes, but has been difficult to achieve at optical frequencies due to the shorter wavelengths, and potential loss.

Regarding the second cloaking phenomenon, it has been long observed that the material properties described by μ and ϵ are intimately related to the metric of space [457]. This is particularly clear when Maxwell's equations are written in differential forms [458]. The metric of space and material properties are inseparable.

In Cartesian coordinates in free space, a plane wave can propagate without reflections. However, one can change the metric of space. The wave will propagate through a distorted space with respect to the Cartesian coordinates, and yet it can propagate

without reflections. Hence, space can be deformed. Since metric and material properties are multiplied together, one can distort space with changing material properties. For instance, a point can be morphed into a sphere. In the original space, a point is invisible to a plane wave. In the distorted space, the wave will travel around the sphere without reflection. Hence, such material can be used to make an object invisible. However, one needs to engineer materials with μ and ϵ ranging from zero to infinity in order to be able to distort space fully [459, 460].

The above two ideas have given rise to a flurry of activity in this area, generally called the metamaterial or transformation optics area [461–463]. The promise of super-resolution and the possibility of cloaking to make objects invisible have induced a large amount of funding in this arena. Even though the original goals may not have been achieved, there has been much new knowledge created on the making of artificial materials due to the large amount of resource being invested.

1.14 Small Antennas

Antennas are used to radiate electromagnetic energy to free space, mainly for communication purposes. The first famous radiation experiment was done by Hertz [35] to confirm the wave nature of an electromagnetic field. One can model a Hertzian dipole current as

$$\mathbf{J}(\mathbf{r}) = I\ell\,\delta(\mathbf{r})\hat{z} \tag{1.159}$$

where $\hat{z}$ is a unit vector pointing in the z direction. The field produced by this current source is

$$\mathbf{E}(\mathbf{r}) = \mathrm{i}\omega\mu\left(\bar{\mathbf{I}} + \frac{\nabla\nabla}{k^2}\right)\cdot\hat{z}I\ell\,\frac{\mathrm{e}^{\mathrm{i}k|\mathbf{r}|}}{4\pi|\mathbf{r}|}. \tag{1.160}$$

In the far field, when $kr \to \infty$, the above can be approximated by replacing $\nabla = ik\hat{r}$ where $\hat{r}$ is a unit vector pointing in the r direction. For a Hertzian dipole, $I = \mathrm{i}\omega Q$ where Q is the charge on the dipole. Consequently,

$$\mathbf{E}(\mathbf{r}) \approx -\omega^2\mu(\hat{\theta}\hat{\theta} + \hat{\phi}\hat{\phi})\cdot\hat{z}Q\ell\,\frac{\mathrm{e}^{\mathrm{i}k|\mathbf{r}|}}{4\pi|\mathbf{r}|}. \tag{1.161}$$

It is seen that the radiation field is proportional to ω^2 because it is proportional to the acceleration of the charge Q. Strangely enough, a DC current loop does not radiate even though the electrons carrying the current are traveling in a circle, and hence, experiencing centrapetal acceleration. The reason is because of charge neutrality: for every electron carrying the current, a positive charge is present to neutralize the electron charge, but an electron alone traveling in a circle will radiate.

The effective aperture of an antenna is given by

$$A_{\mathit{eff}} = G\frac{\lambda^2}{4\pi} \tag{1.162}$$

where G is the antenna gain, and λ is the wavelength of the operating frequency. For small antennas, the above formula gives the erroneous concept that the aperture of the antenna becomes larger without a bound as the wavelength increases. This is incorrect, because as the frequency lowers, the radiation resistance of the antenna becomes

smaller. Finally, copper loss or material loss starts to dominate in the antenna, precluding the effective aperture from increasing without bound. In other words, the gain of the antenna drops as the frequency lowers.

A small antenna like a Hertzian dipole is a poor radiator because the dipole moment $Q\ell$ of the antenna is small. This dipole moment can be enlarged by enlarging the size of the dipole. Since a Hertzian dipole is capacitive, one can make the antenna resonate with an inductor to drive more current, and hence charge into the antenna to make it radiate more. Alternatively, one can make the dipole into a half-wave dipole so that it can self resonate to enhance the current on the antenna.

Due to the growth in the cellular phone industry, antennas have to be designed to be as inconspicuous as possible. Hence, the field of small antennas has been in vogue [464–472].

An antenna can be made into a resonating structure to enhance its radiation efficiency, such as in half-wave dipole, microstrip patch, etc. A Hertzian dipole is a small antenna, but with poor radiation efficiency because of its non-resonating nature. An inductor can be used to resonate the antenna and hence increase the current amplitude on the antenna, but at the peril of increasing loss coming from the inductor as well as increasing the Q (quality factor) of the antenna.

The Q of an antenna is defined to be [473]

$$Q = 2\pi \frac{\text{energy stored}}{\text{energy radiated per cycle}} = \frac{f_r}{\Delta f} \tag{1.163}$$

where f_r is the resonance frequency while Δf is the bandwidth. Hence, a high-Q antenna has a narrow bandwidth, which is undesirable. The Q of the antenna is also reflective of its bandwidth. A small dipole has high Q because it has much stored energy in the near field, and radiates little. The fundamental limit for the Q of a small antenna has been derived by Chu in [474]. That and others [469, 475] have improved on the tightness of the bound derived by Chu.

The alternative has been to build inductors into the antenna, which also contribute to the radiation of the antenna. This has been the concept of many small antenna designs. The resonating structure has been made smaller by using meandering line to reduce the size of the antenna. It has also exploited the inductor as radiating magnetic dipole in addition to having a radiating electric dipole. In the case of a microstrip patch, a simple microstrip patch resonator requires about half-wavelength for its resonance. Attempts have been made by using tortuous lines on a patch to increase the patch inductance so as to achieve a resonance at a lower frequency [470]. Also, one has used metamaterials to improve the efficiency for small antennas [476].

1.15 Conclusions

Electromagnetic theory and Maxwell's equations were completed in 1864. They are over 150 years old now, but their usefulness in science and technology has not diminished, as they are fundamental to many engineering technologies, especially electrical engineering technologies. From the very beginning, electrical technology grew because of the need for power transfer and communication. The importance of these two needs has not diminished in the modern world, but more technologies have emerged, such

as wireless communication, remote sensing, and emerging applications in renewable energies and wireless power transfer.

The onset of quantum mechanics brings new possibilities to electromagnetic technologies in the area of nano-optics, quantum optics, quantum communications, cryptography, and computing. All these systems use electromagnetic technologies, old and new. Therefore, electromagnetics will remain an important area of study, impacting many technologies for many years to come.

Bibliography

1 Faraday, M. (1843). On static electrical inductive action. *Philos. Mag*. 22 (144): 200–204. Faraday, M. (1839). *Experimental Researches in Electricity and Magnetism*. vol. 1. London: Taylor & Francis; vol. 2, London: Richard & John E. Taylor, 1844; vol. 3, London: Taylor and Francis, 1855. Reprinted by Dover, 1965. Also see Faraday, M. (1858). Remarks on static induction. *Proc. Roy. Inst*. (12 February 1858).

2 Ampére, A.M. (1823). Mémoire sur la théorie des phénoménes électrodynamiques. *Mem. Acad. R. Sci. Inst. France* 6: 228–232.

3 Gillmore, C.S. (1971). *Charles Augustin Coulomb: Physics and Engineering in Eighteenth Century France*. Princeton, NJ: Princeton University Press.

4 Gauss, C.F. (1841). General theory of terrestrial magnetism. In: *Scientific Memoirs*, vol. 2 (ed. R. Taylor), 184–251. London: R & J. E. Taylor.

5 Maxwell, J.C. (1865). A dynamical theory of the electromagnetic field. *Philos. Trans. R. Soc. London* 155: 459–512.

6 Maxwell, J.C. (1873). *A Treatise of Electricity and Magnetism*. 2 vols. Oxford: Clarendon Press. Also see Harman, P. M. (ed.) (1995). The Scientific Letters and Papers of James Clerk Maxwell, Vol. II, 1862–1873. Cambridge, UK: Cambridge University Press.

7 Woodruff, T.S. III (1984). *The Early Years of Radio Astronomy*. Cambridge, UK: Cambridge University Press.

8 Carlsmith, D. (2013). Particle Physics. *Upper Saddle.* River, NJ: Pearson Education, Inc.

9 Jackson, J.D. (1962). *Classical Electrodynamics*. New York, NY: Wiley.

10 Chew, W.C. and Sen, P.N. (1982). Dielectric enhancement due to electrochemical double layer: thin double layer approximation. *J. Chem. Phys.* 77 (9): 4683–4693.

11 Altman, M.D., Bardhan, J.P., White, J.K., and Tidor, B. (2008). Accurate solution of multi-region continuum biomolecule electrostatic problem using linearized Poisson-Boltzmann equation with curved boundary elements. *J. Comput. Chem.* 30 (1): 132–153.

12 Yoon, B.J. and Lenhoff, A.M. (1990). A boundary element method for molecular electrostatics with electrolyte effects. *J. Comput. Chem.* 11 (9): 1080–1086.

13 Yokota, R., Barba, L., Narumi, T., and Yasuoka, K. (2012). Scaling fast multipole methods up to 4000 GPUs. *Proceedings of the ATIP/A*CRC Workshop on Accelerator Technologies for High-Performance Computing: Does Asia Lead the Way?*

14 Wang, F., Yam, C.Y., Chen, G.H. et al. (2007). Linear scaling time-dependent density-functional tight-binding method for absorption spectra of large systems. *Phys. Rev. B* 76 (4): 045114(1)–045114(6).

15 Ionescu, A.M. and Riel, H. (2011). Tunnel field-effect transistors as energy-efficient electronic switches. *Nature* 479: 329–337.

16 Ferain, I., Colinge, C.A., and Colinge, J.-P. (2011). Multigate transistors as the future of classical metal-oxide-semiconductor field-effect transistors. *Nature* 479: 310–316.

17 del Alamo, J.A. (2011). Nanometre-scale electronics with III-V compound semiconductors. *Nature* 479: 317–323.

18 Phillips, J.R. and White, J.K. (1997). A precorrected-FFT method for electrostatic analysis of complicated 3-D structures. *IEEE Trans. Comput. Aided Des.* 16 (10): 1059–1072.

19 Zauharand, R.J. and Morgan, R.S. (1988). The rigorous computation of the molecular electric potential. *J. Comput. Chem.* 9 (2): 171–187.

20 Juffer, A.H., Botta, E.F.F., Van Keulen, B.A.M. et al. (1991). The electric potential of a macromolecule in a solvent: a fundamental approach. *J. Comput. Phys.* 97 (1): 144–171.

21 Kuo, S.-H., Tidor, B., and White, J. (2008). A meshless, spectrally accurate, integral equation solver for molecular surface electrostatics. *ACM J. Emerging. Technol. Comput.* 4 (2, Art. 6).

22 Holst, M.J. and Said, F. (1995). Numerical solution of the non-linear Poisson-Boltzmann: developing more robust and efficient methods. *J. Comput. Chem.* 16 (3): 337–364.

23 Baker, N., Holst, M., and Wang, F. (2000). Adaptive multilevel finite element solution of the Poisson Boltzmann equations II: refinement at solvent accessible surfaces in biomolecular systems. *J. Comput. Chem.* 21 (15): 1343–1352.

24 Lu, B., Zhou, Y., Holst, M., and McCammon, J. (2008). Recent progress in numerical methods for the Poisson-Boltzmann equation in biophysical applications. *Commun. Comput. Phys.* 3 (5): 973–1009.

25 Cai, W. (2013). *Computational Methods for Electromagnetic Phenomena: Electrostatics in Solvation, Scattering, and Electron Transport*. Cambridge: Cambridge University Press.

26 Chau, K.T., Li, W.L., and Lee, C.H.T. (2012). Challenges and opportunities of electric machines for renewable energy. *Prog. Electromagn. Res. B* 42: 45–74.

27 Li, G., Zhu, R., and Yang, Y. (2012). Polymer solar cells. *Nat. Photonics* 6: 153–161.

28 Atwater, H.A. and Polman, A. (2010). Plasmonics for improved photovoltaic devices. *Nat. Mater.* 9: 205–213.

29 Yoon, J., Baca, A.J., Park, S.-I. et al. (2008). Ultrathin silicon solar microcells for semitransparent, mechanically flexible and microconcentrator module designs. *Nat. Mater.* 7: 907–915.

30 Shin, J.C., Kim, K.H., Yu, K.J. et al. (2011). $In_xGa_{1-x}As$ nanowires on silicon: one-dimensional heterogeneous epitaxy, bandgap engineering, and Photovoltaics. *Nano Lett.* 11 (11): 4831–4838.

31 Li, X.H., Choy, W.C.H., Huo, L. et al. (2012). Dual plasmonic nanostructures for high performance inverted organic solar cells. *Adv. Mater.* 24 (22): 3046–3052.

32 Zhang, D., Choy, W.C.H., Wang, C.C.D. et al. (2011). Polymer solar cells with gold nanoclusters decorated multi-layer graphene as transparent electrode. *Appl. Phys. Lett.* 99 (22): 223302(1)–223302(3).

33 Yaghjian, A.D. (2014). Reflections on Maxwell's treatise. *Prog. Electromagn. Res.* 149: 217–249.

34 Nahin, P.J. (2002). *Oliver Heaviside: The Life, Work, and Times of an Electrical Genius of the Victorian Age*. JHU Press.

35 Hertz, H.R. (1888). On the propagation velocity of electrodynamic effects (in German: Ueber die Ausbreitungsgeschwindigkeit der electrodynamischen Wirkungen). *Ann. Phys.* 270 (7): 551–560.

36 Tesla, N. (1982). *My Inventions*. (Parts I through V published in the *Electrical Experimenter* monthly magazine from February through June 1919. Part VI published October 1919.) Reprint edition with introductory notes by B Johnson, Barnes, and Noble.

37 Marconi, G. Transmitting electrical signals, (using Ruhmkorff coil and Morse code key). US Patent 586,193, filed December 1896, patented July 1897.

38 Einstein, A. (1905). On the electrodynamics of moving bodies (in German: Zur elektrodynamik bewegter körper). *Ann. Phys.* 17: 891.

39 Dirac, P.A.M. (1927). The quantum theory of the emission and absorption of radiation. *Proc. R. Soc. London, Ser. A* 114 (767): 243–265.

40 Schweber, S.S. (1994). *QED and the Men Who Made It: Dyson, Feynman, Schwinger, and Tomonaga*. Princeton, NJ: Princeton University Press.

41 Mandel, L. and Wolf, E. (1995). *Optical Coherence and Quantum Optics*. Cambridge, UK: Cambridge University Press.

42 Scully, M.O. and Zubairy, M.S. (1997). *Quantum Optics*. Cambridge, UK: Cambridge University Press.

43 Loudon, R. (2000). *The Quantum Theory of Light*. Oxford, UK: Oxford University Press.

44 Gerry, C. and Knight, P. (2005). *Introductory Quantum Optics*. Cambridge, UK: Cambridge University Press.

45 Fox, M. (2006). *Quantum Optics: An Introduction*, vol. 15. Oxford, UK: Oxford University Press.

46 Garrison, J. and Chiao, J. (2014). *Quantum Optics*. Oxford, UK: Oxford University Press.

47 Milonni, P.W. (1994). *The Quantum Vacuum: An Introduction to Quantum Electrodynamics*. San Diego, CA: Academic Press.

48 Cartan, É. (1945). *Exterior Differential Systems and Its Applications (in French: Les systemes différentiels extérieurs et leurs applications géométriques)*. Hermann.

49 Warnick, K.F. and Russer, P.H. (2014). Differential forms and electromagnetic field theory. *Prog. Electromagn. Res.* 148: 83–112.

50 Yang, C.N. and Mills, R.L. (1954). Conservation of isotopic spin and isotopic gauge invariance. *Physiol. Rev.* 96 (1): 191–195.

51 Hooft, G.T. (ed.) (2005). *50 Years of Yang-Mills Theory*. Singapore: World Scientific.

52 Misner, C.W., Thorne, K.S., and Wheeler, J.A. (1973). *Gravitation*. New York, NY: Macmillan.

53 Teixeira, F.L. and Chew, W.C. (1999). Differential forms, metrics, and the reflectionless absorption of electromagnetic waves. *J. Electromagn. Wave* 13 (5): 665–686.

54 Feynman, R.P. (1985). *QED: The Strange Story of Light and Matter*. Princeton, NJ: Princeton Science.

55 Styer, D. (2012). Calculation of the anomalous magnetic moment of the electron, [Online]. Available: http://www.oberlin.edu/physics/dstyer/StrangeQM/Moment.pdf

56 Aoyama, T., Hayakawa, M., Kinoshita, T., and Nio, M. (2012). Tenth-order QED contribution to the electron g-2 and an improved value of the fine structure constant. *Phys. Rev. Lett.* 109 (11): 111807.

57 Clauser, J.F. (1974). Experimental distinction between the quantum and classical field-theoretic predictions for the photoelectric effect. *Phys. Rev. D: Part. Fields* 9 (4): 853–860.

58 Kimble, H.J., Dagaenais, M., and Mandel, L. (1977). Photon antibunching in resonance fluorescence. *Phys. Rev. Lett.* 39 (11): 691–695.

59 Aspect, A., Dalibard, J., and Roger, G. (1982). Experimental test of Bell's inequalities using time-varying analyzers. *Phys. Rev. Lett.* 49 (25): 1804–1807.

60 Griffiths, D.J. (2004). *Introduction to Quantum Mechanics*. Harlow, Essex: Pearson Education.

61 Miller, D.A.B. (2008). *Quantum Mechanics for Scientists and Engineers*. New York, NY: Cambridge University Press.

62 Ryu, C.J., Liu, A.Y., Sha, W.E.I., and Chew, W.C. (2016). Finite-difference time-domain simulation of the Maxwell-Schrodinger system. *IEEE J. Multiscale Multiphys. Comput. Tech.* 1: 40–47. http://dx.doi.org/10.1109/JMMCT.2016.2605378.

63 Xiang, Z.-L., Ashhab, S., You, J.Q., and Nori, F. (2013). Hybrid quantum circuits: superconducting circuits interacting with other quantum systems. *Rev. Mod. Phys.* 85 (2): 623–653.

64 Cohen-Tannoudji, C., Dupont-Roc, J., and Grynberg, G. (1992). *Atom-Photon Interactions: Basic Processes and Applications*. New York, NY: Wiley.

65 Datta, S. (2005). *Quantum Transport: Atom to Transistor*. New York, NY: Cambridge University Press.

66 Lamoreaux, S.K. (1997). Demonstration of the Casimir force in the 0.6 to 6 μm range. *Phys. Rev. Lett.* 78 (1): 5–8.

67 Casimir, H.B.G. (1948). On the attraction between two perfectly conducting plates. *Proc. K. Ned. Akad. Wet.* 51: 793–795.

68 Casimir, H.B.G. and Polder, D. (1948). The influence of retardation on the London-van der Waals forces. *Physiol. Rev.* 73: 360–372.

69 Novotny, L. and Hecht, B. (2008). *Principles of Nano-Optics*. New York, NY: Cambridge University Press.

70 Dung, H.T., Knöll, L., and Welsch, D.-G. (1998). Three-dimensional quantization of the electromagnetic field in dispersive and absorbing inhomogeneous dielectrics. *Phys. Rev. A* 57 (5): 3931–3942.

71 Scheel, S. and Buhmann, S.Y. (2008). Macroscopic quantum electrodynamics concepts and applications. *Acta Phys. Slov.* 58 (5): 675–809.

72 Tai, C.T. (1994). Dyadic Green Functions in Electromagnetic Theory, *2e*. Piscataway, NJ: IEEE Press.

73 Chew, W.C. (2014). Vector potential electromagnetics with generalized gauge for inhomogeneous media: formulation. *Prog. Electromagn. Res.* 149: 69–84.

74 Kong, J.A. (1986). *Theory of Electromagnetic Waves*. New York, NY: Wiley.

75 Ishimaru, A. (1991). *Electromagnetic Wave Propagation, Radiation, and Scattering*. Upper Saddle River, NJ: Prentice Hall.

76 Chew, W.C. (1995). *Waves and Fields in Inhomogeneous Media*, vol. 522. IEEE Press. First Printing 1990.

77 Yaghjian, A.D. (1980). Electric dyadic Green's functions in the source region. *Proc. IEEE* 68 (2): 248–263.

78 Green, G. (1828). *An Essay on the Application of Mathematical Analysis to the Theories of Electricity and Magnetism*. Nottingham: T. Wheelhouse. Also, see Challis, L. and Sheard, F. (2003). The green of Green functions. *Physics Today* (December 2003), pp. 41–46.

79 Lancaster, T. and Blundell, S.J. (2014). *Quantum Field Theory for the Gifted Amateur*. OUP Oxford.

80 Chew, W.C., Liu, A.Y., Salazar-Lazaro, C., and Sha, W.E.I. (2016). Quantum electromagnetics: a new look, Part I. *IEEE J. Multiscale Multiphys. Comput. Tech.* 1: 73–84.

81 Chew, W.C., Liu, A.Y., Salazar-Lazaro, C., and Sha, W.E.I. (2016). Quantum electromagnetics: a new look, Part II. *IEEE J. Multiscale Multiphys. Comput. Tech.* 1: 85–97.

82 Chen, Y.P., Sha, W.E.I., Choy, W.C.H. et al. (2012). Study on spontaneous emission in complex multilayered plasmonic system via surface integral equation approach with layered medium Green's function. *Opt. Express* 20 (18): 20210–20221.

83 Sha, W.E.I., Liu, A.Y., and Chew, W.C. Dissipative quantum electromagnetics: a Novel Approach, accepted by *JMMCT*.

84 Dirac, P.*A*.M. (1928). The quantum theory of the electron. *Proc. R. Soc. London, Ser. A* 117 (778): 610–624.

85 Anderson, C.D. (1932). The apparent existence of easily deflectable positives. *Science* 76 (1967): 238–239.

86 Heaviside, O. (1888). On electromagnetic waves, especially in relation to the vorticity of the impressed forces, and the forced vibration of electromagnetic systems. *Philos. Mag.* 25: 130–156.

87 Chew, W.C. (2004). Computational electromagnetics: the physics of smooth versus oscillatory fields. *Philos. Trans. R. Soc. London, Ser. A* 362 (1816): 579–602.

88 Morse, S.F.B. (1869). *Examination of the Telegraphic Apparatus and the Processes in Telegraphy*. Washington, WA: Philip and Solomons.

89 Pohl, R.W. (1924). *Einführung in die Physik*, vol. 3. Göttingen: Springer.

90 Novotny, L. and Hecht, B. (2006). *Principles of Nano-Optics*. Cambridge, UK: Cambridge University Press.

91 Rokhlin,V. Yale University, New Haven, CT, private communication.

92 Van Dyke, M.D. (1964). *Perturbation Methods in Fluid Mechanics*. New York, NY: Academic Press.

93 Chew, W.C., Tong, M.S., and Hu, B. (2008). *Integral Equations Methods for Electromagnetic and Elastic Waves*. Morgan & Claypool.

94 Dirac, P.*A*.M. (1927). The quantum theory of the emission and absorption of radiation. *Proc. R. Soc. London, Ser. A* 114 (767): 243–265.

95 Gerry, C. and Knight, P. (2004). *Introductory Quantum Optics*. Cambridge, UK: Cambridge University Press.

96 Fox, M. (2006). *Quantum Optics: An Introduction*. Oxford, UK: Oxford University Press.

97 Cohen-Tannoudji, C., Dupont-Roc, J., and Grynberg, G. (1997). *Photons and Atoms: Introduction to Quantum Electrodynamics*. New York, NY: Wiley.

98 Miller, D.A.B. (2008). *Quantum Mechanics for Scientists and Engineers*. New York, NY: Cambridge University Press.

99 Chew, W.C. (2016). Lecture Notes: Quantum Mechanics Made Simple. Internet: http://wcchew.ece.illinois.edu/chew/course/QMAll20161206.pdf (6 December 2016).

100 Keller, J.B. (1962). Geometrical theory of diffraction. *J. Opt. Soc. Am.* 52 (2): 116–130.

101 Kouyoumjian, R.G. (1965). Asymptotic high-frequency methods. *Proc. IEEE* 53 (8): 864–876.

102 Kouyoumjian, R.G. and Pathak, P.H. (1974). A uniform geometrical theory of diffraction for an edge in a perfectly conducting surface. *Proc. IEEE* 62 (11): 1448–1461.

103 Lee, S.W. and Deschamps, G.A. (1976). A uniform asymptotic theory of electromagnetic diffraction by a curved wedge. *IEEE Trans. Antennas Propag.* 24 (1): 25–34.

104 Hansen, R.C. (ed.) (1981). *Geometric Theory of Diffraction*. Piscataway, NJ: IEEE Press.

105 Pathak, P.H. (1992). High-frequency techniques for antenna analysis. *Proc. IEEE* 80 (1): 44–65.

106 Born, M. and Wolf, E. (1964). *Principles of Optics: Electromagnetic Theory of Propagation, Interference and Diffraction of Light*, 1e. London, UK: Macmillan. Cambridge, UK: Cambridge University Press, 1999.

107 Mandel, L. and Wolf, E. (1995). *Optical Coherence and Quantum Optics*. Cambridge, UK: Cambridge University Press.

108 Stroke, G.W. (1966). *An Introduction to Coherent Optics and Holography*. New York, NY: Academic Press.

109 Haus, H.A. (2000). *Electromagnetic Noise and Quantum Optical Measurements*. Berlin: Springer-Verlag.

110 Viktorov, I.A. (1967). *Rayleigh and Lamb Waves: Physical Theory and Applications*. New York, NY: Plenum Press.

111 Stoneley, R. (1928). The dispersion of waves in a double superficial layer. *Geophys. J. Int.* 1 (s10): 527–532.

112 Faraday, M. (1857). Experimental relations of gold (and other metals) to light. *Philos. Trans. R. Soc. London* 147: 145–181.

113 Mie, G. (1908). Beiträge zur optik trüber medien, speziell kolloidaler metallösungen. *Ann. Phys.* 330 (3): 377–445.

114 Choudhuri, A.R. (1998). *The Physics of Fluids and Plasma*. Cambridge, UK: Cambridge University Press.

115 Chew, W.C., Jin, J.M., Michielssen, E., and Song, J.M. (eds.) (2001). *Fast and Efficient Algorithms in Computational Electromagnetics*. Boston, MA: Artech House.

116 Strutt Rayleigh, J.W. (Lord Rayleigh) (1976). *Theory of Sound*. New York, NY: Dover Publications (originally published 1877).

117 Strutt Rayleigh, J.W. (Lord Rayleigh) (1897). On the passage of electric waves through tubes, or the vibrations of dielectric cylinders. *Philos. Mag.* 43: 125–132.

118 Bowman, J.J., Senior, T.B.A., Uslenghi, P.L.E., and Asvestas, J.S. (1970). *Electromagnetic and Acoustic Scattering by Simple Shapes*. Amsterdam: North-Holland Publishing Co.

119 Debye, P. (1909). Der lichtdruck auf kugeln von beliebigem material. *Ann. Phys.* 4 (30): 57.

120 Strutt Rayleigh, J.W. (Lord Rayleigh) (1871). On the scattering of light by small particles. *Philos. Mag*., Series 4, 41: 447–454.

121 Abramowitz, M. and Stegun, I.A. (1965). *Handbook of Mathematical Functions*. New York, NY: Dover Publications.

122 Stratton, J.A. (1941). *Electromagnetic Theory*. New York, NY: McGraw-Hill.

123 Harrington, R.F. (1961). *Time-Harmonic Electromagnetic Fields*. New York, NY: McGraw-Hill.

124 Collin, R.E. (1991). *Field Theory of Guided Waves*. Piscataway, NJ: IEEE Press.

125 Balanis, C.A. (1989). *Engineering Electromagnetics*. New Jersey, NJ: Wiley.

126 Jin, J.M. (2010). *Theory and Computation of Electromagnetic Fields*. New York, NY: Wiley.

127 Sommerfeld, A. (1909). Über die ausbreitung der wellen in der drahtlosen telegraphie. *Ann. Phys.* 28 (25): 665–737.

128 Weyl, H. (1919). Ausbreitung electromagnetischer wellen über einem ebenen leiter. *Ann. Phys.* 365 (21): 481–500.

129 Kong, J.A. (1972). Electromagnetic field due to dipole antennas over stratified anisotropic media. *Geophysics* 37 (6): 985–996.

130 Sommerfeld, A. (1896). Mathematische Theorie der Diffraction. *Math. Ann.* 47 (s319): 317–374.

131 Heins, A.E. (1982). The Sommerfeld half-plane problem revisited I: the solution of a pair of coupled Wiener-Hopf integral equations. *Math. Methods Appl. Sci.* 4 (1): 74–90.

132 Ziolkowski, R.W. (1987). Exact solution of the Sommerfeld half-plane problem: a path integral approach without discretization. *J. Electromagn. Waves Appl.* 1 (4): 377–402.

133 Wiener, N. and Hopf, E. (1931). Ueber eine Klasses singulärer Integralgleichungen. *S.-B. Deutsch. Akad. Wiss. Berlin KI. Math. Phys. Tech*. 696–706.

134 Banos, A. (1966). *Dipole Radiation in the Presence of a Conducting Half-Space*. Oxford: Pergamon Press.

135 Felsen, L.B. and Marcuvitz, N. (1972). *Radiation and Scattering of Waves*. Englewood Cliffs, NJ: Prentice-Hall.

136 Chew, W.C. (1983). The singularities of a Fourier-type integral in a multicylindrical layer problem. *IEEE Trans. Antennas Propag.* 31 (4): 653–655.

137 Bleistein, N. and Handelsman, R.A. (1974). *Asymptotic Expansions of Integrals*. New York, NY: Holt Rinehart and Winston.

138 Lewis, R. M. and Keller, J. B. (1964). Asymptotic methods for partial differential equations: the reduced wave equation and Maxwell's equations. *N.Y.U. Research Report No. EM-194*.

139 Watson, G.N. (1918). The diffraction of electric waves by the earth. *Proc. R. Soc. London, Ser. A* 95 (666): 83–99.

140 Li, M.K. and Chew, W.C. (2004). A new Sommerfeld-Watson transformation in 3-D. *IEEE Antennas Wirel. Propag. Lett*. 3 (1): 75–78.

141 Sha, W.E.I. and Chew, W.C. (2009). High frequency scattering by an impenetrable sphere. *Prog. Electromagn. Res.* 97: 291–325.

142 Shore, R.A. and Yaghjian, A.D. (1988). Incremental diffraction coefficients for planar surfaces. *IEEE Trans. Antennas Propag.* 36 (1): 55–70.

143 Batchelor, G.K. (1967). *An Introduction to Fluid Dynamics*. New York, NY: Cambridge University Press.

144 Wentzel, G. (1926). A generalization of the quantum conditions for the purposes of wave mechanics. *Z. Angew. Phys.* 38 (6-7): 518–529.

145 Kramers, H.A. (1926). Wave mechanics and semi-numerical quantisation. *Z. Angew. Phys.* 30 (10-11): 828–840.

146 Brillouin, L. (1926). The undulatory mechanics of Schrödinger: a general method of solution by successive approximations. *C.R. Hebd. Seances Acad. Sci.* 183 (5): 24–26.

147 Kirchhoff, G. (1877). Zur Theorie des Condensators, *144–162*. Berlin: Akad. Monatsber.

148 Chew, W.C. and Kong, J.A. (1981). Asymptotic formula for the capacitance of two oppositely charged discs. *Math. Proc. Cambridge Philos. Soc.* 89: 373–384.

149 Leppington, F. and Levine, H. (1970). On the capacity of the circular disc condenser at small separation. *Cambridge Philos. Soc.* 68 (1): 235–254.

150 Spurling, K.L., Poitras, A.E., McGranaghan, M.F., and Shaw, J.H. (1987). Analysis and operating experience for back-to-back 115 kV capacitor banks. *IEEE Trans. Power Delivery* 2 (4): 1255–1263.

151 Hildebrand, F.B. (1976). *Advanced Calculus for Applications*. Prentice-Hall.

152 Chew, W.C. and Kong, J.A. (1982). Microstrip capacitance for a circular disk through matched asymptotic expansions. *SIAM J. Appl. Math.* 42 (2): 302–317.

153 Poh, S.Y., Chew, W.C., and Kong, J.A. (1981). Approximate formulas for line capacitance and characteristic impedance of microstrip line. *IEEE Trans. Microwave Theory Tech.* 29 (2): 135–142.

154 Michell, J.H. (1894). A map of the complex Z-function: a condenser problem. *Messenger. Math. Cambridge.* 23: 72–78.

155 I'a Bromwich, T.J. (1902). Note on a condenser problem. *Messenger Math. Cambridge* 31: 184–192.

156 Love, A.E.H. (1924). Some electrostatic distributions in two dimensions. *Proc. London Math. Soc.*, Series 2, 22 (1460): 337–369.

157 Chew, W.C. and Kong, J.A. (1981). Asymptotic formula for the resonant frequencies of a circular microstrip antenna. *J. Appl. Phys.* 52 (8): 5365–5369.

158 Chew, W.C. and Kong, J.A. (1981). Asymptotic eigenequations and analytic formulas for the dispersion characteristics of open, wide microstrip lines. *IEEE Trans. Microwave Theory Tech.* 29 (9): 933–941.

159 Dukhin, S. and Shilov, V.N. (1974). *Dielectric Phenomena and the Double Layer in Disperse Systems and Polyelectrolytes*. New York, NY: Wiley.

160 Fixman, M. (1980). Charged macromolecules in external fields. I. The sphere. *J. Chem. Phys.* 72 (9): 5177–5186.

161 Hinch, E.J., Sherwood, J.D., Chew, W.C., and Sen, P.N. (1984). The dielectric response of a dilute suspension of spheres with thin double layers in an asymmetric electrolyte. *J. Chem. Soc., Faraday Trans.* 2 (80): 535–551.

162 Conde, O.M., Pérez, J., and Cátedra, M.F. (2001). Stationary phase method application for the analysis of radiation of complex 3-D conducting structures. *IEEE Trans. Antennas Propag.* 49 (5): 724–731.

163 Carluccio, G., Albani, M., and Pathak, P.H. (2010). Uniform asymptotic evaluation of surface integrals with polygonal integration domains in terms of UTD transition functions. *IEEE Trans. Antennas Propag.* 58 (4): 1155–1163.

164 Ufimtsev, P.Y. (2007). *Fundamentals of the Physical Theory of Diffraction*. New York, NY: Wiley.

165 Wikipedia, Human Computer. Internet: http://en.wikipedia.org/wiki/Human_computer (4 December 2012).

166 Gumbrecht, J. (2011) Rediscovering WWII's female 'computers'. Internet: http://www.cnn.com/2011/TECH/innovation/02/08/women.rosies.math/index.html (8 February 2011).

167 Wikipedia, Mechanical Computer. Internet: http://en.wikipedia.org/wiki/Mechanical_computer (7 December 2012).

168 Ceruzzi, P.E. (1998). *A History of Modern Computing*. Cambridge, MA: MIT Press.

169 ENIA Wikipedia, ENIAC. Internet: http://en.wikipedia.org/wiki/ENIAC (22 December 2012).

170 ILLIAC Wikipedia, ILLIAC. Internet: http://en.wikipedia.org/wiki/ILLIAC (17 December 2012).

171 Zienkiewicz, O.C. (1977). The Finite Element Method*, 3e*. London: McGraw-Hill.

172 Silvester, P.P. and Ferrari, R.L. (1983). *Finite Elements for Electrical Engineers*. Cambridge: Cambridge University Press.

173 Silvester, P.P., Itoh, T., and Pelosi, G. (1996). *Finite Element Software for Microwave Engineering*. New York, NY: Wiley.

174 Jin, J.M. (2002). The Finite Element Method in Electromagnetics*, 2e*. New York, NY: Wiley-IEEE Press.

175 Volakis, J.L., Chaterjee, A., and Kempel, L.C. (1998). *Finite Element Method Electromagnetics: Antennas, Microwave Circuits, and Scattering Applications*. New York, NY: Wiley-IEEE Press.

176 Zhu, Y. and Cangellaris, A.C. (2006). *Multigrid Finite Element Methods for Electromagnetic Field Modeling*. Hoboken, NJ: Wiley-IEEE Press.

177 Yee, K.S. (1966). Numerical solution of initial boundary value problems involving Maxwell's equation in isotropic media. *IEEE Trans. Antennas Propag.* 14: 302–307.

178 Taflove, A. (1995). *Computational Electrodynamics: The Finite Difference Time Domain Method*. Boston: Artech House.

179 Harrington, R.F. (1968). *Field Computation by Moment Method*. New York, NY: Macmillan.

180 Richmond, J. (1965). Scattering by a dielectric cylinder of arbitrary cross section shape. *IEEE Trans. Antennas Propag.* 13 (3): 334–341.

181 Rao, S.M., Wilton, G.R., and Glisson, A.W. (1982). Electromagnetic scattering by surfaces of arbitrary shape. *IEEE Trans. Antennas Propag.* 30 (3): 409–418.

182 Nakhla, M.S. and Vlach, J. (1976). A piecewise harmonic balance technique for determination of periodic response of nonlinear systems. *IEEE Trans. Circuits Syst.* 23 (2): 85–91.

183 Gilmore, R.J. and Steer, M.B. (1991). Nonlinear circuit analysis using the method of harmonic balance-A review of the art. Part I. Introductory concepts. *Int. J. Microwave Millimeter-Waves Comput.-Aided Eng.* 1 (1): 22–37.

184 Yamada, S., Bessho, K., and Lu, J. (1989). Harmonic balance finite element method applied to nonlinear AC magnetic analysis. *IEEE Trans. Magn.* 25 (4): 2971–2973.

185 Parrón, J., Collado, C., Mateu, J. et al. (2001). General electromagnetic simulation tool to predict the microwave nonlinear response of planar, arbitrarily-shaped HTS structures. *IEEE Trans. Appl. Supercond.* 11 (1): 399–402.

186 Newton, I. *Methodus fluxionum et serierum infinitarum*, 1664–1671.

187 Raphson, J. *Analysis aequationum universalis*, London, 1690.

188 Fletcher, R. (1987). Practical Methods of Optimization*, 2e*. New York, NY: Wiley.

189 Medgyesi-Mitschang, L.N., Putnam, J.M., and Gedera, M.B. (1994). Generalized method of moments for three-dimensional penetrable scatterers. *J. Opt. Soc. Am. A* 11 (4): 1383–1398.

190 Sommerfeld, A. (1949). *Partial Differential Equation*. New York, NY: Academic Press.

191 Garabedian, P.R. (1964). *Partial Differential Equations*. New York, NY: Wiley.

192 Courant, R. and Hilbert, D. (1953–1962). *Methods of Mathematical Physics*. New York, NY: Interscience Publishers.

193 Mautz, J.R. and Harrington, R.F. (1978). *H*-field, *E*-field, and combined-field solutions for conducting bodies of revolution. *A. E. Ü.* 32: 157–164.

194 Harrington, R.F. (1989). Boundary integral formulations for homogenous material bodies. *J. Electromagn. Waves Appl.* 3 (1): 1–15.

195 Müller, C. (1969). *Foundation of the Mathematical Theory of Electromagnetic Waves*. Berlin: Springer-Verlag.

196 Werner, P. (1963). On the exterior boundary value problem of the perfect reflection for the stationary electromagnetic wave fields. *J. Math. Anal. Appl.* 7: 348–396.

197 Schenck, H.A. (1968). Improved integral formulation for acoustic radiation problems. *J. Acoust. Soc. Am.* 44 (1): 41–58.

198 Mitzner, K.M. (1968). Numerical solution of the exterior scattering problem at the eigen-frequencies of the interior problem, *URSI Meeting Digest*, 75, Boston.

199 Burton, *A. J.* and Miller, G.F. (1971). The application of integral equation methods to the numerical solution of some exterior boundary value problems. *Proc. R. Soc. London, Ser. A* 323 (1553): 201–210.

200 Bolomey, J.C. and Tabbara, W. (1973). Numerical aspects on coupling between complementary boundary value problems. *IEEE Trans. Antennas Propag.* 21 (3): 356–363.

201 Mittra, R. and Klein, C.A. (1975). Stability and convergence of moment method solutions. *Numer. Asymp. Tech. Electromagn.* 3: 129–163.

202 Morita, N. (1979). Resonant solutions involved in the integral equation approach to scattering from conducting and dielectric cylinders. *IEEE Trans. Antennas Propag.* 27 (6): 869–871.

203 Yaghjian, A.D. (1981). Augmented electric- and magnetic-field integral equations. *Radio Sci.* 16: 987–1001.

204 Peterson, A.F. (1990). The interior resonance problem associated with surface integral equations of electromagnetics: numerical consequences and a survey of remedies. *Electromagnetics* 10 (3): 293–312.

205 Chew, W.C. and Song, J.M. (2007). Gedanken experiments to understand the internal resonance problems of electromagnetic scattering. *Electromagnetics* 27 (8): 457–471.

206 Song, J.M., Shu, W.W., and Chew, W.C. (2007). Numerical resonances in method of moments. *IEEE APS Int. Symp. Dig.* 4861–4864.

207 Wilton, D.R. (1992). Review of current status and trends in the use of integral equations in computational electromagnetics. *Electromagnetics* 12 (3-4): 287–341.

208 Mautz, J.R. and Harrington, R.F. (1979). A combined-source solution for radiation and scattering from a perfectly conducting body. *IEEE Trans. Antennas Propag.* 27 (4): 445–454.

209 Andriulli, F.P., Cools, K., Bagci, H. et al. (2008). A multiplicative Calderon preconditioner for the electric field integral equation. *IEEE Trans. Antennas Propag.* 56 (8): 2398–2412.

210 Cools, K., Andriulli, F.P., Olyslager, F., and Michielssen, E. (2009). Improving the MFIE's accuracy by using a mixed discretization. *IEEE Antennas Propag. Soc. Int. Symp*. 1–4.

211 Bagci, H., Andriulli, F.P., Cools, K. et al. (2010). A Calderon multiplicative preconditioner for coupled surface-volume electric field integral equations. *IEEE Trans. Antennas Propag.* 58 (8): 2680–2690.

212 Petrov, G. (1940). Application of Galerkin's method to a problem of the stability of the flow of a viscous liquid." (Russian). *Prikad. Matem. i Mekh* 4 (3): 3–12.

213 Belytschiko, T., Lu, Y.Y., and Gu, L. (1994). Element-free Galerkin methods. *Int. J. Numer. Methods Eng.* 37 (2): 229–256.

214 Brooks, A.N. and Hughes, T.J.R. (1982). Streamline upwind/Petrov-Galerkin formulations for convection dominated flows with particular emphasis on the incompressible Navier-Stokes equations. *Comput. Meth. Appl. Mech. Eng.* 32 (1–3): 199–259.

215 Saad, Y. (2003). *Iterative Methods for Sparse Linear Systems*. SIAM.

216 Chan, T.F. and Ng, M.K. (1999). Galerkin projection methods for solving multiple linear systems. *SIAM J. Sci. Comp.* 21 (3): 836–850.

217 Graglia, R.D. (1993). On the numerical integration of the linear shape functions times the 3D Green's function or its gradient on a plane triangle. *IEEE Trans. Antennas Propag.* 41 (10): 1448–1456.

218 Graglia, R.D., Wilton, D.R., and Peterson, A.F. (1997). Higher order interpolatory vector bases for computational electromagnetics. *IEEE Trans. Antennas Propag.* 45 (3): 329–342.

219 Greengard, L. and Rokhlin, V. (1987). A fast algorithm for particle simulations. *J. Comput. Phys.* 73: 325–348.

220 Willis, D.J., Peraire, J., and White, J.K. (1997). A combined pFFT-multipole tree code, unsteady panel method with vortex particle wakes. *Int. J. Numer. Methods Fluids* 53: 1399–1422.

221 Bleszynski, E., Bleszynski, M., and Jaroszewicz, T. (1996). AIM: Adaptive integral method for solving large-scale electromagnetic scattering and radiation problems. *Radio Sci.* 31 (5): 1225–1251.

222 Lu, C.C. and Chew, W.C. (1994). Multilevel algorithm for solving boundary-value scattering. *Microwave Opt. Technol. Lett.* 7 (10): 466–470.

223 Song, J.M. and Chew, W.C. (1995). Multilevel fast-multipole algorithm for solving combined field integral equations of electromagnetic scattering. *Microwave Opt. Technol. Lett.* 10 (1): 14–19.

224 Velamparambil, S., Chew, W.C., and Song, J.M. (2003). 10 million unknowns, is it that large. *IEEE Antennas Propag. Mag.* 45 (2): 43–58.

225 Trefethen, L.N. and Bau, D. (1997). *Numerical Linear Algebra*, No. 50. SIAM.

226 Saad, Y. (1989). Krylov subspace methods on supercomputers. *SIAM J. Sci. Stat. Comput.* 10: 1200–1232.

227 Saad, Y. (1981). Krylov subspace methods for solving large unsymmetric linear systems. *Math. Comput.* 37: 105–126.

228 Saad, L.Y. and Schultz, M.H. (1986). GMRES: a generalized minimal residual algorithm for solving nonsymmetric linear systems. *SIAM J. Sci. Stat. Comput.* 7 (3): 856–869.

229 Trefethen, L.N. (1990). *Approximation theory and numerical linear algebra*. In: *Algorithms for Approximation II*, Chapman, London (eds. J.C. Mason and M.G. Cox).

230 Nachtigal, N.M., Reddy, S.C., and Trefethen, L.N. (1992). How fast are nonsymmetric matrix iterations. *SIAM J. Matrix Anal. Appl.* 13 (3): 778–795.

231 Driscoll, T.A., Toh, K.-C., and Trefethen, L.N. (1998). From potential theory to matrix iterations in six steps. *SIAM Rev.* 40: 547–578.

232 Liesen, J. and Tichy, P. (2004). Convergence analysis of Krylov subspace methods. *GAMM-Mitteilungen* 27 (2): 153–173.

233 Siefert, C. and de Sturler, E. (2006). Preconditioners for generalized saddle-point problems. *SIAM J. Numer. Anal.* 44 (3): 1275–1296.

234 Lee, R. and Cangellaris, A.C. (1992). A study of discretization error in the finite element approximation of wave solution. *IEEE Trans. Antennas Propag.* 40 (5): 542–549.

235 George, J.A. (1973). Nested dissection of a regular finite element mesh. *SIAM J. Numer. Anal.* 10: 345–363.

236 George, A. and Liu, J.W.H. (1976). An algorithm for automatic nested dissection and its application to general finite element problems. In: *Proceedings of the Sixth Conference on Numerical Mathematics and Computing, Winnipeg, Manitoba*, 59–94.

237 Irons, B.M. (1970). A frontal solution scheme for finite element analysis. *Int. J. Numer. Methods Eng.* 2: 5–32.

238 Axelsson, O. and Barker, V.A. (1984). *Finite Element Solution of Boundary Value Problems: Theory and Computation*. Academic Press.

239 Bayliss, A. and Turkel, E. (1980). Radiation boundary conditions for wave-like equations. *Commun. Pure Appl. Math.* 33: 707–725.

240 Engquist, B. and Majda, A. (1977). Absorbing boundary conditions for the numerical simulation of waves. *Math. Comput.* 31: 629–651.

241 Fang, J. and Mei, K.K. (1988). A super-absorbing boundary algorithm for solving electromagnetic problems by time-domain finite-difference method. *IEEE AP-S Int. Symp. Dig.* 2, 472–474.

242 Liao, Z.P., Wong, H.L., Yang, B.P., and Yuan, Y.F. (1984). A transmitting boundary for transient wave analysis. *Sci. Sin., Ser. A* 27 (10): 1063–1076.

243 Lindman, E.L. (1975). Free space boundary conditions for the time dependent wave equation. *J. Comput. Phys.* 18: 66–78.

244 Mur, G. (1981). Absorbing boundary conditions for the finite-difference approximation of the time-domain electromagnetic-field equations. *IEEE Trans. Electromagn. Compat.* 23: 377–382.

245 Randall, C.L. (1988). Absorbing boundary conditions for the elastic wave equation. *Geophysics* 53 (5): 611–624.

246 Wagatha, L. (1983). Approximation of pseudodifferential operators in absorbing boundary conditions for hyperbolic equations. *Numer. Math.* 42: 1–64.

247 Higdon, R.L. (1987). Numerical absorbing boundary conditions for the wave equation. *Math. Comput.* 49: 65–90.

248 Mittra, R., Ramahi, O.O., Khebir, A. et al. (1989). A review of absorbing boundary conditions for two and three-dimensional electromagnetic scattering problems. *IEEE Trans. Magn.* 25 (4): 3034–3039.

249 Ziolkowski, R.W. (2008). FDTD absorbing boundary conditions: From global lookback schemes to metamaterial PMLs. *Antennas and Propagation Society International Symposium, 2008. AP-S 2008. IEEE*: 1–4 (5–11 July 2008).

250 Alavikia, B., Ramahi, O.M.(2010). Limitation of using absorbing boundary condition to solve the problem of scattering from a cavity in metallic screens. *Antennas and Propagation Society International Symposium (APSURSI), 2010 IEEE*: 1–4 (11–17 July 2010).

251 Berenger, J.-P. (1994). A perfectly matched layer for the absorption of electromagnetic waves. *J. Comput. Phys.* 114: 185–200.

252 Chew, W.C. and Weedon, W.H. (1994). A 3-D perfectly matched medium from modified Maxwell's equations with stretched coordinates. *Microwave Opt. Technol. Lett.* 7 (13): 599–604.

253 Sacks, Z.S., Kingsland, D.M., Lee, R., and Lee, J.-F. (1995). A perfectly matched anisotropic absorber for use as an absorbing boundary condition. *IEEE Trans. Antennas Propag.* 43 (12): 1460–1463.

254 Katz, D.S., Thiele, E.T., and Taflove, A. (1994). Validation and extension to three dimensions of the Berenger PML absorbing boundary condition for FD-TD meshes. *IEEE Microwave Guided Wave Lett.* 4 (8): 268–270.

255 Mittra, R. and Pekel, U. (1995). A new look at the perfectly matched layer (PML) concept for the reflectionless absorption of electromagnetic waves. *IEEE Microwave Guided Wave Lett.* 5 (3): 84–86.

256 Navarro, E.A., Wu, C., Chung, P.Y., and Litva, J. (1994). Application of PML superabsorbing boundary condition to non-orthogonal FDTD method. *Electron. Lett.* 30 (20): 1654–1656.

257 Gribbons, M., Lee, S.K., and Cangellaris, A.C. (1995). Modification of Berenger's perfectly matched layer for the absorption of electromagnetic waves in layered media. In: *11th Annual Review of Progress in ACES*, 498–503.

258 Andrew, W.V., Balanis, C.A., and Tirkas, P.A. (1995). A comparison of the Berenger perfectly matched layer and the Lindman higher-order ABC's for the FDTD method. *IEEE Microwave Guided Wave Lett.* 5 (6): 192–194.

259 Fang, J. and Wu, Z. (1995). Generalized perfectly matched layer—an extension of Berenger's perfectly matched layer boundary condition. *IEEE Microwave Guided Wave Lett.* 5 (12): 451–453.

260 Abarbanel, S. and Gottlieb, D. (1998). On the construction and analysis of absorbing layers in CEM. *Appl. Numer. Math.* 27: 331–340.

261 Teixeira, F.L. and Chew, W.C. (1997). PML-FDTD in cylindrical and spherical grids. *IEEE Micro. Guided Wave Lett.* 7 (9): 285–287.

262 Chew, W.C. and Liu, Q.H. (1996). Perfectly matched layers for elastodynamics: A new absorbing boundary condition. *J. Comput. Acoust.* 4 (4): 341–359.

263 Zeng, Y.Q., He, J., and Liu, Q.H. (2001). The application of the perfectly matched layer in numerical modeling of wave propagation in poroelastic media. *Geophysics* 66 (4): 1258–1266.

264 Cheng, C., Lee, J.-H., Lim, K.H. et al. (2007). 3D quantum transport solver based on the perfectly matched layer and spectral element methods for the simulation of semiconductor nanodevices. *J. Comput. Phys.* 227: 455–471. https://doi.org/10.1016/j.jcp.2007.07.028.

265 Peng, Z., Wang, X.C., and Lee, J.F. (2011). Integral equation based domain decomposition method for solving electromagnetic wave scattering from non-penetrable objects. *IEEE Trans. Antennas Propag.* 59 (9): 3328–3338.

266 Chew, W.C. and Wang, Y.M. (1990). A fast algorithm for solution of a scattering problem using a recursive aggregate tau matrix method. *Microwave Opt. Technol. Lett.* 3 (5): 164–169.

267 Chew, W.C. and Lu, C.C. (1995). The recursive aggregated interaction matrix algorithm for multiple scatterers. *IEEE Trans. Antennas Propag.* 43 (12): 1483–1486.

268 Chew, W.C. and Lu, C.C. (1993). NEPAL–An algorithm for solving the volume integral equation. *Microwave Opt. Technol. Lett.* 6 (3): 185–188.

269 Lu, C.C. and Chew, W.C. (1995). The use of Huygens' equivalence principle for solving 3D volume integral equation of scattering. *IEEE Trans. Antennas Propag.* 43 (5): 500–507.

270 Chew, W.C. and Lu, C.C. (1993). A fast recursive algorithm to compute the wave scattering solution of a large strip. *J. Comput. Phys.* 107: 378–387.

271 Michielssen, E., Boag, A., and Chew, W.C. (1996). Scattering from elongated objects: direct solution in $O(N \log^2 N)$ operations. *IEEE Proc. Microwaves Antennas Propag*. 143 (4): 277–283. IET.

272 Chai, W. and Jiao, D. (2008). An H2-matrix-based integral-equation solver of linear-complexity for large-scale full-wave modeling of 3D circuits. In: *Electrical Performance of Electronic Packaging*, 283–286. IEEE-EPEP.

273 Guo, H., Liu, Y., Hu, J., and Michielssen, E. (2017). A butterfly-based direct integral-equation solver using hierarchical LU factorization for analyzing scattering from electrically large conducting objects. *IEEE Trans. Antennas Propag.* 65 (9): 4742–4750.

274 Borup, D.T. and Gandhi, O.P. (1984). Fast-Fourier transform method for calculation of SAR distributions in finely discretized inhomogeneous models of biological bodies. *IEEE Trans. Microwave Theory Tech.* 32 (4): 355–360.

275 Shen, C.Y., Glover, K.J., Sancer, M.I., and Varvatsis, A.D. (1989). The discrete Fourier transform method of solving differential-integral equations in scattering theory. *IEEE Trans. Antennas Propag.* 37 (8): 1032–1041.

276 Zwamborn, P. and van den Berg, P.M. (1992). The three-dimensional weak form of the conjugate gradient FFT method for solving scattering problems. *IEEE Trans. Microwave Theory Tech.* 40 (9): 1757–1766.

277 Catedra, M.F., Gago, E., and Nuno, L. (1989). A numerical scheme to obtain the RCS of three-dimensional bodies of size using the conjugate gradient method and the fast Fourier transform. *IEEE Trans. Antennas Propag.* 37 (5): 528–537.

278 Phillips, J.R. and White, J.K. (1994). Efficient capacitance computation of 3D structures using generalized pre-corrected FFT methods. In: Proceedings of the 3rd

Topical Meeting on Electric Performance of Electronic Packaging, *Nov*. 2–4, Monterey, CA.

279 Lumme, K. and Rahola, J. (1994). Light scattering by porous dust particles in the discrete-dipole approximation. *Astrophys. J.* 425: 653–667.

280 Bleszynski, E., Bleszynski, M., and Jaroszewicz, T. (1994). A fast integral-equation solver for electromagnetic scattering problems. *IEEE APS Int. Symp. Dig.* 416–419.

281 Chan, C.H. and Tsang, L. (1995). A sparse-matrix canonical-grid method for scattering by many scatterers. *Microwave Opt. Technol. Lett.* 8 (2): 114–118.

282 Gan, H. and Chew, W.C. (1995). A discrete BCG-FFT algorithm for solving 3D inhomogeneous scatterer problems. *J. Electromagn. Waves Appl.* 9 (10): 1339–1357.

283 Chew, W.C., Lin, J.H., and Yang, X.G. (1995). An FFT T-matrix method for 3D microwave scattering solution from random discrete scatterers. *Microwave Opt. Technol. Lett.* 9 (4): 194–196.

284 Lin, J.H. and Chew, W.C. (1996). BiCG-FFT T-matrix method for solving for the scattering solution from inhomogeneous bodies. *IEEE Trans. Microwave Theory Tech.* 44 (7): 1150–1155.

285 Seo, S.M. and Lee, J.F. (2005). A fast IE-FFT algorithm for solving PEC scattering problems. *IEEE Trans. Magn.* 41 (5): 1476–1479.

286 Kim, H. and Ling, H. (1993). On the application of fast wavelet transform to the integral- equation solution of electromagnetic scattering problems. *Microwave Opt. Technol. Lett.* 6 (3): 168–173.

287 Steinberg, B.Z. and Leviatan, Y. (1993). On the use of wavelet expansions in the method of moments. *IEEE Trans. Antennas Propag.* 41 (5): 610–619.

288 Wagner, R.L., Otto, G.P., and Chew, W.C. (1993). Fast waveguide mode computation using wavelet-like basis functions. *IEEE Microwave Guided Wave Lett.* 3 (7): 208–210.

289 Sabetfakhri, K. and Katehi, L.P.B. (1994). Analysis of integrated millimeter-wave and submillimeter-wave waveguides using orthonormal wavelet expansion. *IEEE Trans. Microwave Theory Tech.* 42: 2412–2422.

290 Wang, G., Pan, G., and Gilbert, B.K. (1995). A hybrid wavelet expansion and boundary element analysis for multiconductor transmission lines in multilayered dielectric media. *IEEE Trans. Microwave Theory Tech.* 43: 664–674.

291 Wagner, R.L. and Chew, W.C. (1995). A study of wavelets for the solution of electro- magnetic integral equations. *IEEE Trans. Antennas Propag.* 43 (8): 802–810.

292 Golik, W.L. (2000). Sparsity and conditioning of impedance matrices obtained with semi-orthogonal and bi-orthogonal wavelet bases. *IEEE Trans. Antennas Propag.* 48 (4): 473–481.

293 Deng, H. and Ling, H. (1999). On a class of predefined wavelet packet bases for efficient representation of electromagnetic integral equations. *IEEE Trans. Antennas Propag.* 47 (12): 1772–1779.

294 Jaffard, S. (1992). Wavelet methods for fast resolution of elliptic problems. *SIAM J. Numer. Anal.* 29 (4): 965–986.

295 Alpert, B., Beylkin, G., Coifman, R.R., and Rokhlin, V. (1993). Wavelet-like bases for the fast solution of second-kind integral equations. *SIAM J. Sci. Comput.* 14 (1): 159–184.

296 Hackbusch, W. (1999). Sparse matrix arithmetic based on H-matrices. Part I: introduction to H-matrices. *Computing* 62 (2): 89–108.

297 Bebendorf, M. (2000). Approximation of boundary element matrices. *Numer. Math.* 86 (4): 565–589.

298 Borm, S., Grasedyck, L., and Hackbusch, W. (2003). Hierarchical matrices. *Lecture Note 21 of the Max Planck Institute for Mathematics in the Sciences*.

299 Bebendorf, M. (2008). *Hierarchical Matrices: A Means to Efficiently Solve Elliptic Boundary Value Problems*. Berlin: Springer.

300 Baharav, Z. (1996). Impedance matrix compression with the use of wavelet expansions. *Microwave Opt. Technol. Lett.* 12 (2): 268–272.

301 Kurz, S., Rain, O., and Rjasanow, S. (2002). The adaptive cross-approximation technique for 3-D boundary-element method. *IEEE Trans. Magn.* 38 (2): 421–424.

302 Zhao, K., Vouvakis, M., and Lee, J.F. (2004). Application of the multilevel adaptive cross-approximation on ground plane designs. *IEEE Int. Symp. Electromagn. Compat.* 1: 124–127.

303 Bebendorf, M. and Grzhibovskis, R. (2006). Accelerating Galerkin BEM for linear elasticity using adaptive cross approximation. *Math. Methods Appl. Sci.* 29 (14): 1721–1747.

304 Guo, H., Hu, J., Shao, H., and Nie, Z. (2011). Multilevel sparse approximate inverse preconditioning for solving dynamic integral equation by H-matrix method. In: *Proc. IEEE Int. Workshop Antenna Tech.*, 124–127.

305 Liberty, E., Woolfe, F., Martinsson, P.G., and Tygert, M. (2007). Randomized algorithms for the low-rank approximation of matrices. *Proc. Natl. Acad. Sci. U.S.A.* 104 (51): 20167–20172.

306 Canning, F.X. (1990). Transformations that produce a sparse moment matrix. *J. Electromagn. Waves Appl.* 4 (9): 983–993.

307 Canning, F.X. (1991). Interaction matrix localization (IML) permits solution of larger scattering problems. *IEEE Trans. Magn.* 27 (5): 4275–4278.

308 Michielssen, E. and Boag, A. (1994). Multilevel evaluation of electromagnetic fields for the rapid solution of scattering problems. *Microwave Opt. Technol. Lett.* 7 (17): 790–795.

309 Michielssen, E. and Boag, A. (1996). A multilevel matrix decomposition algorithm for analyzing scattering from large structures. *IEEE Trans. Antennas Propag.* 44 (8): 1086–1093.

310 Rius, J., Parrón, J., Úbeda, E., and Mosig, J. (1999). Multilevel matrix decomposition algorithm for analysis of electrically large electromagnetic problems in 3-D. *Microwave Opt. Technol. Lett.* 22 (3): 177–182.

311 Appel, A.W. (1985). An efficient program for many-body simulation. *SIAM J. Sci. Stat. Comput.* 6 (1): 85–103.

312 Barnes, J. and Hut, P. (1986). A hierarchical $O(N \log N)$ force calculation algorithm. *Nature* 324 (4): 446–449.

313 Rokhlin, V. (1990). Rapid solution of integral equations of scattering theory in two dimensions. *J. Comput. Phys.* 86 (2): 414–439.

314 Coifman, R., Rokhlin, V., and Wandzura, S. (1993). The fast multipole method for the wave equation: a pedestrian prescription. *IEEE Antennas Propag. Mag.* 35 (3): 7–12.

315 Brandt, A. (1991). Multilevel computations of integral transforms and particle interactions with oscillatory kernels. *Comput. Phys. Commun.* 65 (1–3): 24–38.

316 Rokhlin, V. (1993). Diagonal forms of translation operators for the Helmholtz equation in three dimensions. *Appl. Comput. Harmon. Anal.* 1 (1): 82–93.

317 Chew, W.C., Koc, S., Song, J.M. et al. (1997). A succinct way to diagonalize the translation matrix in three dimensions. *Microwave Opt. Technol. Lett.* 15 (3): 144–147.

318 Brandt, A. (1982). Guide to multigrid development. In: *Multigrid methods*, vol. 96 (eds. W. Hackbusch and U. Trottenberg), 220–312. Berlin: Springer.

319 Song, J.M., Lu, C.C., Chew, W.C., and Lee, S.W. (1998). Fast Illinois solver code (FISC). *IEEE Antennas Propag. Mag.* 40 (3): 27–33.

320 Song, J.M. and Chew, W.C. (2000). Large scale computations using FISC. *IEEE Antennas Propag. Soc. Int. Symp., Salt Lake City, Utah (16–21 July)* 4: 1856–1859.

321 Hastriter, M.L. and Chew, W.C. (2004). Comparing Xpatch, FISC, and ScaleME using a cone-cylinder. *IEEE Antennas Propag. Soc. Int. Symp.* , Monterey, CA (20–25 June) 2: 2007–2010.

322 Taboada, J.M., Araujo, M.G., Bertolo, J.M. et al. (2010). MLFMA-FFT parallel algorithm for the solution of large-scale problems in electromagnetics. *Prog. Electromagn. Res.* 105: 15–30.

323 Pan, X.M., Pi, W.C., Yang, M.L. et al. (2012). Solving problems with over one billion unknowns by the MLFMA. *IEEE Trans. Antennas Propag.* 60 (5): 2571–2574.

324 Ergul, O. and Gurel, L. (2011). Rigorous solutions of electromagnetics problems involving hundreds of millions of unknowns. *IEEE Antennas Propag. Mag.* 53 (1): 18–26.

325 Lee, J., Zhang, J., and Lu, C.C. (2004). Sparse inverse preconditioning of multilevel fast multipole algorithm for hybrid integral equations in electromagnetics. *IEEE Trans. Antennas Propag.* 52 (9): 2277–2287.

326 Yang, M.L. and Sheng, X.Q. (2010). Parallel FE-BI-MLFMA for scattering by extremely large targets with cavities. *International Conference on Electromagnetics in Advanced Applications*, Sydney, Australia (20–24 September 2010).

327 Nie, Z.P., Ma, W.M., Ren, Y. et al. (2009). A wideband electromagnetic scattering analysis using MLFMA with higher order hierarchical vector basis functions. *IEEE Trans. Antennas Propag.* 57 (10): 3169–3178.

328 Shao, H.R., Hu, J., and Nie, Z.P. (2011). Hybrid tangential equivalence principle algorithm with MLFMA for analysis of array structures. *Prog. Electromagn. Res.* 113: 127–141.

329 Kishimoto, S., Ohnuki, S., Ashizawa, Y. et al. (2012). Time domain analysis of nanoscale electromagnetic problems by a boundary integral equation method with fast inverse Laplace transform. *J. Electromagn. Waves Appl.* 26: 997–1006.

330 Kim, B., Song, J.M., and Song, X. (2010). Calculations of the binding affinities of protein-protein complexes with the fast multipole method. *J. Chem. Phys*. 133, Paper 095101.

331 Cui, T.J., Chew, W.C., Chen, G., and Song, J.M. (2004). Efficient MLFMA, RPFMA and FAFFA algorithms for EM scattering by very large structures. *IEEE Trans. Antennas Propag.* 52 (3): 759–770.

332 Hu, J., Nie, Z.P., Wang, J. et al. (2004). Multilevel fast multipole algorithm for solving scattering from 3-D electrically large object. *Chin. J. Radio Sci.* 19 (5): 509–524.

333 Dembart, B. and Yip, E. (1995). A 3D fast multipole method for electromagnetics with multiple levels. *Ann. Rev. Prog. Appl. Comput. Electromagn.* 1: 621–628.

334 Ergin, A.A., Shanker, B., and Michielssen, E. (1999). The plane-wave time-domain algorithm for the fast analysis of transient wave phenomena. *IEEE Antennas Propag. Mag.* 41 (4): 39–52.

335 Darve, E. and Havé, P. (2004). A fast multipole method for Maxwell equations stable at all frequencies. *Philos. Trans. R. Soc. London, Ser. A* 362 (1816): 603–628.

336 Kishimoto, S., Ohnuki, S., Ashizawa, Y. et al. (2012). Time domain analysis of nanoscale electromagnetic problems by a boundary integral equation method with fast inverse Laplace transform. *J. Electromagn. Waves Appl.* 26: 997–1006.

337 Moharam, M.G. and Gaylord, T.K. (1981). Rigorous coupled-wave analysis of planar-grating diffraction. *J. Opt. Soc. Am. A* 71: 811–818.

338 Chew, W.C., Barone, S., Anderson, B., and Hennessy, C. (1984). Diffraction of axisymmetric waves in a borehole by bed boundary discontinuities. *Geophysics* 49 (10): 1586–1595.

339 Druskin, V.L. and Knizhnerman, L.A. (1988). A spectral semi-discrete method for the numerical solution of 3-D nonstationary problems in electrical prospecting. *Izv. Phys. Solid Earth* 24: 63–74.

340 Berrington, K.A., Burke, P.G., Le Dourneuf, M. et al. (1978). A new version of the general program to calculate atomic continuum processes using the R-matrix method. *Comput. Phys. Commun.* 14: 367–412.

341 Svizhenko, A., Anantram, M.P., Govindan, T.R., and Biegel, B. (2002). Two-dimensional quantum mechanical modeling of nanotransistors. *J. Appl. Phys.* 91 (4): 2343–2354.

342 Khan, H.R., Mamaluy, D., and Vasileska, D. (2007). Quantum transport simulation of experimentally fabricated nano-FinFET. *IEEE Trans. Electron Devices* 54 (4): 784–796.

343 Milnikov, G., Mori, N., Kamakura, Y., and Ezaki, T. (2008). R-matrix theory of quantum transport and recursive propagation method for device simulations. *J. Appl. Phys.* 104 (4): 044506.

344 Anantram, M.P., Lundstrom, M.S., and Nikonov, D.E. (2008). Modeling of nanoscale devices. *Proc. IEEE* 96 (9): 1511–1550.

345 Radhakrishnan, K. and Chew, W.C. (2001). Efficient analysis of waveguiding structures. In: *Fast and Efficient Algorithms in Computational Electromagnetics*, Chapter 10. Boston, MA: Artech House.

346 Greengard, L. and Gropp, W.D. (1990). A parallel version of the fast multipole method. *Comput. Math. Appl.* 20 (7): 63–71.

347 Ying, L., Biros, G., and Zorin, D. (2004). A kernel-independent adaptive fast multipole algorithm in two and three dimensions. *J. Comput. Phys.* 196 (2): 591–626.

348 Bagci, H., Yilmaz, A.E., Jin, J.-M., and Michielssen, E. (2008). Time domain adaptive integral method for surface integral equations. *Model. Comput. Electromagn.* 65–104.

349 Pirinoli, P., Matekovits, L., Vecchi, G. et al. (2003). Synthetic functions, multiscale MoM analysis of arrays. *IEEE Antennas Propag. Soc. Int. Symp.* 4: 799–802.

350 Li, M.K. and Chew, W.C. (2007). Wave-field interaction with complex structures using equivalence principle algorithm. *IEEE Trans. Antennas Propag.* 55 (1): 130–138.

351 Qian, Z.-G. and Chew, W.C. (2009). Fast full-wave surface integral equation solver for multiscale structure modeling. *IEEE Trans. Antennas Propag.* 57 (11): 3594–3601.

352 Zhao, J.S. and Chew, W.C. (2000). Integral equation solution of Maxwell's equations from zero frequency to microwave frequencies. *IEEE Trans. Antennas Propag*. James R. Wait Memorial Special Issue 48 (10): 1635–1645.

353 Jiang, L.J. and Chew, W.C. (2005). A mixed-form fast multipole algorithm. *IEEE Trans. Antennas Propag.* AP-53 (12): 4145–4156.

354 Cheng, H., Crutchfield, W.Y., Gimbutas, Z. et al. (2006). A wideband fast multipole method for the Helmholtz equation in three dimensions. *J. Comput. Phys.* 216 (1): 300–325.

355 Wallen, H., Jarvenpaa, S., and Yla-Oijala, P. (2006). Broadband multilevel fast multipole algorithm for acoustic scattering problems. *J. Comput. Acoust.* 14 (04): 507–526.

356 Xia, T., Meng, L.L., Liu, Q.S. et al. (2018). A low-frequency stable broadband multilevel fast multipole algorithm using plane wave multipole hybridization. *IEEE Trans. Antennas Propag.* 66 (11): 6137–6145.

357 Hood, P. (1976). Frontal solution program for unsymmetric matrices. *Int. J. Numer. Methods Eng.* 10 (2): 379–399.

358 Smith, B., Bjorstad, P., and Gropp, W. (2004). *Domain Decomposition: Parallel Multilevel Methods for Elliptic Partial Differential Equations*. Cambridge University Press.

359 Kron, G. (1963). *Diakoptics: The Piecewise Solution of Large Scale Systems*. MacDonald.

360 Lai, C.H. (1994). Diakoptics, domain decomposition, and parallel computing. *Comput. J.* 37 (10): 840–846.

361 Goubau, G., Puri, N.N., and Schwering, F.K. (1982). Diakoptic theory for multielement antennas. *IEEE Trans. Antennas Propag.* 30 (1): 15–26.

362 Schwering, F.K., Puri, N.N., and Butler, C.M. (1986). Modified diakoptic theory of antennas. *IEEE Trans. Antennas Propag.* 34 (11): 1273–1281.

363 Niver, E., Smith, H.H., and Whitman, G.M. (1992). Frequency characterization of a thin linear antenna using diakoptic antenna theory. *IEEE Trans. Antennas Propag.* 40 (3): 245–250.

364 Merugu, L.N. and Fusco, V.F. (1993). Concurrent network diakoptics for electromagnetic field problems. *IEEE Trans. Microwave Theory Tech.* 41 (4): 708–716.

365 Ooms, S. and Zutter, D.D. (1998). A new iterative diakoptics-based multilevel moments method for planar circuits. *IEEE Trans. Microwave Theory Tech.* 46 (3): 280–291.

366 Notaros, B.M. (2008). Higher order frequency-domain computational electromagnetics. Special Issue on Large and Multiscale Computational Electromagnetics. *IEEE Trans. Antennas Propag.* 56 (8): 2251–2276.

367 Olcan, D.I., Stevanovic, I.M., Mosig, J.R., and Djordjevic, A.R. (2007). Diakoptic surface integral-equation formulation applied to large 2-D scattering problems. In: *Proceedings of EuCAP 2007*, 11–16. Edinburgh, UK.

368 Stupfel, B. (1996). A fast-domain decomposition method for the solution of electromagnetic scattering by large objects. *IEEE Trans. Antennas Propag.* 44 (10): 1375–1385.

369 Stupfel, B. (1996). A fast-domain decomposition method for the solution of electromagnetic scattering by large objects. *IEEE Trans. Antennas Propag.* 44 (10): 1375–1385.

370 Stupfel, B. and Mognot, M. (2000). A domain decomposition method for the vector wave equation. *IEEE Trans. Antennas Propag.* 48 (5): 653–660.

371 Lu, Y. and Shen, C.Y. (1997). A domain decomposition finite-difference method for parallel numerical implementation of time-dependent Maxwell's equations. *IEEE Trans. Antennas Propag.* 45 (3): 556–562.

372 Wolfe, C.T., Navsariwala, U., and Gedney, S.D. (2000). Parallel finite-element tearing and interconnecting algorithm for solution of the vector wave equation with PML absorbing medium. *IEEE Trans. Antennas Propag.* 48 (2): 278–284.

373 Boag, A. (2001). A fast multilevel domain decomposition algorithm for radar imaging. *IEEE Trans. Antennas Propag.* 49 (4): 666–671.

374 Xu, F. and Hong, W. (2004). Analysis of two dimensions sparse multicylinder scattering problem using DD-FDTD method. *IEEE Trans. Antennas Propag.* 52 (10): 2612–2617.

375 Liu, P. and Jin, Y.Q. (2005). Numerical simulation of the Doppler spectrum of a flying target above dynamic oceanic surface by using the FEM-DDM method. *IEEE Trans. Antennas Propag.* 53 (2): 825–832.

376 Vouvakis, M.N., Cendes, Z., and Lee, J.F. (2006). A FEM domain decomposition method for photonic and electromagnetic band gap structures. *IEEE Trans. Antennas Propag.* 54 (2): 721–733.

377 Yin, L., Wang, J., and Hong, W. (2002). A novel algorithm based on the domain-decomposition method for the full-wave analysis of 3-D electromagnetic problems. *IEEE Trans. Microwave Theory Tech.* 50 (8): 2011–2017.

378 Hamandi, L., Lee, R., and Ozgdner, F. (1995). Review of domain-decomposition methods for the implementation of FEM on massively parallel computers. *IEEE Antennas Propag. Mag.* 37 (1): 93–98.

379 Barka, A. and Caudrillier, P. (2007). Domain decomposition method based on generalized scattering matrix for installed performance of antennas on aircraft. *IEEE Trans. Antennas Propag.* 55 (6): 1833–1842.

380 Rubia, V. and Zapata, J. (2007). Microwave circuit design by means of direct decomposition in the finite-element method. *IEEE Trans. Microwave Theory Tech.* 55 (7): 1520–1530.

381 Zhao, K., Rawat, V., Lee, S.C., and Lee, J.F. (2007). A domain decomposition method with nonconformal meshes for finite periodic and semi-periodic structures. *IEEE Trans. Antennas Propag.* 55 (9): 2559–2570.

382 Li, Y.J. and Jin, J.M. (2006). A vector dual-primal finite element tearing and interconnecting method for solving 3-D large-scale electromagnetic problems. *IEEE Trans. Antennas Propag*. 54: 3000–3009. 55 (10): 2803–2810, 2007.

383 Collino, F., Ghanemi, S., and Joly, P. (2000). Domain decomposition method for harmonic wave propagation: a general presentation. *Comput. Meth. Appl. Mech. Eng*. 184: 171–211 . Elsevier.

384 Rebollo, T.C. and Vera, E.C. (2004). Study of a non-overlapping domain decomposition method: Poisson and Stokes problems. *Appl. Numer. Math*. 48: 169–194 . Elsevier.

385 Farhat, C. and Roux, F.-X. (1991). A method of finite element tearing and interconnecting and its parallel solution algorithms. *Int. J. Numer. Methods Eng.* 32: 1205–1227.

386 Lee, S.-C., Vouvakis, M.N., and Lee, J.-F. (2005). A nonoverlapping domain decomposition method with nonmatching grids for modeling large finite antenna arrays. *J. Comput. Phys.* 203: 1–21.

387 Zhao, K., Rawat, V., and Lee, J.-F. (2008). A domain decomposition method for electromagnetic radiation and scattering analysis of multi-target problems. *IEEE Trans. Antennas Propag.* 56: 2211–2221.

388 Ilic, M.M. and Notaros, B.M. (2009). Higher order FEM-MoM domain decomposition for 3-D electromagnetic analysis. *IEEE Antennas Wirel. Propag. Lett.* 8: 970–973.

389 Li, M.-K. and Chew, W.C. (2007). Wave-field interaction with complex structures using equivalence principle algorithm. *IEEE Trans. Antennas Propag.* 55 (1): 130–138.

390 Li, M.-K. and Chew, W.C. (2008). Multiscale simulation of complex structures using equivalence principle algorithm with high-order field point sampling scheme. *IEEE Trans. Antennas Propag.* 56 (8): 2389–2397.

391 Sun, L.E., Chew, W.C., and Jin, J.M. (2010). Augmented equivalence principle algorithm at low frequencies. *Microwave Opt. Technol. Lett.* 52 (10): 2274–2279.

392 Ma, Z.H., Jiang, L.J., and Chew, W.C. (2013). Loop-tree free augmented equivalence principle algorithm for low frequency problems. *Microwave Opt. Technol. Lett.* 55 (10): 2475–2479.

393 Shao, H.R., Hu, J., Chew, W.C. (2013). Single source EPA for scattering by array structures. AP-S/URSI *Symposium*, Orlando (July, 2013).

394 Chao, H.Y., Song, J.M., Michielssen, E., and Chew, W.C. (1998). The multilevel fast multipole algorithm for analyzing electromagnetic radiation from complex surface-wire structures. *Antenna Applications Symposium*, Monticello, IL (16–18 September, 1998).

395 Song, J.M., Lu, C.C., and Chew, W.C. (1997). Multilevel fast multipole algorithm for electromagnetic scattering by large complex objects. *IEEE Trans. Antennas Propag.* 45 (10): 1488–1493.

396 Hesford, A.J. and Chew, W.C. (2008). On preconditioning and the eigensystems of electromagnetic radiation problems. *IEEE Trans. Antennas Propag.* 56: 2413–2420.

397 He, S.Q., Sha, W.E.I., Jiang, L.J. et al. (2012). Finite element based generalized impedance boundary condition for modeling plasmonic nanostructures. *IEEE Trans. Nanotechnol.* https://doi.org/10.1109/TNANO.2011.2171987.

398 Ling, H., Chou, R.C., and Lee, S.W. (1989). Shooting and bouncing rays: calculating the RCS of an arbitrarily shaped cavity. *IEEE Trans. Antennas Propag.* 37: 194–205.

399 Engquist, B. and Runborg, O. (2003). Computational high frequency wave propagation. *Acta Numer.* 12: 181–266.

400 Chandler-Wilde, S.N., Graham, I.G., Langdon, S., and Spence, E.A. (2012). Numerical-asymptotic boundary integral methods in high-frequency acoustic scattering. *Acta Numer.* 21: 89–305.

401 Osher, S.J. and Sethian, J.A. (1988). Fronts propagating with curvature-dependent speed: algorithms based on Hamilton-Jacobi formulations. *J. Comput. Phys.* 79: 12–49.

402 Sethian, J.A. (1996). A fast marching level set method for monotonically advancing fronts. *Proc. Natl. Acad. Sci. U.S.A.* 93: 1591–1595.

403 Červený, V., Popov, M.M., and Pšenč´ lk, I. (1982). Computation of wave fields in inho-mogeneous media–Gaussian beam approach. *Geophys. J. R. Astron. Soc.* 70: 109–128.

404 Tanushev, N.M., Engquist, B., and Tsai, R. (2009). Gaussian beam decomposition of high frequency wave fields. *J. Comput. Phys.* 228: 8856–8871.

405 Macdonald, H.M. (1913). The effect produced by an obstacle on a train of electric waves. *Philos. Trans. R. Soc. London, Ser. A* 212: 299–337.

406 Gordon, W.B. (1975). Far-field approximations to the Kirchhoff-Helmholtz representation of scattered fields. *IEEE Trans. Antennas Propag.* 23: 590–592.

407 Ludwig, A.C. (1968). Computation of radiation patterns involving numerical double integration. *IEEE Trans. Antennas Propag.* 16: 767–769.

408 Burkholder, R.J. and Lee, T. (2005). Adaptive sampling for fast physical optics numerical integration. *IEEE Trans. Antennas Propag.* 53: 1843–1845.

409 Obelleiro-Basteiro, F., Rodriguez, J.L., and Burkholder, R.J. (1995). An iterative physical optics approach for analyzing the electromagnetic scattering by large open-ended cavities. *IEEE Trans. Antennas Propag.* 43: 356–361.

410 Burkholder, R.J. and Lundin, T. (2005). Forward-backward iterative physical optics algorithm for computing the RCS of open-ended cavities. *IEEE Trans. Antennas Propag.* 53: 793–799.

411 Wu, Y.M., Jiang, L.J., and Chew, W.C. (2012). An efficient method for computing highly oscillatory physical optics integral. *Prog. Electromagn. Res.* 127: 211–257.

412 Chandler-Wilde, S.N. and Graham, I.G. (2009). Boundary integral methods in high-frequency scattering. In: *Highly Oscillatory Problems* (eds. B. Engquist, T. Fokas, E. Hairer and A. Iserles), 154–193. Cambridge: Cambridge University Press.

413 Doḿlnguez, V., Graham, I.G., and Smyshlyaev, V.P. (2007). A hybrid numerical-asymptotic boundary integral method for high-frequency acoustic scattering. *Numer. Math.* 106: 471–510.

414 Chandler-Wilde, S.N. and Langdon, S. (2007). A Galerkin boundary element method for high frequency scattering by convex polygons. *SIAM J. Numer. Anal.* 45: 610–640.

415 Bruno, O.P. and Kunyansky, L.A. (2001). A fast, high-order algorithm for the solution of surface scattering problems: basic implementation, tests, and applications. *J. Comput. Phys.* 169 (1): 80–110.

416 Perrey-Debain, E., Trevelyan, J., and Bettess, P. (2003). Plane wave interpolation in direct collocation boundary element method for radiation and wave scattering: numerical aspects and applications. *J. Sound Vib.* 261 (5): 839–858.

417 Huybrechs, D. and Vandewalle, S. (2006). On the evaluation of highly oscillatory integrals by analytic continuation. *SIAM J. Numer. Anal.* 44 (3): 1026–1048.

418 Geuzaine, C., Bruno, O., and Reitich, F. (2005). On the O(1) solution of multiple-scattering problems. *IEEE Trans. Magn.* 41 (5): 1488–1491.

419 Davis, C.P. and Chew, W.C. (2008). Frequency-independent scattering from a flat strip with TE_z-polarized fields. *IEEE Trans. Antennas Propag.* 56 (4): 1008–1016.

420 Burridge, R. (1980, 1980). The Gelfand-Levitan, the Marchenko, and the Gopinath-Sondhi integral equations of inverse scattering theory, regarded in the context of inverse impulse-response problems. *Wave Motion* 2: 305–323.

421 Cutrona, L.J. (1970). Synthetic aperture radar , Chapter 23. In: *Radar Handbook* (ed. M.I. Skolnik). New York, NY: McGraw Hill.

422 McCandless, S.W. and Jackson, C.R. (2004). Principles of synthetic aperture radar," Chapter 1. In: *SAR Marine Users Manual* (eds. C.R. Jackson and J.R. Apel), 1–23. NOAA.

423 Devaney, A.J. (1982). A filtered backpropagation algorithm for diffraction tomography. *Ultrason. Imaging* 4 (6): 336–350.

424 Devaney, A.J. (1983). A computer simulation study of diffraction tomography. *IEEE Trans. Biomed. Eng.* 30 (7): 377–386.

425 Tarantola, A. (1984). Inversion of seismic reflection data in the acoustic approximation. *Geophysics* 49: 1259–1266.

426 Chew, W.C. and Wang, Y.M. (1990). Reconstruction of two-dimensional permittivity distribution using the distorted Born iterative method. *IEEE Trans. Med. Imaging* 9: 218–225.

427 Bond, E.J., Bond, E.J., Li, X. et al. (2003). Microwave imaging via space-time beamforming for early detection of breast cancer. *IEEE Trans. Antennas Propag.* 51: 1690–1705.

428 Cui, T.J., Chew, W.C., Aydiner, A.A., and Chen, S. (2001). Inverse scattering of two-dimensional dielectric objects buried in a lossy earth using the distorted Born iterative method. *IEEE Trans. Geosci. Remote Sens.* 39: 339–346.

429 Wang, G.L., Chew, W.C., Cui, T.J. et al. (2004). 3D near-to-surface conductivity reconstruction by inversion of VETEM data using the distorted Born iterative method. *Inverse Prob.* 20: S195–S216.

430 Mojabi, P. and LoVetri, J. (2009). Overview and classification of some regularization techniques for the Gauss-Newton inversion method applied to inverse scattering problems. *IEEE Trans. Antennas Propag.* 57: 2658–2665.

431 Liu, Q.H., Zhang, Z.Q., Wang, T.T. et al. (2002). Active microwave imaging I–2-D forward and inverse scattering methods. *IEEE Trans. Microwave Theory Tech.* 50: 123–133.

432 Cui, T.J., Chew, W.C., Yin, X.X., and Hong, W. (2004). Study of resolution and super resolution in electromagnetic imaging for half-space problems. *IEEE Trans. Antennas Propag.* 52: 1398–1411.

433 Deuflhard, P. (2004). *Newton Methods for Nonlinear Problems. Affine Invariance and Adaptive Algorithms*, Springer Series in Computational Mathematics, 1e, vol. 35. Berlin: Springer.

434 Franchois, A., Joisel, A., Pichot, C., and Bolomey, J.-C. (1998). Quantitative microwave imaging with a 2.45-GHz planar microwave camera. *IEEE Trans. Med. Imaging* 17 (4): 550–561.

435 Van Den Berg, P.M. and Kleinman, R.E. (1997). A contrast source inversion method. *Inverse Prob.* 13 (6): 1607–1620.

436 Abubakar, A., Habashy, T.M., Druskin, V.L. et al. (2008). 2.5D forward and inverse modeling for interpreting low-frequency electromagnetic measurements. *Geophysics* 73: F165–F177.

437 Zhong, Y. and Chen, X. (2007). MUSIC imaging and electromagnetic inverse scattering of multiple-scattering small anisotropic spheres. *IEEE Trans. Antennas Propag.* 55: 3542–3549.

438 Litman, A., Lesselier, D., and Santosa, F. (1998). Reconstruction of a two-dimensional binary obstacle by controlled evolution of a level-set. *Inverse Prob.* 14 (3): 685–706.

439 Torres-Verdín, C. and Habashy, T.M. (1994). Rapid 2.5-dimensional forward modeling and inversion via a new nonlinear scattering approximation. *Radio Sci.* 29: 1051–1079.

440 Cui, T.J. and Chew, W.C. (1999). Fast algorithm for electromagnetic scattering by buried 3-D dielectric objects of large size. *IEEE Trans. Geosci. Remote Sens.* 37: 2597–2608.

441 Cui, T.J. and Liang, C.H. Nonlinear differential equation for the reflection coefficient of an inhomogeneous lossy medium and its inverse scattering solutions. *IEEE Trans. Antennas Propag*. 42 (5): 621–626.

442 Hesford, A.J. and Chew, W.C. (2010). Fast inverse scattering solutions using the distorted Born iterative method and the multilevel fast multipole algorithm. *J. Acoust. Soc. Am.* 128: 679–690.

443 Moghaddam, M. and Chew, W.C. (1992). Nonlinear two-dimensional velocity profile inversion using time domain data. *IEEE Trans. Geosci. Remote Sens.* 30 (1): 147–156.

444 Wang, Y.M. and Chew, W.C. (1992). Accelerating the iterative inverse scattering algorithms by using the fast recursive aggregate T-matrix algorithm. *Radio Sci.* 27 (2): 109–116.

445 Weedon, W.H. and Chew, W.C. (1999). Time-domain inverse scattering using the local shape function (LSF) method. *Inverse Prob.* 9 (5): 551.

446 Chen, F.C. and Chew, W.C. (1998). Experimental verification of super resolution in nonlinear inverse scattering. *Appl. Phys. Lett.* 72 (23): 3080–3082.

447 Ali, M.A. and Moghaddam, M. (2010). 3D nonlinear super-resolution microwave inversion technique using time-domain data. *IEEE Trans. Antennas Propag.* 58 (7): 2327–2336.

448 Gilmore, C., Mojabi, P., Zakaria, A. et al. (2010). On super-resolution with an experimental microwave tomography system. *IEEE Antennas Wirel. Propag. Lett.* 9: 393–396.

449 Lehman, S.K. and Devaney, A.J. (2003). Transmission mode time-reversal super-resolution imaging. *J. Acoust. Soc. Am.* 113: 2742.

450 Lerosey, G., De Rosny, J., Tourin, A. et al. (2004). Time reversal of electromagnetic waves. *Phys. Rev. Lett.* 92 (19): 193904.

451 Pembry, J.B. (2000). Negative refraction makes a perfect lens. *Phys. Rev. Lett.* 85: 3966–3969.

452 Pendry, J.B., Schurig, D., and Smith, D.R. (2006). Controlling electromagnetic fields. *Science* 312: 1780–1782.

453 Schurig, D., Mock, J.J., Justice, B.J. et al. (2006). Metamaterial electromagnetic cloak at microwave frequencies. *Science* 314: 977–980.

454 Cummer, S.A., Popa, B.I., Schurig, D. et al. (2006). Full-wave simulations of electromagnetic cloaking structures. *Phys. Rev. E* 74: 036621.

455 Chew, W.C. (2005). Some reflections on double negative materials. *Prog. Electromagn. Res.* 51: 1–26.

456 Thomas, J.R. and Ishimaru, A. (2002). Transmission properties of material with relative permittivity and permeability close to -1. *Proc. SPIE* 4806: 167–175.

457 Dolin, L.S. (1961). *Izv. Vyssh. Uchebn. Zaved. Radiofizika* 4: 964.

458 Odabasi, H., Teixeira, F.L., and Chew, W.C. (2011). Impedance-matched absorbers and optical pseudo black holes. *J. Opt. Soc. Am. B: Opt. Phys.* 28 (5): 1317–1323.

459 Chen, H. and Chan, C.T. (2007). Acoustic cloaking in three dimensions using acoustic metamaterials. *Appl. Phys. Lett.* 91 (18).

460 Liu, R., Ji, C., Mock, J.J. et al. (2009). Broadband ground-plane cloak. *Science* 323: 366–369.

461 Shu, W.W. and Song, J.M. (2006). Complete mode spectrum of a grounded dielectric slab with double negative metamaterials. *Prog. Electromagn. Res.* 65: 103–123.

462 Cui, T.J., Smith, D.R., and Liu, R. (2009). *Metamaterials: Theory, Design, and Applications*. Springer.

463 Ma, H.F. and Cui, T.J. (2010). Three-dimensional broadband ground-plane cloak made of metamaterials. *Nat. Commun.* 1 (3): 21.

464 Choo, H.S., Rogers, R.L., and Ling, H. (2005). Design of electrically small wire antennas using a pareto genetic algorithm. *IEEE Trans. Antennas Propag.* 53: 1038–1046.

465 Adams, J.J. and Bernhard, J.T. (2009). Tuning method for a new electrically small antenna with low Q. *IEEE Antennas Wirel. Propag. Lett.* 8: 303–306.

466 Hansen, R. and Collin, R.E. (2011). *Small Antenna Handbook*. Wiley.

467 Best, S.R. (2007). A discussion on power factor, quality factor and efficiency of small antennas. *IEEE Antennas Propag. Soc. Int. Symp. Dig.* 2269–2272.

468 Yaghjian, A.D., O'Donnell, T.H., Altshuler, E.E., and Best, S.R. (2008). Electrically small supergain end-fire arrays. *Radio Sci.* 43: 13.

469 Thal, H.L. Jr. (2006). New radiation Q limits for spherical wire antennas. *IEEE Trans. Antennas Propag.* 54: 2757–2763.

470 Wong, H., Luk, K.-M., Chan, C.H. et al. (2012). Small antennas in wireless communications. *Proc. IEEE* 100 (7): 2109–2121.

471 Wong, K.L. (2003). *Planar Antennas for Wireless Communications*. New York, NY: Wiley.

472 Chen, Z.N., See, T.S.P., and Qing, X. (2007). Small printed ultrawideband antenna with reduced ground plane effect. *IEEE Trans. Antennas Propag.* 55: 383–388.

473 Jordan, E.C. and Balmain, K.G. (1968). *Electromagnetic Waves and Radiating Systems*. Upper Saddle River, NJ: Prentice-Hall.

474 Chu, L.J. (1948). Physical limitations of omni-directional antennas. *J. Appl. Phys.* 19: 1163–1175.

475 McLean, J.S. (1996). A re-examination of the fundamental limits on the radiation Q of electrically small antenna. *IEEE Trans. Antennas Propag.* 44: 672–676.

476 Erentok, A. and Ziolkowski, R.W. (2008). Metamaterial-inspired efficient electrically small antennas. *IEEE Trans. Antennas Propag.* 56: 691–707.